Control of *Shigella sonnei* and Adhesive Invasive *Escherichia coli* Infections with A Natural Product Which Inhibits the Bacterial Oxidoreductase DsbA

By

Zainulabedeen Reda Mirza

Thesis submitted to the University of Strathclyde for the degree of Doctor of Philosophy

Strathclyde Institute of Pharmacy and Biomedical Sciences, University of Strathclyde, 161 Cathedral Street, Glasgow, G4 0RE, UK

July 2017

Author’s Declaration

This thesis is the result of the author’s original research. It has been composed by the author and has not been previously submitted for examination which led to the award of a degree.

Signed:

Date:

CONTENT:

Abbreviation:

ActA: *Listeria* surface protein responsible for actin polymerisation

AIEC: adhesive and invasive *Escherichia coli*

AMP: anti-microbial peptide

AMPK: AMP-activated protein kinase

Arps: Actin related proteins

Atg: autophagy related genes

AJC: apical junctional complex

BSA: bovine serum albumin

c-Src: proto-oncogene tyrosine-protein kinase

CD: Crohn's disease

CARD: Caspase activation and recruitment domains

Casp-1: caspase-1

CEACAM6: carcinoembryonic antigen-related cell adhesion molecule 6

CFU: colony-forming unit

COX: cyclooxygenase

Crk: Cytoplasmic regulatory protein

C_T: cycle threshold

CUMS: chronic unpredictable mild stress

Cx: hexameric connexins

DAPI: 4’,6-diamidino-2-phenylindole

DCs: dendritic cells

Di-E-GSSG: dieosin glutathione disulphide

DMBA: 7,12-dimethylbenz[α]anthracene

DMEM: Dulbecco’s modified Eagle’s medium

DMSO: Dimethyl sulphoxide

DsbA: disulphide bond A

DSB: Disulphide bond System

DSS: dextran sulfate sodium

DTT: Dithiothreitol

EC: Epithelial cell

EDTA: Ethylenediaminetetraacetic acid

EGSH: eosin-glutathione

EIEC: Enteroinvasive *Escherichia coli*

FDA: food and drug administration

FlgI: flagellar p-ring protein

FliC: flagellin protein C

EOs: essential oils

EPEC: *Enteropathogenic Escherichia coli*

ER: endoplasmic reticulum

FAE: Follicle-associated epithelium

FOH: farnesol

FPPS: farnesyl pyrophosphate synthase

FSQ: fluorescence self-quenching

GALT: Gut-associated lymphoid tissues

GFP: green fluorescent protein

GGOH: geranylgeraniol

GGPP: geranylgeranyl-pyrophosphate

gipA: growth in PPs protein

GOH: Geraniol

GR: glutathione reductase

GSSG: oxidized glutathione

GSH: reduced Glutathione

H_2O_2: hydrogen peroxide

HCQ: Hydroxychloroquine

Hfq: RNA binding protein

HeLa: Henrietta Lacks cell line

HEK293: Human Embryonic Kidney 293 cells

Hep-2: Hep-2 epidermoid carcinoma cell line

htrA: high temperature requirement A

IBD: inflammatory bowel disease

IcsA: *Shigella* surface protein responsible for actin polymerisation

IcsB: *Shigella* protein for evades autophagy

IFN-γ: Gamma interferon

IL: Interleukin

InsP3: inositol-1,4,5-triphophate

Ipa: Invasion plasmid antigens

IPTG: Isopropyl β-D-1-thiogalactopyranoside

IRF-1: interferon-related factor

JAKs: Janus-associated kinases

LAMP1: Lysosomal-associated membrane protein 1

LPF: Long polar fimbriae

Lpfa: long polar fimbriae

M cells: Microfold cells

MALT: Mucosa-associated lymphoid tissues

MAM: Multivalent adhesion molecule

MCA: 4-methoxycinnamic acid

MDP: muramyl dipeptide

MDR: multidrug-resistant

MEF: mouse embryonic fibroblasts

MetS: fructose-induced metabolic syndrome

MHC: major histocompatibility complex

MIC: minimum inhibitory concentration

MKD: mevalonate kinase deficiency

MOH: Menthol

MOI: multiplicity of infection

MRSA*:* Methicillin-resistant *Staphylococcus aureus*

MS: resolution mass spectrometry

MTT: 3-(4,5-Dimethylthiazol-2-yl)-2,5-diphenyltetrazolium bromide

Mxi: membrane expression of invasion plasmid antigens

NALT: Nasal-associated lymphoid tissue

NF-kB: nuclear factor kappa

NK: Natural killer

NLRP3: oligomerization domain-like receptor family pyrin domain-containing 3

NLRs: NOD-like receptors

NMR: Nuclear magnetic resonance

NOD: Nucleotide-binding oligomerization domain-containing protein

NPFs: Nucleation promoting factors

NSAIDs: Non-steroidal anti-inflammatory drugs

OD: optical density

OmpA: outer membrane protein A

OMVs: outer membrane vesicles

PAGE: polyacrylamide gel electrophoresis

PAM: pamidronate

PBS: phosphate buffered saline

PDI: protein disulphide isomerase

PhoA: alkaline phosphatase

PI3K: phosphatidylinositol-3-kinase

PIs: Phosphoinositides

Pks: polyketide synthase complex

PLC: phospholipase C

PMNs: polymorphonuclear leukocytes

PP: Peyer's patches

PRR: pattern recognition receptor

PVDF: polyvinylidene difluoride

RATP: Response association with trespassing pathogens

RAW 264: mouse leukaemic monocyte macrophage cell line

RFU: relative fluorescence units

RIRK2: receptor-interacting serine/threonine-protein kinase 2

RLRs: RIG-I like receptors

ROS: reactive oxygen species

SAR: structure activity relationship

SDS: sodium dodecyl sulphate

SNPs: Single nucleotide polymorphisms

Spa: surface presentation of invasion plasmid antigens

Spy: Spheroplast protein y

ssRNA: single-stranded RNA

STAT: signal transducer and activator of transcription proteins

TEMED: Tetramethylethylenediamine

TLC: Thin layer chromatography

TLR: Toll-like receptor

TORC1: rapamycin complex 1

TPA: 12-O-tetradecanoylphorbol 13-acetate

TSA: Trypticase soy agar

TSB: Trypticase soy broth

T3SS: Type III secretion system

Vmax: maximum rate of reaction

WASP: Wiskott Aldrich syndrome protein

WHO: World Health Organisation

ZO-1: zonula occludens-1

Acknowledgements:

I would like to thank Dr Jun Yu for his guidance and help with this research project. I would like to thank Dr Veronique Seidel for her advice and help with this research project, particularly with propolin D purification. I would like to thank Dr Christine Dufes for her advice with the research project. I would like to thank Dr Gareth Westrop for his help with the enzymatic kinetic assay. I would like to thank the academic staff of the Strathclyde Institute of Pharmacy and Biomedical Science. I would like to thank my family and friends for their support and help.

Abstract:

Many Gram-negative bacterial pathogens such as *Shigella* and adhesive invasive *Escherichia coli* (AIEC) cause infections characteristic of hyperinflammation. These infections require antimicrobial therapy. However, due to the widespread emergence of multiple drug-resistant strains, alternative strategies must be sought to combating infectious diseases. It has been shown that natural compounds such as propolin D are able to control *Shigella* growth inside host cells. Geraniol is another natural product which has a chemical structure similar to the side chain of propolin D, which possesses properties potentially useful for antimicrobial therapy. qPCR analysis revealed that propolin D caused extensive bacterial envelopE stress, as indicated by a changed expression of key bacterial genes involved in stress responses. Propolin D also enhanced the autophagy activity of the host cells; the intracellular growth of *S. sonnei* was significantly reduced in wild type HEK293 cells but not changed in *ATG5* knockout cells. Propolin D was unable to enhance septin cage as intracellular *S. sonnei* formed actin tails in the presence of propolin D; septin cage would restrict formation of actin tails. Geraniol has been shown to target the major virulence regulator, DsbA, which is vital for *Shigella's* survival in the reducing host cell cytosol. Geraniol and geranyl

acetate inhibited DsbA function *in vitro*; wild type DsbA efficiently reduced fluorescently labelled Di-E-GSSG whereas a mutant protein, DsbA33G, was less potent in this *in vitro* assay. By supplementing acidic and nutrient-poor medium with geraniol the growth of *S. sonnei* and AIEC strains was severely inhibited. Geraniol was effective in protecting of *Galleria. mellonella* larva from *S. sonnei* and AIEC infection. The *Galleria mellonella* larvae were highly tolerant to geraniol – indicating the great potential of geraniol for future *in vivo* and clinical studies. In light of previous reports that geraniol synergistically works with antibiotics and induces IL-10 from macrophages, it was concluded that geraniol holds great potential in treating *Shigella* and AIEC infections.

Chapter 1: Introduction

Bacillary dysentery (shigellosis) predominantly occurs in children and the elderly, resulting in high levels of morbidity and mortality. It is estimated that approximately 165 million shigellosis episodes occur worldwide per year, mostly in developing countries (Peirano *et al.,* 2005). This infectious disease results in or contributes to the death of approximately 1.1 million people each year. Bacillary dysentery is characterised by hyperinflammation in the epithelium of the colon and rectum. The clinical manifestations include bloody diarrhoea, nausea, vomiting and severe abdominal pain. The aetiologic agent of the disease is *Shigella*, which is transmitted mainly through the faecal-oral route via contaminated food or water. *Shigella* is an adapted human pathogen (Peirano *et al.,* 2005). The most severe form of the disease is associated with life-threatening complications due to the Shiga toxin. As an intracellular pathogen, *Shigella* damages the colorectum by invading many types of cells in the gut, including epithelial cells (EC) and macrophages. This invasion is a multistep process involving bacterial adhesion to the cell surface, entry by induced phagocytosis, membrane lysis of the phagocytic vacuole, actin polymerisation and intra- and inter-cellular

dissemination (Allaoui *et al.,* 1992). Treatment and prevention of dysentery are challenging due to widespread resistant strains and lack of effective vaccines (Mani *et al.,* 2016).

Crohn's disease (CD) is another hyperinflammatory disease. Clinical manifestations of CD begin in adulthood and then persist throughout life, with the disease resulting in decreased quality of life and increased disability (Cosnes *et al.,* 2011). Studies have been conducted in different regions to determine the incidence and prevalence of CD (Molodecky *et al.,* 2012). The incidence rates of CD are on the rise worldwide. In countries such as Japan, the incidence doubled (12 million people per year) between 1986 and 1998 (Economou *et al.,* 2009). Studies showed that the annual CD incidence from 1930 to 2008 was 127 million people per year in Europe, 5.0/100,000 persons/year in Asia and the Middle East, and 202 million people per year in North America (Molodecky *et al.,* 2012). One study showed a moderate increase in the period 1991-1995 (50 million people per year) in Germany (Economou *et al.,* 2009). Prevalence ranges are between 26 and 198 cases per 100,000 in populations in North America. The incidence and prevalence of CD have risen over time and the disease

has emerged as a threat to public health around the word (Molodecky *et al.,* 2012). Changes in lifestyle have played a critical role in the rising incidence of the disease at the regional and international level. Moreover, differences in genetic profile may play a role in CD development, as may environmental factors (Molodecky & Kaplan, 2010). Importantly, it has become evident that adhesive invasive *Escherichia coli* (AIEC) infection is a key contributing factor to CD (Eaves-Pyles *et al.,* 2008). Treatment of AIEC is therefore considered an important strategy in the treatment of CD but faces similar challenges from drug-resistant AIEC strains (Dogan *et al.,* 2013).

1.1 Dysentery and Crohn's disease; molecular pathogenesis:

Shigella bacteria are Gram-negative, non-motile, non-spore forming, rod-shaped bacteria that were discovered by Japanese microbiologist Kiyoshi Shiga at the end of the 19th century. *Shigella* includes various strains/serotypes derived from non-pathogenic *Escherichia coli* of diverse origins (Johannes & Romer, 2010). *Shigella* is traditionally divided into four groups: *Shigella dysenteriae* (A; 16 serogroups), *Shigella flexneri* (B, 6 serogroups), *Shigella boydii* (C, 19 serogroups), *Shigella sonnei* (D, 1 serogroup) (Schroeder & Hilbi, 2008). Enteroinvasive *Escherichia coli* (EIEC) are other

E. coli strains that possess similar pathogenic properties that also cause shigellosis. The first primary step in *Shigella* infection is the invasion of and proliferation within the intestinal epithelium and underlying mucosal macrophages of the colorectum, which triggers inflammatory responses. Virulent *Shigella* strains possess a virulence plasmid that encodes many virulence determinants, of which the type III secretion system (T3SS) delivers effector proteins into host cells to initiate invasion (Skoudy *et al.,* 2000).

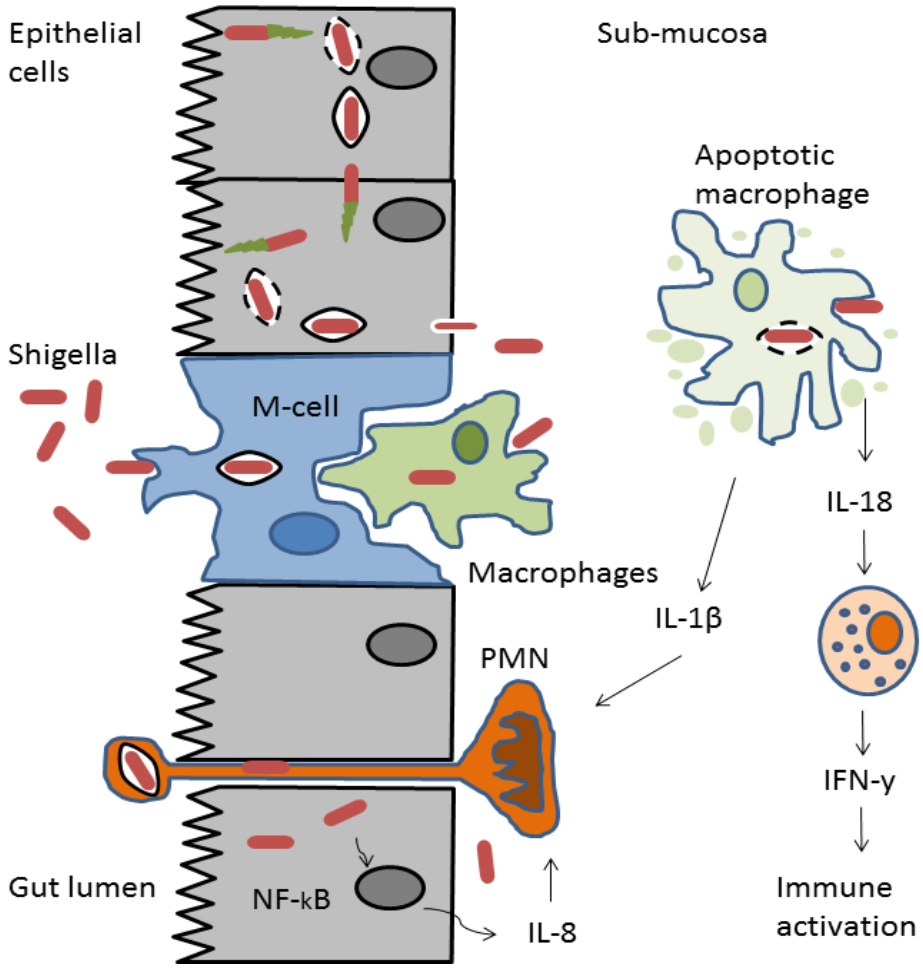

Figure 1: Pathogenesis of *Shigella* spp (adapted from (Schroeder & Hilbi, 2008).

The main step of *Shigella* pathogenesis is the invasion of the intestinal epithelium following transmission through the faecal-oral route and ingestion of contaminated food or water. One hundred microorganisms of *Shigella* are sufficient to cause dysentery, and this low infectious dose compensates for the low tolerance of the bacteria to the acidic environment of the stomach (Schroeder & Hilbi, 2008). *Shigella* reaches the large intestine after passing through the stomach and small intestine. *Shigella* gains access through to the epithelial barrier from the apical side initially via microfold cells (M cells) of the follicle-associated epithelium (FAE) or colonic crypts (Schroeder & Hilbi, 2008). M cells are specialised ECs found in mucosa-associated lymphoid tissues (MALT), and play a critical role in the intestinal immune system (Man *et al.,* 2004). M cells are present in the FAE (~5-10% cells) overlaying the Peyer's patches (PP) of the ileum and lymphoid follicles of the colon. M cells are also located outside the FAE in tissues overlying gut-associated lymphoid tissues (GALT) (Man *et al.,* 2004). Moreover, M cells are also found in the upper respiratory tract within the nasal-associated lymphoid tissue (NALT) (Man *et al.,* 2004). M cells play an important role in protective immune responses against bacterial pathogens such as *Shigella*. For example, M cells

have a role in the induction of specific mucosal immune responses in the Peyer's patches (Man *et al.,* 2004).

After transcytosis via M cells, *Shigella* encounters resident macrophages, which are responsible for engulfing and degrading invading microorganisms. However, virulent *Shigella* actively invades macrophages, escaping from phagosomes and triggering apoptosis, and is then released from apoptotic macrophage into the extracellular milieu. In contrast, plasmid-cured or *ipaB* deletion strains are unable to trigger macrophage invasion and subsequent apoptosis (Lai *et al.,* 2015). The T3SS constituents, IpaB and IpaC, form a translocon on the host cell membrane, enabling translocation of many effector proteins into host cells to initiate cell invasion. *Shigella* T3SS is also responsible for the escape of the bacteria to the cell cytosol (Suzuki *et al.,* 2007). Known as IL-1 converting enzyme, *Shigella* IpaB colocalises with and activates caspase-1 (casp-1), which is associated with the host cell membrane in the macrophage cytoplasm. Casp-1 activation leads to the apoptosis of macrophages and secretion of interleukin (IL-1β) and IL-18 from apoptotic cells, which results in the recruitment of polymorphonuclear leukocytes (PMNs) to the site of infection. PMN

recruitment leads to the release of a cascade of inflammatory of cytokines and the engulfing and killing of bacteria (Schroeder & Hilbi, 2008). IL-1β and IL-18 cytokines mediate acute and massive inflammatory responses: IL-1β signalling lead to the recruitment of neutrophils, leading to hyperinflammation, while IL-18 activates natural killer (NK) cells, which produce gamma interferon (IFN-γ) (Schroeder & Hilbi, 2008). IFN-γ plays an important role in the innate resistance to *Shigella* infection through the activation of macrophages, which prevents *Shigella*-triggered cell death and also destroys the bacteria (Schroeder & Hilbi, 2008).

Shigella attaches to the host cell surface via multivalent adhesion molecule (MAM) protein (Mahmoud *et al.,* 2016). Certain strains lacking MAM deploy a surface protein, IcsA, whose primary role is the polymerisation of actin, which allows attachment of the host cell surface (Brotcke *et al.,* 2014). Thereafter, *Shigella* initiates cell invasion by injecting effector proteins into the host cell cytosol (Alonso & Garcia-del Portillo, 2004). These effector proteins target host regulatory proteins in order to highjack host-signalling cascades. These cascades regulate cytoskeleton dynamics and the release of immunomodulatory molecules which control host cell survival/death (Alonso &

Garcia-del Portillo, 2004). Both host β1/α5 integrins and CD44 (hyaluronic acid receptor) act as receptors for *Shigella* invasion. These two surface molecules interact with *Shigella* IpaB and IpaC, thereby triggering intracellular signalling cascades (Alonso & Garcia-del Portillo, 2004). Intracellular *Shigella* replication causes an inflammatory response that destroys the human colonic epithelium, a process that involves IpaA, IpaB, IpaC, IpgB1, IpgD and VirA. IpaA is secreted upon contact with cell surface and binds to the focal adhesion protein vinculin (Bourdet-Sicard *et al.,* 1999). IpaB also binds to CD44, stimulating cell signalling, which promotes the accumulation of cellular proto-oncogene tyrosine-protein kinase (c-Src), the phosphorylation of cortactin, and the stimulation of oncogene cytoplasmic regulatory protein (Crk). IpaC nucleates host actin when inserted into the host cell plasma (Ogawa & Sasakawa, 2006). Once *Shigella* enters the cytoplasm, IcsA (also known as VirG), expressed at the old pole of the outer membrane, polymerises host cell actin, which leads to the formation of actin tails behind the bacteria. The actin tails propel *Shigella*, advancing its intra- and inter-cellular spread and thus its survival (Steinhauer *et al.,* 1999). IcsB binds to IcsA, which supports evasion of autophagy essential for intracellular survival (Kayath *et al.,* 2010).

Actin-based motility is exploited by several intracellular bacterial pathogens that have the ability to enter the host cytoplasm. Cells require actin polymerisation, which determines the shape, stiffness and movement of the cell surface. The actin cytoskeleton facilitates the transduction of mechanical signals. Many cellular functions, including cell motility, muscle contraction, cell division, cytokinesis, vesicle and organelle movement, and cell signalling, require intracellular forces that are generated by the actin cytoskeleton (Doherty & McMahon, 2008). *Shigella flexneri* and *Listeria monocytogenes* are intracellular pathogens that have the ability to exhibit intracellular actin-based motility. These pathogens exploit a host protein complex called the actin-related protein 2/3 complex (Arp2/3), which is used by host cells to nucleate actin filaments (Pantaloni *et al.,* 2001). Actin-related proteins (Arps) Arp2 and Arp3 of the Arp 2/3 complex are structurally similar to conventional actin. The end of each Arp provides a dock for polymerisation but has no actin nucleation activity. Wiskott-Aldrich syndrome proteins (WASP) possess nucleation-promoting factors (NPFs) that activate actin nucleation through the Arp 2/3 complex (Gouin *et al.,* 2005). NPFs contain several conserved domains, including the C-terminal WASP homology 2 (W) and C-

terminal central and acidic regions (CA), which are required for binding actin monomers and binding to the Arp2/3 complex, respectively. *Listeria monocytogenes* ActA mimics WASP family NPFs, while *S. flexneri* IcsA recruits host family WASP proteins (Teh & Morona, 2013), thus representing two strategies for Arp2/3 complex activation by intracellular pathogens (Gouin *et al.,* 2005).

Shigella uses actin-based motility at rates of 10-15 μm/min following escape from the internalisation vacuole (Heindl *et al.,* 2010). Intracellular *Shigella* can move through the cytoplasm of host cells into adjacent cells through actin polymerisation in a structure called a protrusion. *Shigella* protein IcsA is the protein responsible for this function. IcsA is a type VI autotransporter and is thus able to mediate its own translocation across the outer membrane (Gouin *et al.,* 2005). The level of IcsA expression and activity of IcsP (IcsA specific outer membrane serine protease) are addition factors that determine the level and location of IcsA presentation on the bacterial surface (Magdalena & Goldberg, 2002). The efficiency of the actin tail is dependent on the amount of IcsA α domain exposed on the bacterial old pole (Wing *et al.,* 2004).

Polymerisation of actin allows *Shigella* to spread to adjacent ECs, which elicits a strong inflammatory response. After spreading to adjacent ECs via the protrusion, *Shigella* releases bacterial peptidoglycan fragments, which are sensed by the nucleotide-binding oligomerization domain-containing protein 1 (Nod1)-mediated intracellular surveillance system (Schroeder & Hilbi, 2008). This activates nuclear factor kappa (NF-kB), triggering the up-regulation and secretion of the chemokine IL-8 (Fig 1), which mediates the recruitment of large numbers of PMNs to the site of infection. Production of pro-inflammatory chemokines and cytokines such as IL-8, IL-1β, IL-6 and TNF-α is caused by *Shigella* invasion (Ogawa & Sasakawa, 2006). PMN migration results in damage to the integrity of the epithelial lining, which allows further luminal bacteria to reach the submucosa. ECs tight junctions are weakened by PMNs, which alter tight-junction protein composition. Bacterial infection is exacerbated by the destruction of the epithelial layer, macrophage killing and the massive influx of PMNs. All these steps are necessary for the development of diarrhoea (Schroeder & Hilbi, 2008).

A recent study used a bioimage analysis tool to quantitatively measure pathogenicity and investigate *S. flexneri* invasion in a guinea pig model (Arena *et al.,* 2015). The

primary finding of this study was that *S. flexneri* targets crypts for entry into the colonic mucosa (Arena *et al.,* 2015). Arena *et al.,* 2015 found that *Shigella* was consistently associated with crypts which were seen within whole-mount preparation of infected guinea pig colonic tissue. The study also measured the distance of *Shigella* positions in relation to the crypt mouth at early time points, and they found that the majority were found within 13.6 ± 15.6 μm of the crypt (Arena *et al.,* 2015). This study may change our hypothesis as illustrated in Fig. 1. In other words, translocation via M cell may not necessarily be the main route for *Shigella* invasion. however, it should be noted that *Shigella* showed a significantly greater relative translocation (8.6 ± 1.6 fold increase) through M cells than enterocytes (Roberts *et al.,* 2010). *Shigella* utilising Ca^{2+} jagged edge signals during the invasion of epithelial cells is likely the mechanism of the crypt epithelial cells entry. It has been found that *Shigella* induces a typical Ca^{2+} response at entry sites, which allow local cytoskeletal remodelling for bacteria engulfment (Bonnet & Tran Van Nhieu, 2016). The local and global Ca^{2+} responses depend on an inositol-1,4,5-triphophate (InsP3) signal. Response association with trespassing pathogens (RATP) is some of local Ca^{2+} responses induced by *Shigella*. This RATP involves phospholipase C (PLC)-β1 and δ1 activated at *Shigella* entry sites, which lead to the

accumulation of InsP3. The opening of the InsP3 receptor and Ca^{2+} release is triggered by an increase in InsP3 levels. The Ca^{2+} chelator BAPTA and transfection of InsP3-5 phosphate inhibited local Ca^{2+} response, impairing *Shigella* induced actin foci formation. This indicates that they likely participate in the invasion process. Calpain activation by cytosolic Ca^{2+} increased participation in the cytoskeleton reorganisation essential for bacterial entry is another implication of local Ca^{2+} response. Calpain targets components regulating cytoskeleton reorganisation such as Src tyrosine kinase and cortactin, which are known also to be implicated in *Shigella* invasion. A Ca^{2+} dependent motor protein myosin II has also been implicated in *Salmonella* invasion into the host cell, and it is also seen to be recruited in *Shigella* entry foci. *Shigella* elicits a global Ca^{2+} response with slow dynamic after a local Ca^{2+} response. These responses amplify *Shigella* entry through the release of ATP in the extracellular milieu via hexameric connexin (Cx) hemichannels. Cellular function in an autocrine or paracrine manner such as ca^{2+} signalling is stimulated by secreted ATP. Global increase Ca^{2+} in the cell triggers the opening of connexion hemichannels at the plasma membrane, and this favours *Shigella* invasion and spreading through purinergic receptor signals (Bonnet & Tran Van Nhieu, 2016).

Crohn's disease (CD) is an inflammatory bowel disease (IBD), the cause of which is multifactorial and includes genetic, immune-related, environmental and infectious factors (Molodecky & Kaplan, 2010). Next-generation sequencing techniques have identified alterations of the gut microbiota composition in IBD. Dysbiosis is the shift in the balance of the gut microbiota. The gut microbiota is composed of four major phyla: the Firmicutes (49-76%) and Bacteroidetes (16-23%), followed to a lesser extent by the Proteobacteria and Actinobacteria. It has been observed that altered composition of gut microbiota in IBD patients involves a reduction in Firmicutes and an increase in Proteobacteria (Matsuoka & Kanai, 2015). A recent study found that the Firmicute, Faecalibacterium *prausnitzii* is in lower abundance, while Enterobacteriaceae, such as mucosa-associated *E. coli*, is higher in Crohn's disease (Wright *et al.,* 2015). Darfeuille-Michaud *et al*. (1998) reported a group of adhesive invasive *Escherichia coli* (AIEC) that were involved in early and chronic ileal lesions of CD patients. One of the AIEC strains isolated from an ileal biopsy of a patient with CD was LF82, which is a true invasive pathogen (Boudeau *et al*., 1999; see below). Infection by AIEC is one of

the important contributing factors of CD. AIEC infection contributes to the acute and chronic mucosal inflammation in patients with CD. Darfeuille-Michaud *et al*. (2004) demonstrated that AIEC strains were found in 21.7% of CD chronic lesions in ileal specimens, 36.4% of early CD lesions in neoterminal ileal specimens, and 22.2% of the healthy mucosa of CD patients. Similar muscosa-associated *E. coli* have been observed in the colon of CD patients (Martin *et al.,* 2004; Martinez-Medina *et al.,* 2009)

The pathogenesis of AIEC involves several steps: the ability of the pathogen to disrupt the integrity of EC, penetration of the epithelial monolayer, replication in the epithelium, dissemination and the induction of a chronic hyperinflammatory immune response (Wine *et al*., 2010). The first step in AIEC pathogenesis in the ileum is adhesion to the carcinoembryonic antigen-related cell adhesion molecules 6 (CEACAM6), which act as a receptor for AIEC in ECs (Barnich *et al*., 2007). Through CEACAM6, AIEC strain LF82 expresses type I pili, thereby adhering to the brush border of inflamed ileal enterocytes in CD patients. Gut inflammation results in of abnormally high intestinal expression of CEACAM6 in patients with CD (Carvalho *et al*., 2009). It has also been shown that the interaction between AIEC LF82 type 1 pili and CD ileal enterocytes

occurs via mannose residues of CEACAM6 expressed on the apical side of CD intestinal epithelium (Barnich *et al*., 2007). In the presence of 2% of D-mannose, AIEC strain LF82 is unable to adhere to the brush border of ileal enterocytes from CD patients. This suggests that adherence of AIEC strain LF82 via type 1 pili is a mechanism of entry of CD-associated AIEC strains (Barnich *et al*., 2007). Overexpression of CEACAM6 occurs as a result of stimulation by proinflammatory cytokines IFN-γ or TNFα, or infection of the epithelial by AIEC (Barnich *et al*., 2007). Colonic-mucosa associated *Escherichia coli* show increased abundance in CD, and they adhere to and invade epithelial cells, replicate within macrophages, as well as translocate across M cells (Prorok-Hamon *et al.,* 2014). Colonic mucosa-associated AIEC are able to adhere to and invade intestinal epithelial cells in the using afimbrial adhesion encoded by the *afa* operon. Replication within macrophages or translocation through M cells, was not conferred by the presence of *afa-1* operon (Prorok-Hamon *et al.,* 2014). In addition, colonic mucosa-associated *E. coli* harboured long polar fimbriae (LpfA) and can use this adhesin to target and translocate across M cells (Prorok-Hamon *et al.,* 2014), as per ileal AIEC (Chassaing *et al.,* 2011; Dogan *et al.,* 2014). Increased prevalence in CD of colonic mucosally associated AIEC isolate possessing

afa together with *lpfA* and *fimH* (Prorok-Hamon *et al.,* 2014). These colonic-mucosa associated AIEC also possesses the polyketide synthase gene complex (*pks*), which is responsible for producing the genotoxin colibactin, inducing inflammation-associated colorectal cancer in mice. Prorok-Hamon *et al.,* 2014 found that colonic mucosa associated diffusely adherent *afa* positive *E. coli* expressing *lpfA* and *pks* are increased in IBD. Long polar fimbriae (LPF) play essential roles as a key factor for AIEC that target PPs (Chassaing *et al.,* 2011). It has been found that the AIEC *ΔlpfA* mutant is impaired in its ability to translocate across M cell monolayers and to interact with murine M cells *in vivo* (Chassaing et al., 2011). In addition, AIEC harboring the *lpf* operon is higher in CD patients (Chassaing et al., 2011). It has been observed that mucosa associated AIEC, such as HM605, translocate across M cells while it could not readily cross epithelial cells (Roberts *et al.,* 2010). This suggested that mucosa associated AIEC HM605 invasion of the gut epithelium occurs mainly through M cells.

Activation of the innate immune response through Toll-like receptor 4 and 5 (TLR) in macrophages is mediated by LPS and flagellin, respectively (Sasaki *et al*., 2007). This activation results in upregulation of TNFα, which attracts macrophages to the site of

inflammation in order to eliminate AIEC. AIEC LF82 strain replicates and survives within macrophages and induces the formation of a spacious phagosome, which persists within phagocytic cells for a long period. Colonic mucosal AIEC strains are able to replicate inside macrophages compared to *E. coli* K-12 (Subramanian *et al.,* 2008). Colonic mucosal AIEC HM605 is one of the colonic mucosal strains which are able to replicate within macrophages vacuoles ((Mpofu *et al.,* 2007; Subramanian *et al.,* 2008). Colonic AIEC are able to survive within macrophages in the presence of *Saccharomyces cerevisiae* mannan (Mpofu *et al.,* 2007). AIEC HM605 is able to survival within monocytes from 24% ± 10.5% in the absence of *S. cerevisiae* mannan, will increase to 114% ± 22.7% survival in the presence of mannan (Mpofu *et al.,* 2007). AIEC HM427, HM670, HM580 and HM95 were also shown to survive with monocytes in this study. This showed microbial mannan inhibits bacterial killing by macrophages. Colonic AIEC isolate persistence in macrophages, also likely involves factors such as high temperature requirement A protein and DsbA (Tawfik *et al.,* 2014; Prorok-Hamon *et al.,* 2014). Macrophages infected with AIEC LF82 release high levels of TNFα cytokines (Glasser *et al*., 2001). In contrast to *Shigella* infection, AIEC LF82 does not induce secretion of IL-1β from macrophages (Glasser *et al*., 2001).

AIEC strains also induce high expression of inflammatory cytokine IL-8 from epithelial cells. Pathogenicity features of AIEC include the regulation of cytokine expression, including the up-regulation of TNFα (Sasaki *et al*., 2007). AIEC also results in the dissociation of F-actin, zonula occludens-1 (ZO-1) and E-cadherin from the apical junctional complex (AJC), resulting in decreased epithelial barrier function (Sasaki *et al*., 2007). AIEC LF82 induces differential secretion of proinflammatory cytokine IL-8 and CCL20 from polarised intestinal ECs. This induction of proinflammation cytokines by AIEC contributes to the chronic inflammation detected in CD (Eaves-Pyles *et al*., 2008). AIEC colonises CD ileal lesions and produces outer membrane vesicles (OMVs) which contribute to the bacterial invasion process. Flagella isolated from colonic mucosa-associated AIEC HM427 is also able to cause significant proinflammatory cytokine IL-8 release (Subramanian *et al.,* 2008). Flagellae has been observed associated with OMVs, with flagellin being a major stimulant for the IL-8 response to the bacteria (Subramanian *et al.,* 2008 b). OMVs can deliver bacterial effectors, vesicle components and virulence factors to host cells. OmpA, a multifaceted protein located

on the surface of OMVs, has multiple roles in adhesion, invasion and persistence of intracellular bacteria (Rolhion *et al*., 2010). Gp96, an endoplasmic reticulum (ER) associated stress response protein which is expressed in patients with CD, acts as the host receptor for OmpA present in OMVs, and assists in the adhesion and invasion of a *ΔompA* mutant strain. Overexpression of gp96 on the apical surface of ileal EC in CD patients promotes invasion by AIEC (Rolhion *et al*., 2010). AIEC bacteria are able to replicate in ECs. It has been found that AIEC are present in membrane-bound compartments after infection (Wine *et al*., 2010). Lysosomal-associated membrane protein 1 (LAMP1) is a late endosomal marker that co-localises with AIEC, suggesting that AIEC is directed to the endosomal pathway (Wine *et al*., 2010).

It has been shown that AIEC LF82 strain prevents IFN-γ induced tyrosine phosphorylation of signal transducer and activator of transcription proteins (STAT) (Ossa *et al*., 2013). These STAT proteins are transcription factors that are important in mediating cytokine signalling. It has also been found that the activation of interferon-related factor (IRF-1) is blocked by inhibition of STAT tyrosine phosphorylation by AIEC strain LF82 (Ossa *et al*., 2013). STAT proteins become activated through interaction

with tyrosine phosphorylation cytokine receptor Janus-associated kinases (JAKs) (Bromberg & Darnell, 2000). The secretion of bacterial factors such as heat factor, sensitivity to proteinase-K, and growth sensitivity in apical and basolateral infections causes inactivation of the IFN$_{\Upsilon}$/JAKs/STAT1 signalling in epithelial and immune cells, which promotes AIEC survival and contributes to acute and chronic inflammation in CD (Ossa *et al.*, 2013). AIEC adheres to and invades intestinal ECs and then replicates in mature phagolysosomes within macrophages; LF82 strain of AIEC survives within macrophages (Darfeuille-Michaud *et al.*, 2004). The survival and replication in large vacuoles within macrophage is the hallmark of these CD-associated AIEC strains. Aphthous ulcers of the mucosa, mural abscesses, macrophage and epithelioid cell granuloma are key characteristic pathological elements of CD (Bringer *et al.*, 2007). A recent study used confocal laser endomicroscopy and conventional histopathology to characterise lymphoid follicles (LFs), highlighting 'red rings' as the first manifestation of early CD lesions (Krauss *et al.,* 2012). LFs with red ring sign (RRS) progressed to early aphthous ulcers as seen by follow up endoscopy, which showed in patients with the first manifestation of CD (Krauss *et al.,* 2012).

The innate immune response to invading bacteria and development of CD is linked to mutations of *NOD2* [also called caspase activation and recruitment domain 15 (*CARD15*)] in CD patients (Darfeuille-Michaud *et al*., 2004). These mutations result in impaired immune responses required to destroy invading bacteria. Two studies demonstrate that *NOD2* mutations contribute to CD pathogenesis: NOD2 provides critical host anti-bacterial defence and pro-inflammatory responses, and acts to regulate innate immune responses (Boyapati *et al*., 2015). *NOD2* encodes a cytosolic pattern recognition receptor (PRR), which detects peptidoglycan from intracellular bacteria. NOD2 is expressed in intestinal epithelial cells and monocyte-derived immune cells. Defective NOD2 function affects cellular activities, including microbial sensing, epithelial cell function, anti-microbial peptide (AMP) production, antigen presentation, intracellular bacteria killing and innate immune signalling such as TLR function (Boyapati *et al*., 2015). NOD2 recognises peptidoglycan product muramyl dipeptide (MDP), which triggers autophagy. This leads to controlled antigen presentation and bacterial replication, while MDP acts on dendritic cells in connection with TLR ligands (Khor *et al*., 2011). *NOD2* mutations result in immune tolerance. Patients with CD-associated *NOD2* mutations do not respond to MDP stimulation. NOD2 effects MDP-

independent pathways such as type 1 IFN response to single-stranded RNA (ssRNA) stimulation, and regulation of T-cell response. NOD-like receptors (NLRs) and RIG-I like receptors (RLRs) are two innate immune receptors which also regulate intestinal inflammation and immunity. NLRs and RLRs recognise pathogen-associated molecular patterns. Tight regulation of these pathways is essential for intestinal homoeostasis. Over-activation of NLRs causes detrimental effects due to mutations in *NOD2* and *NLRP3*, which in turn results in Blau syndrome and cryopyrinopathies, respectively (Khor *et al*., 2011). Another gene associated with CD is *CARD9*, which encodes a CD-adaptor protein. Signals from many innate immune receptors are integrated by CARD9 protein, which is important for recognition of viral, bacterial and fungal motifs (Khor *et al*., 2011). NF-kB factor is implicated in CD; its activation by CARD9 and dectin-2 enhances the production of TH17-class of cytokines such as IL-1β and IL-23. Defective CARD9 function renders patients susceptable to mucocutaneous candidiasis. Diverse signalling is integrated by both CARD9 and NOD2. A deficiency of CARD9 and NOD2 would constitute a predisposition to CD (Khor *et al*., 2011).

Following CARD9 and NOD2, defects in the autophagy genes *ATG16L1*, *IRGM* and *LRRK2* have been associated with CD pathogenesis (Boyapati *et al*., 2015). Autophagy is a conserved process in all mammalian cells and is required for intracellular homoeostasis by removing intracellular microbes and contributing to the degradation of cytosolic contents and organelles. Increased risk of CD is associated with mutation of *ATG16L1,* as ATG16L1 plays an important role in triggering all forms of autophagy. ATG16L1 forms complex with ATG12-ATG5, which defines the site of microtubule-associated protein 1 light chain 3 (LC3)-PE conjugation during autophagosome formation (Boyapati *et al*., 2015). Mutation of *ATG16L1* results in diminished autophagy. It has been shown that there are links between *ATG16L1* and *NOD2* in defining disease association pathways. NOD2 induces autophagy via receptor-interacting serine/threonine-protein kinase 2 (RIRK2), ATG5, ATG7 and ATG16L1 in dendritic cells (DCs). This generates major histocompatibility complex (MHC) class II for antigen-specific $CD4^+$ T-cell responses in DCs (Boyapati *et al*., 2015). Defects in autophagy have been shown in epithelial and dendritic cells containing CD-associated *ATG16L1* and *NOD2* mutants (Khor *et al*., 2011). Dysentery and CD share predisposing host genes *NOD2* and *ATG16L1*, as they are necessary

for sensing bacteria. The association between CD and *ATG16L1* assists autophagy in the pathogenesis of CD (Prescott *et al.*, 2007). Mutation of *NOD2* prevents recruitment of ATG16L1 to the plasma membrane, which results in the destruction of invading bacteria by autophagosome (Travassos *et al.*, 2010). These results show that communication with the immune system and intracellular processes are affected by the relationship between NOD2, ATG16L1 and autophagy (Khor *et al.*, 2011).

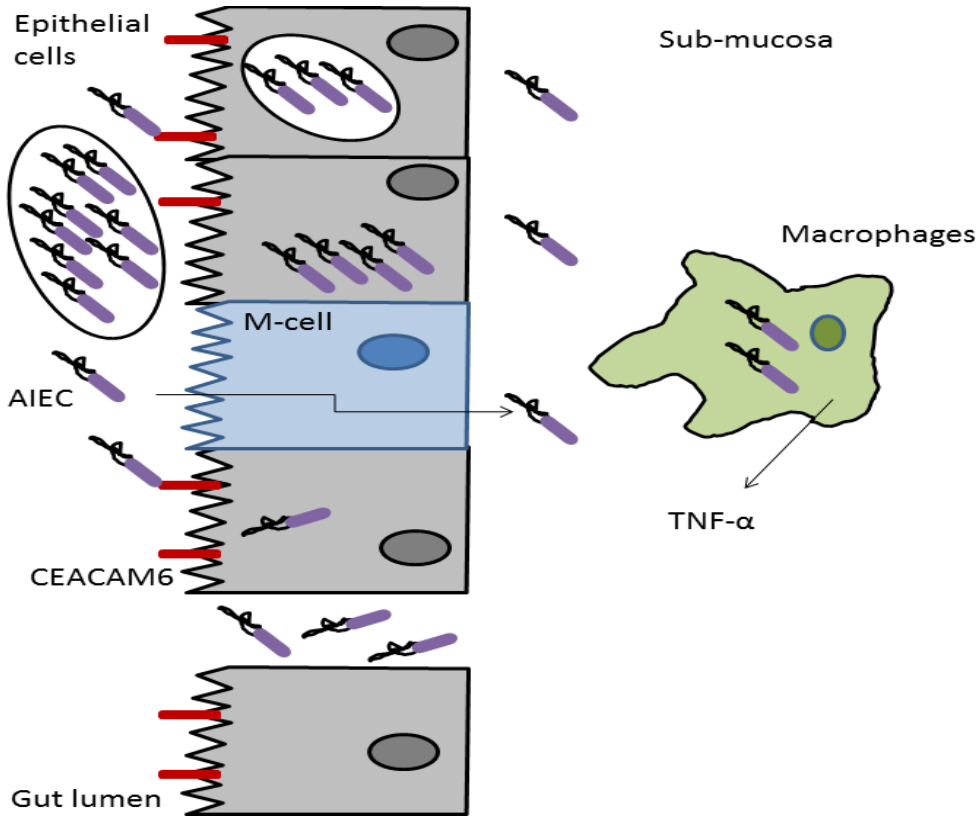

Figure 2: Contribution of AIEC to CD pathogenesis (Martinez-Medina & Garcia-Gil, 2014). The purple rod represents AIEC. CEACAM6 receptors on epithelial cells are coloured in red. Black circle represent biofilm.

1.2 The cell cytosol is a highly reducing niche:

Shigella escapes into the host cell cytosol by lysing the membrane–bound vacuole after invasion of epithelial cells (Torres, 2004). The host cell cytosol is a highly reducing environment due to the presence of high levels (~10 mM) of reduced glutathione (GSH), which is the result of the activity of glutathione reductase (GR). This enzyme reduces oxidised glutathione disulphide (GSSG) to the sulfhydryl form GSH (Carlberg & Mannervik, 1985).

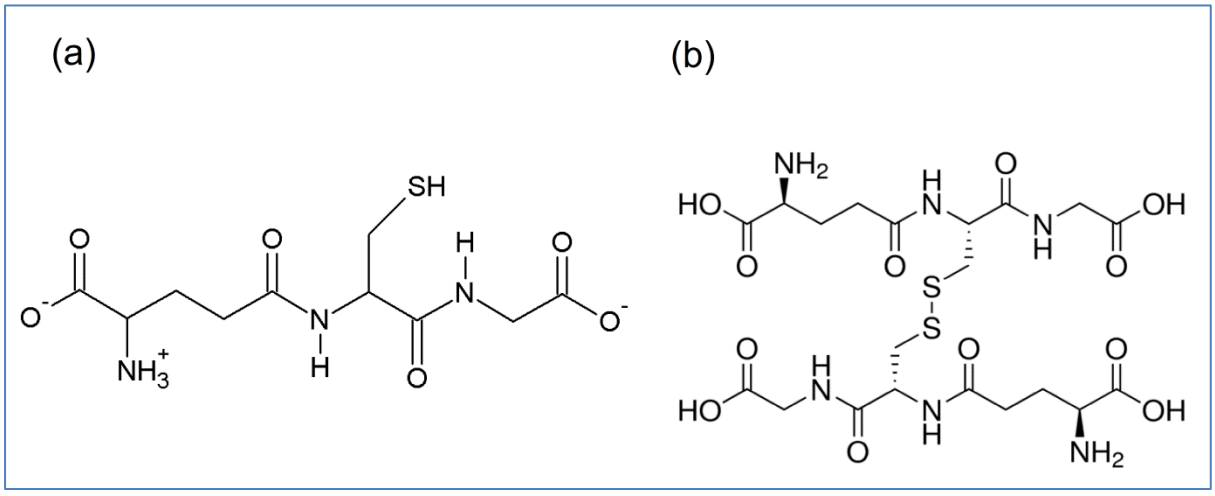

Figure 3: Structures of (a) reduced (GSH) and (b) oxidised (GSSG) glutathione.

GSH is a tripeptide compound synthesised in the cell cytosol which has many functions in the cell, including anti-oxidant defence, regulation of the cell cycle and gene expression (Dickinson & Forman, 2002). GSH also plays a role as a mediator of many

physiological reactions, including the metabolism of xenobiotics, thiol disulphide exchange reaction and cellular signalling (Mari *et al.*, 2009). GSH consists of three amino acids, glutamate, cysteine and glycine, which are linked by γ peptide linkage between the carboxyl (-COOH) group of glutamate and the amine ($-NH_2$) group of cysteine, and α peptide linkage between the cysteine and glycine units (Fig. 3). GSH is an anti-oxidant which prevents damage to important cellular components caused by reactive oxygen species (ROS). Glutathione exists in either reduced (GSH) or oxidised (GSSG) forms. GSH reduces disulphide bonds by donating an electron to form GSSG (Appenzeller-Herzog, 2011).

1.3 DsbA as the major virulence regulator:

Disulphide bond formation is a key step in protein folding, which is necessary for secreted proteins to gain biological function. Protein misfolding can be the result of failure in disulphide formation, which leads to aggregation and degradation. Disulphide bond proteins (Dsb) localised in the periplasm catalyse disulphide bond formation in Gram-negative bacteria (Lasica & Jagusztyn-Krynicka, 2007). Gram-negative bacteria contain a set of Dsb periplasmic redox proteins, including DsbA, DsbB, DsbC DsbD,

DsbE and others, which are involved in disulphide bond exchange and balancing of the redox potential. Each protein possesses an active site with conserved residues Cys-X-X-Cys (Lasica & Jagusztyn-Krynicka, 2007). A key protein in the catalysis of disulphide bond formation in Gram-negative bacteria is DsbA, which is a periplasmic disulphide oxidoreductase required for disulphide bond formation in certain proteins such as alkaline phosphatase PhoA (PhoA) and outer membrane protein A (OmpA). The formation of disulphide bonds in Gram-negative bacteria such as *E. coli* can be divided into two steps: the oxidation of cysteine residues to form a disulphide (DsbA and DsbB), and the isomerisation of incorrect disulphide bond to the correct form (DsbC, DsbG and DsbD). Two electrons are donated to or taken away from the cysteine pair in the formation and breakage of a disulphide bond, respectively (Lasica & Jagusztyn-Krynicka, 2007). The oxidation and reduction reactions are associated with NADPH and the quinine electron transfer chain.

Mutations in *dsb* genes have a diverse influence on Gram-negative bacteria, including loss of stability and function of disulphide bridges, which attenuates bacterial virulence. It has been shown that Dsb proteins have roles in biogenesis of flagella, adhesion

fimbriae, secretion machineries and influence secreted virulence factors and bacterial virulence (Lasica & Jagusztyn-Krynicka, 2007). Heras *et al*. (2009) demonstrated that Dsb proteins contribute to the virulence properties of the bacterial pathogen, and that mutations in *dsbA* affect different stages of the infection process, including adhesion, host cell manipulation and cellular spread. Fimbriae and pili of Gram-negative bacteria mediate adhesion process. Fimbrial biogenesis and function require the correct folding of fimbrial subunits and assembly proteins in the bacterial periplasm (Heras *et al*., 2009). Assembly of P fimbrae (virulence factor) is inhibited by DsbA mutations in *E. coli* due to the inability of the periplasmic chaperone PapD to bind P fimbrial subunits. In addition, formation of the disulphide bond in P fimbrial adhesion requires DsbA. DsbA catalyses disulphide bond formation in the B subunit of the AB toxins, which is a critical step in the biogenesis of the cholera toxin of *Vibro. cholera*, pertussis toxin of *Bordetella. pertussis* and heat-labile enterotoxin of enterotoxigenic *E. coli* (Heras *et al*., 2009). Bacterial virulence requires motility for cellular spread and survival. DsbA has been shown to catalyse the formation of a disulphide bond between two cysteine residues of flagellar p-ring protein (FlgI), which assembles around the rod to form the L-ring. Subsequent integration of flagellin protein C (FliC), which polymerises to form

the filaments of bacterial flagella, is prevented by lack of correctly folded FlgI protein, which prevents cellular spread and survival of the bacterial pathogen (Heras *et al.*, 2009).

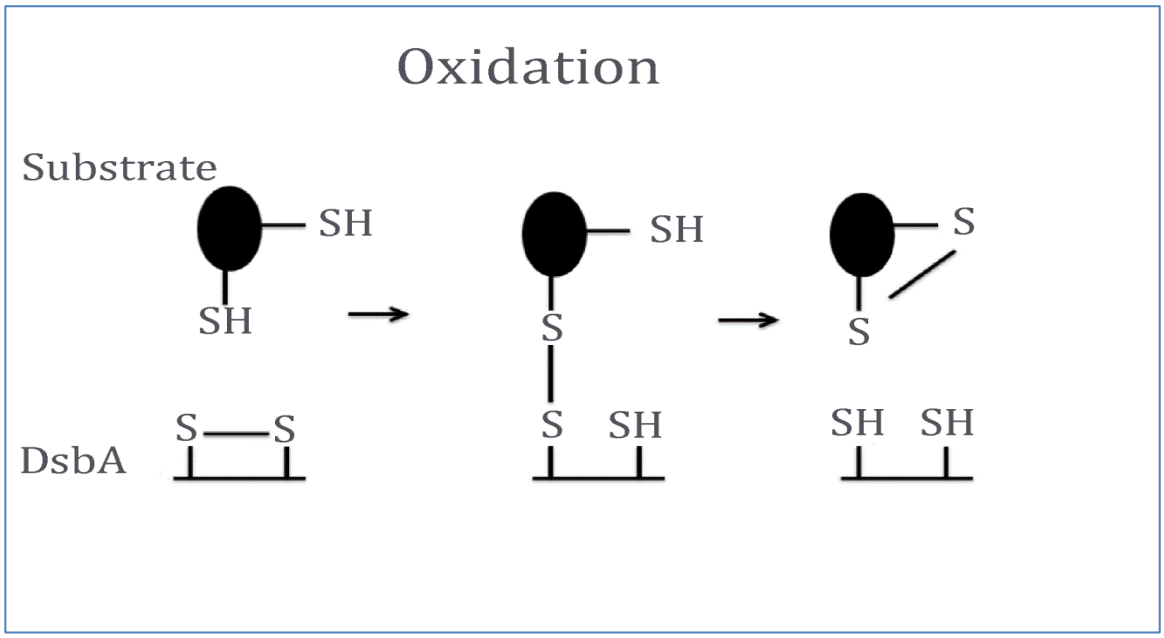

Figure 4. Putative mechanism of DsbA that catalyses the formation of disulphide bond in a substrate.

DsbA is also required for balancing the redox potential in the periplasm. In the host cell cytosol, reduced glutathione (GSH) with a molar weight of 307.32 g/mol penetrates the bacterial periplasm through the major porins in the outer membrane. DsbA is hypothesised to be the main component in reducing the redox potential produced by GSH, as shown in Fig. 3 and 4. DsbA has been shown previously to play an important

role in intracellular survival and virulence of *Shigella.* *Shigella dsbA* mutants are incapable of proliferating inside EC, and inactivation of *Shigella dsbA* reduced virulence in a guinea pig keratoconjunctivitis model (Sereny test negative) (Yu, 1998). DsbA has several important roles in *Shigella* pathogenesis: Intracellular *Shigella* survival depends on DsbA, while inactivation of DsbA reduces *Shigella* virulence, which was confirmed through using complementation in which *Shigella* virulence was restored by a pDsbA plasmid (Yu, 1998). This study found that the *dsbA* mutant can penetrate host cells, secretes Ipa proteins and retains the capacity for *icsA*-mediated movement. However, the *dsbA* mutant is defective in intracellular growth, suggesting that DsbA is important for intracellular *Shigella* survival and pathogenesis. In addition, the *dsbA* mutant is found trapped in double-membrane-bounded vacuoles, and appears to be lysed within the double membranes (Yu, 1998).

The *Shigella* virulence plasmid contains a 31-kb region that harbours three operons: *ipa* (invasion plasmid antigens), *mxi* (membrane expression of invasion plasmid antigens) and *spa* (surface presentation of invasion plasmid antigens). The *ipaBCD* genes in the *ipa* operon encode three invasins, IpaB, IpaC and IpaD, which play an

important role in epithelial cell invasion. These three proteins are secreted onto the bacteria surface, where they facilitate invasion. The transport of the three Ipa proteins across the inner and outer membranes requires the activation of genes from the *spa* and *mxi* operons, including *spa47, spaI3, spa32, spa33, spa24, spa9, spa29*, and *spa40* and *mxiHIJMEDA*. Spa32 is located in the outer membrane. The release of Ipa proteins is affected by the lack of disulphide bond formation in Spa32 in *Δspa32/19* and *Δspa32/292*, two mutants in which Cys-19 and Cys-292 were replaced by Ser residues, respectively (Watarai *et al*., 1995). The release of IpaB, C and D from *S. flexneri* is triggered by adhesion with host cells, and Spa32 plays a very important role in releasing Ipa proteins. *ΔdsbA*, *Δspa32/19* and *Δspa32/292* mutants showed a reduction in the release of Ipa proteins, suggesting that DsbA catalyses disulphide bond formation in Spa32, which is required for assembly of functional proteins (Watarai *et al*., 1995).

Studies have also shown that DsbA may be essential for AIEC bacteria to grow and survive in an acidic and nutrient-poor medium that partially mimics the harsh environment encountered by bacteria within the phagocytic vacuole (Bringer *et al*.,

2007). Bringer *et al*. (2007) studied *dsbA* to confirm that AIEC strain LF82 requires *dsbA* to adhere to intestinal epithelial and survive within macrophages. It has been found that *dsbA* transcription is highly upregulated under stress conditions. AIEC mutant LF82-*ΔdsbA* was unable to survive within macrophages. In addition, AIEC mutant LF82-*ΔdsbA* has a decreased ability to adhere to epithelial cells. Flagella and type 1 pili are not expressed by AIEC mutant LF82-*ΔdsbA* (Bringer *et al*., 2007). Thus, the loss of the ability of the *dsbA* mutant strain to adhere to EC is connected to the loss of type 1 pilus and flagellar expression. DsbA is therefore essential for the survival of LF82 bacteria in the host. In addition, growth and survival of AIEC LF82 bacteria in acidic and nutrient poor medium require DsbA (Bringer *et al*., 2007).

1.4 Autophagy as a defence mechanism against intracellular pathogens:

Autophagy is a conserved cellular process which is critical for cell death, cellular responses to starvation and innate immunity, including selective degradative removal of pathogenic bacteria (Luzio *et al*., 2007). Autophagy is also essential in the degradation of both intrinsic and estrogenic components by the lysosome. Intracellular bacteria are destroyed by autophagy pathways, and are engulfed in intracytosolic

membrane-bound vacuoles called autophagosomes (Xu & Elissa, 2010). Chaperone-mediated autophagy, microautophagy and macroautophagy are three autophagy pathways involved in the delivery of cytoplasmic constituents for degradation by the lysosome. In chaperone-mediated autophagy, the chaperone protein Hsc70 recognises cytoplasmic substrates before they are translocated into the lysosomal lumen for degradation. Microautophagy occurs when the lysosomal membrane engulfs small parts of the cytoplasm (Mizushima & Komatsu, 2011). Macroautophagy (autophagy) is a degradation process that involves autophagosome formation. Macroautophagy is an important mechanism for the degradation of cytoplasmic components involving lysosomal enzymes. The phagophore is an isolation membrane that isolates a small part of the cytoplasm. Isolation of the phagophore results in the formation of a double membrane structure, known as an autophagosome. The autophagosome fuses with the endosome before finally fusing with the lysosome. Lysosomal enzymes are used to degrade the inner membrane and to enclose cytoplasmic materials. Mitochondria (mitophagy), peroxisomes (pexophagy) and intracellular bacteria (xenophagy) are three additional specific types of macroautophagy that have recently been discovered. Macroautophagy is completed through the interaction of more than 30 autophagy-

related genes (*atg*). Proteins encoded by these genes are divided into subgroups: the Atg1/ULK1 protein-kinase complex, the Atg9 Atg2-Atg18 complex, the vesicular protein-sorting (Vps34)-Atg6/beclin1 class III phosphoinositide 3 kinase (PI3K) complex, the Atg12 conjugation system, and the Atg8/LC3 conjunction system (Tanida, 2011).

Atg1/ULK1 (UNC51-like kinases) complex is the first autophagy complex and is regulated by rapamycin complex 1 (TORC1) in a nutrient-dependent manner. TORC1 is one of the main regulators of autophagy induction (Burman & Ktistakis, 2000). Strong autophagy induction occurs following inactivation of TORC1 (Mizushima *et al.*, 2011). The Atg9 Atg2-Atg18 complex is activated during cell starvation, and is essential in the autophagy pathway (Tanida, 2011). The PI3K complex regulates autophagosome generation and degradation (Munz, 2011). The Vps34-Atg6/beclin1 PI3K complex is responsible for phosphatidylinositol 3-phosphate (PI3P) synthesis in the ER. Phosphoinositides (PIs) are created by the phosphorylation of phosphatidylinositol on the inositol ring structure. Three classes of PI3K enzymes are responsible for phosphorylating the 3' OH of PI. These enzymes are responsible for

production and synthesis of PI3P, which regulates the formation of omegasomes and isolation membranes. Omegasomes, shaped like the Greek letter omega (Ω), are formed from endoplasmic ER followed by the formation of an isolation membrane (Tanida, 2011). Double FVVE domain-containing protein 2 (DFCP1) as a PI3P-binding protein is localised to PI3P on the omegasome under starvation conditions. The DFCP1 omegasome formation is positively regulated by the Atg14-Vps34-beclin1 PI3-kinase complex, and thus the isolation membrane is formed inside the ring of the omegasome (Tanida, 2011).

The Atg12 conjugation system is critical in the autophagy process and is involved in the elongation of the isolation membrane and formation of the autophagosome. This complex utilises Atg12, Atg5, Atg7, Atg10 and Atg16, which are essential for the Atg8/LC3 complex (Mizushima *et al.*, 2011). The Atg8/LC3 complex is the last complex of the autophagy pathway and is essential for isolation membrane elongation and selective cargo delivery into the autophagosome (Mizushima *et al.*, 2011). Activation of Atg7, Atg3 and Atg12 complex conjugates cleaves LC3 to phosphatidylethanolamine (PE), generating LC3-PE (also known as LC3-II). Transport of autophagosome is

associated with the cellular localisation of Atg8/LC3 in the autophagosome (Lee & Lee, 2016). LC3 is an autophagic substrate that is degraded by autophagy, and is involved in monitoring the number of autophagosomes (Lee & Lee, 2016). Atg8/LC3 is necessary for autophagosome formation and also acts as an adaptor protein for selective autophagy. After autophagosome formation, the autophagosome fuses with a lysosome to form the autolysosome, which is required for autophagy degradation. In this step, Atg4B delipidates LC3-II on the outer membrane of the autophagosome to recycle LC3-I for autophagosome formation. Lysosomal hydrolases degrade the intra-autophagosomal contents of the autolysosome (Figure 5).

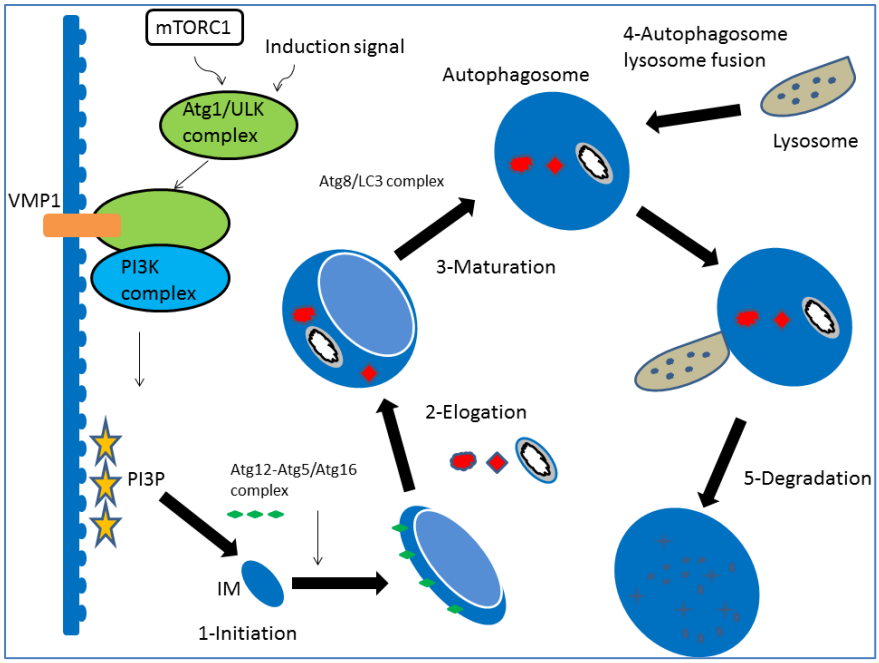

Figure 5: Autophagy pathways (adapted from (Tanida, 2011). The small red represent cytoplasmic components

Many pathogenic microorganisms have strategies for their survival and replication in host cells; they either reside in an intracellular compartment or escape to the cytoplasm. Survival of intracellular pathogens requires avoiding the lysosome or tolerating and adapting to the harsh environment of the lysosome. Each pathogen has its own specific mechanisms for survival inside host cells, including preventing lysosome fusion, delaying phagolysosome biogenesis, and escaping the phagosome. *Escherichia coli* K1 is one example of a pathogen that prevents lysosome fusion by the K1 capsule. Moreover, *Salmonella enterica* and *Mycobacterium tuberculosis* can delay phagolysosome biogenesis through the production of phosphoinositide phosphatases, which delay phagolysosome formation by altering phosphoinositide phosphate concentrations in the phagosome membrane. *Shigella* evades autophagic delivery to the lysosome through IcsB, which masks the part of IcsA required for triggering autophagy (Luzio *et al.*, 2007). IcsB interferes with the autophagic process by interrupting the interaction between IcsA and Atg5 (Ogawa & Sasakawa, 2006; Xu & Elissa, 2010).

1.5 Septin cage as a defence mechanism against intracellular pathogens:

Certain bacteria are degraded by autophagy, while others become compartmentalised in a septin cage. Septins are GTP-binding proteins that were first discovered in *Saccharomyces cerevisiae* (Byers & Goetsch, 1976). *Saccharomyces cerevisiae* has a highly ordered ring of 10-nm filaments in the neck of the bud that is associated with plasma membrane. Mammalian cells have 6 nm actin-containing filaments in the contractile ring, which forms a less ordered structure. The ordered ring of *Saccharomyces cerevisiae* disappears when cytokinesis begins, and is formed during early bud formation (Byers & Goetsch, 1976). There are 14 human septin proteins subdivided into four groups that interact to generate hetero-oligomeric complexes. These septins are formed at *Shigella* entry sites into mammalian cells. It has been shown that septin assembles into rings at sites of actin polymerisation (Mostowy *et al*., 2010). *Shigella ΔicsA* and *Listeria ΔactA* are both unable to polymerise actin and are also unable to recruit septin. It had been shown that septins are incorporated into a cage that forms around bacterial pathogens, preventing them from spreading from cell to cell (Mostowy *et al*., 2010). Inactivation of the septin cage increases the number of *Shigella* with actin tails, thereby enhancing *Shigella* cell-to-cell spread. *Shigella*–

induced septin cages are formed after the initial phase of actin polymerisation, and actin tail formation and dissemination of *Shigella* is prevented by septin caging (Mostowy *et al*., 2010). Septin binds to actin through anillin or myosin II. Anillin is a conserved multi-domain protein which is a prime candidate for scaffolding and organising the cytoskeleton and its regulators. In contrast, myosin II is recruited to septin-caged *Shigella* and colocalises with actin and septin filaments (Mostowy *et al*., 2010).

Septin has a role in host innate immunity in which it prevents intracellular *Shigella* dissemination and directs bacteria towards autophagy for degradation (Mostowy *et al*., 2010). Analyses of a *Shigella* mutant lacking IcsB showed that escape of *Shigella* from autophagy is IcsB-dependent (Phalipon & Sansonetti, 2007). Septin cages were seen to form around *Shigella* IcsB mutants more frequently than around wild-type *Shigella*. These facts indicate that septin cage assembly and autophagy contribute to the same process, as both septin cages (SEPT2 or SEPT9) and autophagy (p62, Atg5, Atg6 or Atg7) markers do not accumulate around intracellular bacteria when depleted by siRNA (Mostowy & Cossart, 2011). This avoidance of autophagy occurs by preventing

ubiquitinated protein recruitment, p62 recognition, and LC3 recruitment. Overall, these studies show that septin cage formation is a key mechanism of host defence for control of intracellular bacteria growth (Mostowy *et al.*, 2010).

1.6 The challenge of antimicrobial resistance in therapy:

AIEC and *Shigella* are known for their ability to invade the human gut and cause CD and shigellosis, respectively. While some AIEC and *Shigella* strains remain sensitive to antibiotics (agents that can kill bacterial pathogens), the majority of contemporary strains are multidrug-resistant (MDR). MDR has been observed in CD-associated AIEC isolates, many of which are resistant to ciprofloxacin, clarithromycin, rifampicin, tetracycline and trimethoprim/sulfamethoxazole (Dogan *et al.*, 2013). Dogan *et al.* 2013 also found that resistance was associated with *tetA*, *tetB*, *tetC*, bla_{TEM-1}, bla_{OXA-1}, *sulI*, *sulII*, *dhfrI*, *dhfrVII*, *ant(3")-Ia* and *catI* genes. Increased resistance to tetracycline (87%), trimethoprim-sulfamethoxazole (94%) and ampicillin (85%) have been observed for certain *Shigella* strains (Ashkenazi *et al.*, 2003). These MDR *Shigella* strains are now prevalent globally, especially in countries undergoing transition to industrialisation (Steele *et al.*, 2012). These resistant strains cannot be killed or inhibited by

antimicrobial agents. Currently, there are no vaccines available for shigellosis, although many health organisations such as the World Health Organisation (WHO) are trying to develop such vaccines (Steele *et al*., 2012). One study in the development of *Shigella* vaccine uses generalised modules that are derived from outer membrane particles from *Shigella* (Steele *et al*., 2012). This membrane antigen-based vaccine conferred cross-protection against heterologous serotypes. Another approach involves the use of IpaB and IpaD proteins of the *Shigella* type III secretion system. High-level cross-serotype protection is induced by both IpaB and IpaD, which are highly immunogenic when delivered mucosally (Steele *et al*., 2012). However, none of these vaccines has been proven to be effective in preventing shigellosis.

S. sonnei can be divided into 4 lineages according to phylogenetic analysis of over 100,00 single nucleotide polymorphisms (SNPs), with lineage III being the predominant lineage in the current pandemic (Holt *et al.*, 2013). Research has shown that lineage III has been more successful than either lineage I or II and was found to be the main MDR *S. sonnei* (Holt *et al.*, 2013). Earlier studies by Holt indicated the recent global dissemination of *S. sonnei* from Europe and demonstrated that the current *S. sonnei*

population descends from a common ancestor that has diversified into several distinct lineages with unique characteristics (Holt *et al.*, 2012). All lineage III strains are MDR and show resistance to most antimicrobial agents. Quinolone resistance has increased among *Shigella* populations globally, especially in Asia and Africa. The current pandemic is associated with MDR clones. The MDR of *S. sonnei* highlights the importance of vaccination for the control and prevention of shigellosis. It has been found that humans are protected from *S. sonnei* infection by exposure to *Plesiomonas shigelloides*, which shares O antigen with *S. sonnei*. The shared O antigen is cross-reactive and has been proposed to be a good vaccine candidate. This will help produce an anti-*Shigella* vaccine, a goal that has yet to be achieved (Holt *et al.*, 2012).

1.7 Natural products as therapy agents against bacterial pathogens:

Resistance to antibiotics has led scientists to find alternative therapeutic agents. Certain plants possess antimicrobial activity, which could be used to treat microbial infections. Medicinal plants are important sources of natural compounds that exhibit antimicrobial activity (Rios & Recio, 2005). Some natural compounds, including those belonging to the flavonoid family, possess activity in modulating *Shigella*-host

interactions (Xu *et al*., 2011). These compounds have also been shown to possess other anti-infective activity (Chirumbolo, 2010).

Table 1: Example of plants exhibiting antimicrobial activity (Cowan, 1999)

Scientific name	Compound	Class	Activity
Malus sylvestris	Phloretin	Flavonoid derivative	Bacteria, fungi and viruses
Camellia sinensis	Catechin	Flavonoid	*Shigella*, *Vibrio*, *Streptococcus. mutans* and Virus
Millettia thonningii	Alpinumisoflavone	Flavone	Schistosoma
Petalostemum	Petalostemumol	Flavonol	Bacteria, fungi

A number of flavonoids possess antimicrobial activity, inhibiting or killing microorganisms. These antimicrobial flavonoids have been used in medicine for the treatment of different infectious diseases (Cushnie & Lamb, 2005). However, the mechanisms behind their antimicrobial effect have yet to be determined. Inhibition of energy metabolism, inhibition of cytoplasmic membrane function, and inhibition of nucleic acid synthesis are some of the examples of the antimicrobial mechanisms of various flavonoids (Cushnie & Lamb, 2005). Natural products have been used to counter many diseases, including atherosclerosis, peptic ulcers, and rheumatoid

arthritis (Patel, 2008). The loss of intestinal fluid and electrolytes in persistent diarrhoea causes patient death. One of the solutions to this problem is the use of green banana and pectin (Rabbani *et al*., 2004). Rabbani *et al*. (2004) showed that green banana and pectin can improve small intestinal permeability and reduce fluid loss. Green banana treatment in children with persistent diarrhoea reduced lactulose recovery which indicates an improvement of permeability; pectin produced similar results (Rabbani *et al*., 2004). Green bananas have been shown to be useful in the treatment of diarrheal diseases, due to the fact that they are rich in amylase-resistant starch, which stimulates fatty acid production. Rabbani *et al*. (2004) demonstrated the positive results of green banana treatment in children with shigellosis. Reduction of faecal inflammatory cells, clearance of faecal blood and mucus, reduction of the daily number of stools and reduction of stool volume are some of the effects of green banana on childhood shigellosis (Rabbani *et al*., 2009). Rabbani *et al*. (2009) showed that green banana could serve as a useful adjunct in the management of shigellosis. Moreover, the study by Roberts *et al*. (2013) found that soluble plantain fibre blocks epithelial adhesion of bacteria and M cell translocation of intestinal pathogens. Adhesion to CaCo2 cells by *Salmonella* typhimurium, *Shigella sonnei*, enerotoxigenic *E. coli* and

Clostridium difficile is inhibited by plantain non-starch polysaccharide (Roberts *et al.*, 2013). Soluble plantain non-starch polysaccharide has been investigated to assess its effect on the translocation of *Escherichia coli* across M cells. Soluble plant fibres, plantain and broccoli reduced translocation of *E. coli* across M cells. This reduction could contribute to the impact of AIEC in Crohn's disease (Roberts *et al.*, 2010).

1.8 Flavonoids as antimicrobial substances:

Flavonoids are polyphenolic in nature and to date over 4000 structurally unique flavonoids had been identified (Patel, 2008). The chemical structure of flavonoids consists of two aromatic rings (A and B) interconnected by a three-carbon atom heterocyclic ring C (Fig. 6a). The modification of these flavonoids, especially in the C ring, could change their structure and function. Accordingly, flavonoids are classified into six main groups: flavanones, flavones, isoflavones, flavonols, flavanols and anthocyanins (Patel, 2008). These flavonoids, referred to as bioflavonoids, are found naturally in plants and exert diverse biological activities, for example by acting as anti-oxidants. The bioflavonoids' capacity to act as anti-oxidants implies that they may have important roles in preventing many diseases, including ulcers, inflammation, viral

infection and diarrhoea. Flavonoids possess anti-microbial, anti-inflammatory, anti-viral activity (Chirumbolo, 2010). Coronary heart disease can be prevented through flavonoids' function as anti-oxidants. The most powerful flavonoids for the protection against reactive oxygen species are the flavones and catechins. Flavonoids have the ability to act as an anti-ulcer agents against peptic ulcers associated with *Helicobacter pylori* infection (Chirumbolo, 2010). Quercetin has been shown to play a critical role in the prevention and treatment of peptic ulcers. Non-steroidal anti-inflammatory drugs (NSAIDs) use a cyclooxygenase (COX) enzyme, which plays an important role as an inflammatory mediator. Quercetin has been shown to inhibit the cyctooxygenase pathway (Patel, 2008).

1.9 Antimicrobial activity of propolis:

Propolis is a resinous substance produced by honey bees by mixing saliva and beewax with exudate gathered from tree buds and sap flows. This 'bee glue' is collected from cracks in tree bark and from leaf buds by honeybees. Bees use propolis to protect hives from deadly intruders. Propolis is also used as a defence mechanism against microbial contamination and for keeping the hive interior warm. Propolis samples were

tested to compare their effects on a variety of Gram-positive and Gram-negative bacteria using a microdilution assay. The results showed that propolis had a high anti-bacterial activity against Gram-positive bacteria but was less effective against Gram-negative (Seidel *et al.*, 2008). There are many types of propolins such as propolin C, D, G and H (Raghukumar *et al.*, 2010). Propolin D show a broad spectrum of activity, including anti-oxidant, antibacterial and anti-inflammatory activities (Raghukumar *et al.*, 2010). This flavonoid compound has been shown to exert a positive influence on health and diet and to prevent many serious diseases (Patel, 2008). Propolin D was identified as the most active against MRSA (Methicillin-resistant *Staphylococcus aureus*) with minimum inhibitory concentrations (MIC) in the range of 16-32 mg/L. However, no activity was observed against Gram-negative bacteria *Pseudomonas. aeruginosa* or *E. coli* (Raghukumar *et al.*, 2010).

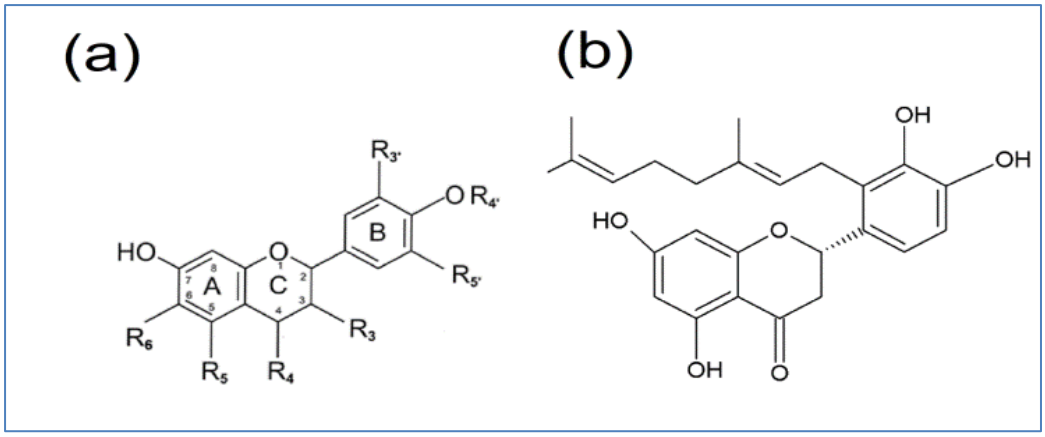

Figure 6. (a) General chemical structure of flavonoids. The two aromatic rings (A) and (B) are interconnected by a three carbon atom heterocyclic ring (C). (b) Chemical structure of propolin D, which has a geraniol side chain attached to the aromatic ring B.

1.10 The inhibition of *S. sonnei* growth in the cell in the presence of various natural compounds:

Several natural compounds have previously been tested on host cells infected with *Shigella* to determine their effects. A number of these compounds, such as 4-methoxycinnamic acid (MCA), propolin D and totarol, were shown to reduce intracellular colony forming units (CFU) at a MIC of 18 µg/ml. Propolin D essentially inhibits intracellular bacterial growth. Actin tails and protrusion were observed in the presence of propolin D, suggesting that propolin D plays no role in preventing bacterial escape from the phagosomes or cell-to-cell spread. Host cells treated with propolin D

alone or together with chloroquine produced similar number of intracellular CFUs, indicating that propolin D does not prevent *Shigella* escape from phagosomes; chloroquine specifically targets the phagosome, which would result in reduced intracellular CFU if the bacteria remain in the phagosomes. Since propolin D is ineffective toward Gram-negative bacteria *in vitro* (Raghukumar *et al*., 2010) propolin D either promotes host cell defence or inhibits *Shigella* only when the bacteria is in the host cell cytosol (Xu *et al*., 2011).

1.11 Biological functions of essential oils:

Other important antimicrobial plant extracts include essential oils (EOs), which are the fragrance substances of plants. EOs from plants are liquid, volatile, limpid, rarely coloured organic solvents. EOs are natural products which play important roles in the protection of plants. They are strongly scented due to the presence of aromatic molecules of secondary metabolites, and represent potential sources of antimicrobial activity, including antibacterial, antifungal and antiviral properties; they can slow and even inhibit bacterial growth (Nazzaro *et al*., 2013). Monoterpenes (C10), sesquiterpenes (C15) and diterpenes (C20) are three primary terpenoids present in

EOs. Geraniol (GOH) is an aromatic oily dietary monoterpene obtained from plant parts, including flowers, seeds, wood, buds, leaves, fruits and roots, and is found in aromatic essentil oils (see Fig 7). Ninety percent of palmarosa oil consists of both geraniol and geranyl acetate (Dubey & Luthra, 2001). Geraniol possesses many of the activities of EOs (Solorzano-Santos & Miranda-Novales, 2012). Hydrophobicity is an important characteristic of EOs, enabling them to partition with lipids of the bacteria cell membrane. This disturbs the cell structure, causing extensive leakage of critical molecules and ions from bacterial cells (Solorzano-Santos & Miranda-Novales, 2012). Their antimicrobial activity can be enhanced by using them in combination with other antimicrobials (Solorzano-Santos & Miranda-Novales, 2012). Cinnamaldehyde, geraniol, thymol analogues, menthol (MOH) and carvacrol are some examples of the components of EOs.

EOs show antimicrobial activity against both Gram-positive and Gram-negative bacteria. The antibacterial activity of various EOs has been tested against Gram-negative bacteria *in vitro*, including *Klebsiella* spp*, E. coli*, *Enterobacter aerogenes* and *Pseudomonas. aeruginosa*. Certain EOs can increase and even restore the

antimicrobial efficacy of certain antibiotics against multi-drug resistant bacteria. Activity in modulating the drug resistance of several Gram-negative bacterial species such as *Enterobacter aerogenes*, *E. coli* and *P. aeruginosa* was observed for geraniol, which targets efflux mechanisms (Solorzano-Santos & Miranda-Novales, 2012). Studies have shown that geraniol can restore the antibiotic activity of the β–lactam ampicillin and penicillin against MDR isolates of Gram-negative species, (Lorenzi *et al*., 2009). The antibacterial activity of various EOs has also been tested against Gram-positive bacteria *in vitro*. The antibacterial activities of the selected EOs components carveol, carvone and citronellol were determined against *Escherichia coli* and *Staphylococcus aureus* (Lopez-Romero *et al*., 2015). Lopez-Romero *et al*. (2015) found that citronellol was the most effective against both *Escherichia coli* and *Staphylococcus aureus*, followed by citronellal, carveol and carvone.

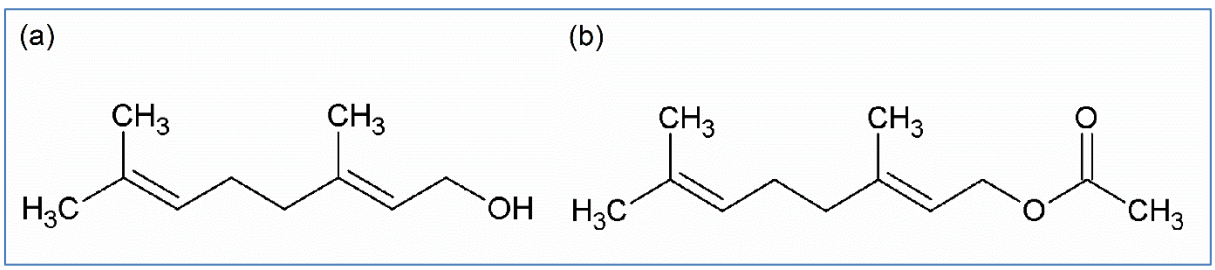

Figure 7. Chemical Structure of geraniol (a) and geranyl acetate (b).

Monoterpenes have also been tested for their effect on mevalonate kinase deficiency (MKD). MKD is an auto-inflammatory disease caused by a mutation affecting the second enzyme of the mevalonate pathway (mevalonate kinase, MK/*MVK*) (Marcuzzi *et al*., 2008). This results in a shortage of intermediate compounds, including geranylgeranyl-pyrophosphate (GGPP), which triggers inflammation (Marcuzzi *et al*., 2011). Monoterpenes such as GOH, farnesol (FOH), geranylgeraniol (GGOH) and MOH have isoprenoid structures (Marcuzzi *et al*., 2008). These monoterpenes can be metabolised by downstream farnesyl pyrophosphate synthase (FPPS) to restore the mevalonate pathway and to ease inflammation (Marcuzzi *et al*., 2011). Geraniol, farnesol, geranylgeraniol and menthol have been shown to inhibit inflammatory marker levels induced by LPS. The level of inflammatory marker induced by pamidronate (PAM) is reduced by GOH, which could be used as a novel therapeutic approach in the treatment of MKD (Marcuzzi *et al*., 2011).

1.12 Objective:

The overall aim of this research project was to unravel the mechanisms of how flavonoids could control *Shigella* intracellular proliferation as described by Xu *et al*. (2011). Additionally, a flavonoid library was screened to identify other related compounds with similar activity to propolin D which is capable of limiting *Shigella* intracellular growth, and to unravel these underlying mechanisms. Flavonoids activities were also detected in the cell. *In vitro* activities of propolin D were then investigated in inhibiting the growth of *S. sonnei*. Envelope stress responses of *S. sonnei* wild-type and *ΔdsbA* were then investigated. Purified DsbA and its inhibition activities on the reduction of Di-E-GSSG by geranyl or geranyl acetate were studied. Lastly, the potential of natural compounds was investigated in the treatment of CD via control of AIEC infection, as CD and shigellosis share inflammations in nature, and DsbA is the master virulence regulator in both AIEC and *Shigella*.

Chapter 2: Materials and methods

2.1 Bacterial strains, cell-lines and natural compounds:

Shigella sonnei strain No. 86 is a wild-type clinical isolate from the Scottish *Salmonella* and *Shigella* Reference Lab (Xu *et al*., 2014). Adherent-invasive *Escherichia coli* (AIEC) LF82 (the paradigm ileal CD isolate) (Darfeuille-Michaud *et al*., 1998), HM427, HM605, and HM615 (colonic mucosally associated CD isolates) (Martin *et al*., 2004; Subramanian *et al*., 2008) are AIEC strains used in this study. Bacteria were routinely grown at 37 °C in Luria-Bertani broth or Trypticase soy broth (TSB) (Sigma). SOC media, M9 minimal medium and acidic, nutrient-poor medium (see Appendix A) were also used to grow *S. sonnei* and test various compounds for anti-*Shigella* activity *in vitro*. Ampicillin (100 g/mL), kanamycin (25 g/mL), and chloramphenicol (12.5 g/mL) were used as appropriate for selecting bacteria containing plasmids.

Natural compounds used in the research: DT6, DT12, DT13, DT17, DT20, DT62, propolin D, eriodictyol, geraniol and geranyl acetate (Table 1).

Sample code	Sample name	Source	Percentage of Purity
DT6	5-Methoxyflavone	The compound was kindly provided by Prof. Deniz Tasdemir	100%
DT12	Chrysin(5,7-dihydroxylflavone)	The compound was kindly provided by Prof. Deniz Tasdemir	100%
DT13	6,7-Dihydroxyflavone	The compound was kindly provided by Prof. Deniz Tasdemir	100%
DT17	3',4',7-trihydroxyflavone	The compound was kindly provided by Prof. Deniz Tasdemir	100%
DT20	7,8-dimethoxyflavone	The compound was kindly	100%

		provided by Prof. Deniz Tasdemir	
DT62	(-)-Catechin	The compound was kindly provided by Prof. Deniz Tasdemir	100%
PD	Propolin D	The assays were done with what was isolated by me. (see section 2.2)	89.6%
Erio	Eriodictyol	Sigma (catalogue No 4049-38-1)	≥95%
Geraniol	Geraniol	Sigma (catalogue No 106-24-1)	98%
Geranyl acetate	Geranyl acetate	Sigma (catalogue No 105-87-3)	≥97%

Table 1. Natural compounds used in this study.

2.2 Propolin D purification and structural elucidation:

Propolin D was purified as previously reported (Raghukumar *et al.*, 2010). Propolis extraction was used to isolate propolin D by using column chromatography on silica gel 60. Gel filtration chromatography was performed by using Sephadex LH-20-100 (Sigma-Aldrich UK). Thin layer chromatography (TLC) analysis was performed by using silica gel PF_{256} pre-coated plates. The plates were heated at 110°C for 2 min after which plates were visualized under UV light (λ = 254 nm) and by spraying with *p*-anisaldehyde sulphuric acid reagent. First, a portion of the active ethyl acetate extract (1 g) was fractionated by gel filtration using Sephadex® LH-20-100 (Sigma-Aldrich UK). All fractions were collected and analysed by TLC using either one or two successive developments with *n*-hexane/ethyl acetate/acetic acid (5 : 3 : 0.4 v/v). 5 mg of propolin D was isolated after elution with 2% v/v methanol in dichloromethane that led to the isolation of the compound of interest. High-resolution mass spectrometry (MS) data were recorded using electrospray ionization (ESI) on a Finnigan LTQ-Orbitrap mass spectrometer operating in positive ESI mode. Nuclear

magnetic resonance (NMR) spectra were recorded, either in DMSO-d6 or CDCl3, on a JEOL Lambda Delta 400 spectrometer operating at 400 MHz (^{1}H) and 100 MHz (^{13}C). NMR data analysis was similar to previous study (Raghukumar *et al.*, 2010) (see Appendix B).

2.3 Cell cultures:

Human embryonic kidney 293 cell-line (HEK 293) (ECACC number 85120602), human epithelial cell-line (HeLa cells) (ECACC number 93021013), Hep-2 epidermoid carcinoma cell-line (ECACC number 86030501) and RAW 264 mouse leukaemic monocyte macrophage cell-line (ECACC number 85062803) were used in this study. All cell-lines were cultured in Dulbecco's modified Eagle's medium (DMEM) (see Appendix A) under 5% CO_2 atmosphere at 37°C. Penicillin and streptomycin (Sigma) were added to DMEM to the final concentrations of 100 Units and 400µg per mL respectively. Cells were washed 3 times with sterile phosphate-buffered saline (PBS) before cells were trypsinised and were resuspended in DMEM. Cell suspensions were counted using a haemocytometer under microscope. Cells

were seeded either in culture flask for passaging or to 24-well plates for experiments described below.

2.4 Bacterial cell electroporation:

Shigella bacteria were cultured overnight (O/N) at 37 °C in Trypticase soy agar (TSA) supplemented with 0.1% w/v Congo red. A single smooth red colony was selected from O/N cultured agar plate and inoculated into 5-10 mL TSB in a 30 mL polystyrene tube. The bacterial culture was incubated with shaking (200 rpm) for 3 hours until approximately OD600nm ≈ 0.6. The bacterial culture was transferred to a 50 mL centrifuge tube (on ice). The tubes were spun for 10 min at 6660 x *g* at 4°C. Tubes were placed on ice and supernatant was removed. The pellet was resuspended with dH_2O and tubes were centrifuged for 10 min at 6660 x *g* at 4°C. The pellet was resuspended with 5-10 mL of 10% glycerol after supernatant was removed. Then cell pellet was resuspended with 2 mL of 10 % v/v glycerol after the supernatant was removed. The resuspended bacteria were added to centrifuge

tubes. The tubes were centrifuged at 10,200 x *g* for 5 min at 4°C. The cell pellet was resuspended with 70µl of 10% v/v glycerol after the supernatant was discarded. 1 µg of DNA was added to the tube. Bacteria were electroporated at 1.8 KV. One mL of TSB broth was added to the tube after each sample after electroporation. The samples were incubated for 1 h at 37°C. One hundred µl of the bacteria were added to TSA plate before plating out on agar. The plates were incubated at 37°C overnight.

2.5 Gentamicin-killing assay:

Mammalian cells were seeded to 24 wells plates at 10,400 cells/well and cultured to 80% confluency. Overnight bacterial cultures were subcultured (1:100 dilution) in 5 mL TSB/LB broth at 37 °C for approximately 2 hours to early exponential phase (OD600nm approximately 0.3). Ten µL or 50 µL of bacteria were added to cells, which gives an MOI (multiplicity of infection) of 10 or 50 respectively. To enhance *Shigella* invasion, a centrifugation was performed at 3330 x *g* for 10 min at room temperatures. The bacteria were incubated for 40 min at 37°C 5% CO_2 incubator

before the extracellular bacteria were removed by 3 washes with sterile 1X PBS. Fresh DMEM medium containing gentamicin (50 µg/mL) and natural products (18µg/mL i.e. 9 µl stock in 1mL) were added for further incubation. Each 24-well plate was incubated for 5 h at 37°C under 5% CO_2 (Xu *et al.*, 2011).

The cells were washed with 1X PBS 2-3 times before they were lysed with 1 mL of 0.1% v/v Triton X-100 in dH_2O in each well. Cell lysates were diluted 1:10 or 1:100. A 100µL sample of diluted cell lysate was plated out on a LB agar plate and incubated at 37°C overnight to determine the intracellular CFU.

2.6 Microscopy of infected cells:

For Giemsa stain, cells were grown on sterile 13mm glass coverslips. After experiments (for example gentamicin-killing assay), cells were washed with 1X PBS for 5 min, and then fixed for 15-30 min with 3.7% w/v paraformaldehyde in PBS (pH 7.4). Cells were washed with dH_2O for 3 times. Giemsa was diluted 1:20 and which was used to stain cells 10 min at room temperature. Cells then were washed with dH_2O for 2-3 times. Giemsa-stained coverslips were mounted to a glass slide with a drop of 50% glycerol. Cells were viewed under a light microscope.

For immunofluorescence microscopy, cells were cultured and processed the same way as above. After fixation cells with 3.7% w/v paraformaldehyde (pH 7.4), cells were washed with 1X PBS three times for 5 min followed by washing with 1mL of 50mM NH_4Cl 3 times before cells were treated with PBS containing 0.1% v/v Triton X-100 for 10 min at room temperature. Cells were washed with 1X PBS for 2 times after cells were washed again with 1 mL of 50mM NH_4Cl for 3 min. 5% w/v BSA (bovine serum albumin) containing phalloidin ALEXA Fluor 594 conjugate (2mg/mL) (Invitrogen Molecular Probes) were made for actin stain; 300µL of the solution per well. Cells were incubated for 20-30 min before washed with 1X PBS 3 times. Culture cells were mounted on glass slides using ProLong™ Antifade mountant (Invitrogen Molecular probes). Images were obtained using a Leica confocal microscope (Leica Microsystems).

2.7 MTT assay to assess for cytotoxicity of the flavonoids:

MTT (3-(4,5-Dimethylthiazol-2-yl)-2,5-diphenyltetrazolium bromide) was purchased from Sigma-Aldrich. Mammalian cells were seeded into 96 well plates to about 60-80% confluency. The cells then were treated with each of the compounds 9µL per

mL for 6 h or overnight. MTT (5 µg/mL in PBS) was added to each well of the 96-well plates. The plate was incubated for 1-2 h until purple precipitation was visible. The cell culture medium was removed, and 100 µL dimethyl sulfoxide (DMSO) was added to each well to solubilise the purple precipitates. Absorbance was measured at 540 nm (A540) and recorded with a Spectramax microplate reader (Molecular Devices) as previously described (Xu *et al.*, 2011).

2.8 Acridine orange stain for viewing the flavonoid compounds:

The gentamicin-killing assay as described in section 2.5 was used in this experiment before cells were treated with different natural compounds (18 µg/mL) for 5 h at 37°C under 5% CO_2. Cells were washed with 1X PBS three times for 5 min, and then fixed for 15-30 min with 3.7% w/v paraformaldehyde (pH 7.4). Cells then were washed with 1X PBS, three times, each for 5 min. one mL of 50mM NH_4Cl was used to wash cells for 10 min 3 times before cells were treated with PBS containing 0.1% v/v Triton X-100 for 10 min at room temperature. Cells were stained with acridine orange by adding 5 µg/mL (Sigma) in 1mL of 5% w/v BSA for each well. Cells were incubated for 15 min before being washed with 1X PBS 3 times. Coverslips were mounted on

glass slides with ProLong™ Antifade Mountant (Invitrogen Molecular Probes). Images were obtained using a Leica confocal microscope (Leica Microsystems).

2.9 Test of various compounds for anti-*S. sonnei* activity *in vitro:*

Adapted *S. sonnei* strains in M9 minimal medium (Sigma) were grown in M9 broth containing various supplements, and growth curves were obtained by measuring optical density (OD) at OD600nm using a WPA spectrophotometer at various time intervals.

2.10 MTT assay to quantify *S. sonnei* growth in reducing M9 medium:

An MTT assay was used to quantify *Shigella* in M9 broth to determine the effect on *S. sonnei* growth by various compounds. Overnight bacterial cultures were subcultured in 96-well plates; each well contained 100 µL M9 broth. Compounds, at 42 µM, as well as different concentrations of GSH were added to each of the wells. After overnight incubation, 96-well plates were centrifuged to bring bacteria down. MTT (5 µg/mL in PBS) was added to each well of the 96-well plates. The plate was incubated for 0.5 to 1 h until purple precipitation was visible and 100 µL DMSO was

added to each well. Absorbance of each plate at 540 nm (A540) was recorded with a Spectramax microplate reader (Molecular Devices).

2.11 Construction of deletion mutants of *S. sonnei* using red λ recombination system:

By electroporation, wild-type *S. sonnei* strain No. 86 was transformed with the plasmid, pKD46, which expresses red λ recombinase (Datsenko & Wanner, 2000). The preparation of cells and the electroporation protocol were followed as previously described (see section 2.4). Primers were designed to amplify the Kan-cassette from plasmid pKD4; the Kan-cassette is flanked with repeated flippase recognition target (FRT) sites. Each of the primers contains 51 base pairs (bp) of either 5'- or 3'-end of the *Shigella* genes to be deleted followed by 20 bp of repeated FRT sequence. (Table 2) lists primers used for deleting *S. sonnei icsA* and *icsB* genes. PCR conditions were set 34 µL of dH_2O, 10 µL of My Taq™ buffer (Bioline), 1 µL of DNA (pKD4), 2 µL of each primer (forward and reverse) and 1 µL of My Taq DNA polymerase (Bioline).The thermal cycling program of PCR for IcsA and IcsB was run

at 95 °C for 10 min, 30 cycles at 95 °C for 1 min, 68 °C at 1 min and 72 °C for 1 min followed by 72 °C for 10 min.

Oligo name	Sequence (5'-3')	Source
icsA-F: for deletion	ATGAATCAAATTCACAATTTTTTTGTAATATGACCCAATGTTCACAG GGGTGTGTAGGCTGGAGCTGCTTCG	Sigma
icsA –R: for deletion	TCAGAAGGTATATTTCACACCCAAAATACCTTGGGTGTCTCTGTAACT GTTATGGGAATTAGCCATGGTCC	Sigma
icsB-F: for deletion	CTATATATTAGAATGAGAGTTATTCAATAAAAGCTTATTGACCTGTAA TATGTGTAGGCTGGAGCTGCTTCG	Sigma
icsB-R: for deletion	ATGATCCTCAAAATTAGCAATTTCATTGACGCAAGCAATACAAAAGGG CCTATGGGAATTAGCCATGGTCC	Sigma
icsA-F: for sequencing verification	ATGACCCAATGTTCATAGGG	Sigma
icsA-R: for	CACACCCAAAATACCTTGGG	Sigma

sequencing verification		
icsB-F: for sequencing verification	CAATAAAAGCTTATTGACCTG	Sigma
icsB-R: for sequencing verification	GCCAAGCAATACAAAAGGGCC	Sigma

Table 2. Primers used for deletion *icsA* and *icsB* and verification of the deletions.

Agarose gels (1% w/v) were prepared by adding 0.5 g of agarose in glass flask to 50 mL of prepared TAE buffer (see Appendix A). The flask was microwaved for 90 min to dissolve the agarose. Three µL of SYBR Safe DNA gel stain (Invitrogen Molecular Probes) was added before the gel was poured to set for 20 min. The gel was transferred to the electrophoresis tank before filling with 1X TAE butter. The DNA samples were mixed with DNA loading dye stain before it was added to the wells. DNA molecular weight markers, the 10 µL HyperLadder 1 (Bioline), was added to the

first well. Electrophoresis was performed at 100 V for 30 min. The gel was scanned with the gel imager (Syngene).

The QIAquick PCR purification kit was used for PCR product purification. All centrifugation was carried out at 17,900 x *g* (13,000 rpm). 1:250 volume of pH indicator was added to buffer PB. The colour of the buffer changed to yellow to indicate a pH ≤ 7.5. Forty five µL of 3 PCR samples were combined together in one microcentrifuge tube. The PCR reaction was added to buffer PB. Ten µL of 3 M sodium acetate pH 5.0 was added and mixed for the colour to turn yellow. A QIAquick column was placed in a 2 mL collection tube before the reaction volume of microcentrifuge tube was added to the QIAquick column. The sample was applied to the QIAquick column to bind amplicon DNA and was centrifuged for 1 min. The QIAquick column was removed from the spin column and the flowthrough liquid discarded before the QIAquick column was returned to the collection tube. The column was washed by adding 750 µL of buffer PE to the QIAquick column and was centrifuged for 1 min. The QIAquick column was removed from the spin column, and flowthrough wash discarded before the QIAquick column returned to the collection tube. The column was centrifuged once again for 1 min to remove residual wash

buffer. The QIAquick column was carefully transferred to a clean 1.5 mL microcentrifuge tube. Fifty µL of buffer EB was applied to the centre of the column without touching the membrane with the pipette tip. The tube was incubated at room temperature for 1 min and centrifuged for 1 min. The collected product was transferred to a clean PCR tube.

DpnI restriction enzyme was used after PCR purification using a PCR product showing a single strong band of about 1.5Kb. Five µL of 10X restriction enzyme buffer 4 was added to 45 µL PCR purified product. A 1 µL aliquot of 1,000 units DpnI restriction enzyme was added. The tube was incubated for 3 hours at 37°C (Datsenko & Wanner, 2000). DNA precipitation was used for removing enzymes and salts, and concentrating the DNA. Twenty four µL Sodium acetate (3M) and 25 µL dH_20 were added to the sample to bring the volume of sample to 100 µL. Two volumes of 100% ethanol were then added. The sample was frozen at -80 °C. The sample was then centrifuged 10,200 x *g* at 4 °C for 20 min before being washed with 70% ethanol. The sample then was resuspended in dH_20 (10 µL) after the tube was air dried to remove the ethanol.

S. sonnei No. 86 containing pKD46 was cultured overnight (O/N) at 30 °C. The single red colony was selected from O/N culture agar plate. The culture was set at 30 °C because the plasmid is temperature sensitive which can be cured at 37 °C. The culture was in 20 mL LB containing 100 µg/mL ampicillin in a small conical flask. Twenty µl of 1M of L-arabinose was added to the culture when OD600 nm ≈ 0.1 to induce recombinase expression from pKD46. The strain was inoculated for 3 hours until OD600 nm ≈ 0.6. 5-10 mL of the bacteria culture was added to 50 mL centrifuge tube (all tubes were kept on ice). The tubes were spun for 10 min at 6660 x *g* at 4 °C. Tubes were placed on ice and supernatant was removed. The pellet was resuspended in dH_20 and tubes were centrifuged for 10 min at 6660 x *g* at 4 °C. The pellet was resuspended with 5-10 mL of 10% v/v glycerol after supernatant was removed. Then cell pellet was resuspended with 2 mL of 10% v/v glycerol after supernatant was removed. The resuspended bacteria were added to centrifuge tubes. The tubes centrifuged at 10,200 x *g* for 5 min at 4 °C. Linear PCR products were then electroporated into electrocompetent cells. The cell pellet was resuspended with 70 µL of 10% glycerol after supernatant was discarded. Five µL of DNA Kan-cassette for mutating *icsA* or *icsB* was added to the tube. Bacteria were

electroporated at 1.8KV. The cuvette was dried to prevent arcing. The pulse after the cuvette was placed in the sample chamber. One mL of SOC media was added to the tube after each sample was electroporated. The samples were incubated for 1 h at 37 °C. Subsequently, 500 µL of the bacteria were added to kanamycin agar before plating out. The plates were incubated at 37 °C. pCP20 plasmid, which expresses FRT recombinase, was used to eliminate the Kan-cassette. The *icsA*-Kan and *icsB*-Kan mutants were transformed with pCP20 by using electroporation. The cell component and cell electroporation protocol were followed (see section 2.4). One mL of SOC media was added to the tube after each sample was electroporated. The samples were incubated for 1 h at 30 °C. The bacteria were then plated out onto agar with ampicillin and left overnight. Colonies were picked and then a few transformants were non-selectively grown on TSA (no antibiotics) at 43 °C overnight. The colonies were then screened for sensitivity to kanamycin and ampicillin on antibiotic-selection agar. A single colony was picked and streaked onto a set of three plates: kanamycin, ampicillin and non-antibiotic. The plates were incubated at 37 °C overnight (Datsenko & Wanner, 2000). The majority of colonies lost the Kan-cassette through FRT-mediated recombination. PCR verification was used to verify the

deletion of the *icsA* or *icsB* genes. Fresh overnight colonies were isolated in 20 µL water. The 20 µL water samples were suspended in boiling water bath 95 °C for 10 min to effect genomic DNA isolation. DNA bands for *icsA* and *icsB* were amplified and examined by agarose gel electrophoresis.

2.12 Isolation of periplasmic protein, His-tag purification, SDS-PAGE and Western blot:

Two strains of *S. sonnei ΔdsbA*/pDsbA-6XHis and *ΔdsbA*/pDsbA33G-6XHis were constructed. Two strains of *S. sonnei ΔdsbA*/pDsbA-6XHis and *ΔdsbA*/pDsbA33G-6XHis were cultured overnight at 37 ^{o}C. The overnight cultures were subcultured 1:100 for two hours in a shaking-incubator at 37 °C 250 rpm. A 800 µL aliquot of 20 mg/mL Isopropyl β-D-1-thiogalactopyranoside (IPTG) was added to the culture. Incubation was continuing for further 2 hours. The cultures were transferred to the 50 mL tube for centrifuge for 6660 x *g* 4 °C for 10 min. The supernatant was removed, and the pellet was washed with 0.1M sodium phosphate buffer, pH 7.0. The cultures were centrifuged for 6660 x *g* 4 °C for 10 min. The supernatant was removed, and

the pellet was resuspended in 2 mL PBS containing 2000U of polymyxin B. The suspension pellet was incubated on ice for 15 min. The culture was centrifuged for 10 min at 4 °C. The supernatant (periplasmic proteins) was transferred to a new tube after centrifugation. The periplasmic proteins were stored in -80^{o}C freezer.

To purify 6XHis tagged DsbA or DsbA33G from the crude periplasmic preps, a His-tag Ni^{2+} affinity chromatography column was used (GE Healthcare). Syringe or pump tubing was filled with distilled water. The column was connected to the syringe. The column was washed with 5 column volumes of distilled water. Then, the column was equilibrated with at least 5 column volumes of binding buffer. The protein sample that contained DsbA was applied using the syringe. The column was then washed with 10 mL of binding buffer before it was eluted with 5 mL of elution buffer into 5 Eppendorf tubes.

Sodium dodecyl sulphate Polyacrylamide gels (SDS-PAGE) (10%) were prepared and mounted using a Mini-Protean (Bio-Rad) Polyacrylamide gel electrophoresis (PAGE) system. Clamp, gel plates and spaces of the system were assembled. After clamping into the stand, the resolving gel mix was setup. 10% w/v ammonium persulphate and Tetramethylethylenediamine (TEMED) were added to gel mix. The

resolving gel mix was prepared. The 10% polyacrylamide resolving gel mix was poured into the assembly gel plates. The gel was left at room temperature to set. Next, the stacking gel mix was prepared. The mix was poured above resolving gel before the plate comb was inserted. The gel was allowed to set for 1 h at room temperature. Running buffer was added to SDS-PAGE after the gel was set. Proteins samples, DsbA-6XHis and DsbA33G-6XHis, were prepared for SDS-PAGE. Five µL of Precision plus protein dual colour standard (BioRAD) was added to one well of each gel. Protein samples were each mixed with protein loading buffer (see Appendix A) before added to the well. The gel was run for 1 h at 120V with protein running buffer (see Appendix A). Transfer of proteins from the polyacrylamide gel was performed in a Mini Trans-Blot system (Bio-Rad). A polyvinylidene difluoride (PVDF) membrane was activated by immersion in 100% methanol for 3 min. The transfer was performed for 60 min, at 0.4 A in transfer buffer (see Appendix A). The membrane was blocked by incubation in a solution containing 5% w/v non-fat milk in TBS (see Appendix A) for 60 min at room temperature. Then, the membrane was incubated at 23 °C for 1 hour with mouse anti-His epitope tag primary antibody (Thermo Scientific) diluted at 1:20,000 in TBS. The membrane was washed with

TBS-T (containing 0.1% Tween 20) three times. Anti-His Antibody (Thermo Scientific) was added to the membrane and incubated overnight. The membrane was washed with TBS-T and incubated with ALEXA FLOUR 680 conjugated anti-mouse Ig secondary antibody diluted at 1:10,000 in TBS at 4 °C for 2 h (Blondel *et al.*, 2013).

2.13 RNA isolation and qPCR analysis for gene expression:

Overnight bacterial cultures were subcultured (1:50) until OD600nm reached 0.6-1.0. One mL of cultured bacteria was taken to a 1.5 mL microcentrifuge tube. The tube was centrifuged for 2 min at 14,000 x *g*. one hundred µL of M9 broth and 500 µL of RNA*later* were added to pellet after the supernatant was removed. The resuspended culture was centrifuged before the supernatant was removed. The pellet was suspended in 100 µL of fresh TE buffer containing lysozyme (0.4 mg/mL). The tube was tapped gently to mix the contents after which it was incubated for 5 min. A 75 µL sample of cell lysis buffer was added. Followed by 350 µL of RNA dilution buffer and mixed by inversion. A 200 µL volume of 95% ethanol was added to clear the lysate and mixed by inversion 4 times. Then it was transferred to a spin

column (Qiagen). The spin column was centrifuged at 14,000 x *g* for one min. A 600 µL volume of RNA wash solution was added to spin column. It was then centrifuged for one min, and the supernatant was discarded. DNA clean-up solution mix (see Appendix A) was prepared before 50 µL of that DNA clean-up solution was added to spin column. The column was centrifuged at 14,000 x *g* for 1 min. Spent solution was discarded, and 600 µL of RNA wash solution was added. It was centrifuged again for 1 min and spent solution was discarded. A 250 µL volume of RNA wash solution was then added before it was centrifuged again for 1 min. The column was transferred to elution tube. One hundred µL of nuclease free water was added to the membrane. The column was centrifuged for 1 min to elute the RNA.

One µg of total RNA from each of the above RNA samples was used to synthesize cDNA using the cDNA synthesis kit (Qiagen). Then, the total cDNA was utilized for real-time reverse transcription-PCR (RT-PCR) with a SensiMixPlus SYBR (Qiagen) kit using a Corbett Rotor Gene 6000 instrument (Life Sciences Ltd). Standard curve was constructed by plotting C_T values against concentration dilution factors. The samples were run in triplicate, and the results were recorded as mean cycle

threshold (C_T) values. The mean C_T was used to calculate ΔC_T values with the formula: ΔC_T = mean C_T target gene – mean C_T control gene. RT-qPCR was normalised by using reference (housekeeping) gene (*cysG*). The normalized mean was calculated with the formula: ΔC_T = mean C_T of the internal control *cysG* gene - the mean C_T of the target gene. $\Delta\Delta C_T$ values were calculated with the formula: the ΔC_T value of the same gene - ΔC_T value of the target gene in control. The $\Delta\Delta C_T$ values were expressed as follows: ln 2ˆ(-$\Delta\Delta C_T$), where 2 reflects the RT-PCR efficiency (Yu *et al.*, 2009).

Oligo name	Sequence (5'-3')	Description (i.e gene function)
cysG-F	CATCGCGATTATGCCCAGAG	Encodes multifunctional enzyme which catalyses SAM-dependent methylations of uroporphyrinogen III
cysG-R	GTGAGCGTACCGTCAATCAC	Encodes multifunctional enzyme which catalyses SAM-dependent methylations of uroporphyrinogen III
dsbA-F	AACCCAGACCATTCGTTCAG	Encodes a periplasmic enzyme which Catalyse oxidation of disulphide bond into substrate protein
dsbA-R	TATCCATACCCTGCGGATTC	Encodes a periplasmic enzyme which Catalyse

		oxidation of disulphide bond into substrate protein
fkpA-F	TCTTGGTCGGAGAGTTTGCT	Encodes a periplasmic enzyme which exhibits both cis/trans peptidyl-prolyl isomerase (PPIase) and chaperone activates
fkpA-R	CCAATCACTTTTGCTGCTGA	Encodes a periplasmic enzyme which exhibits both cis/trans peptidyl-prolyl isomerase (PPIase) and chaperone activities
rseB-F	TCAGTGTCCATCCACACGAT	Encodes a periplasmic enzyme which modulates the activities of sigma-E (RpoE)
rseB-R	TTTTGAACCGGGACTTGAAC	Encodes a periplasmic enzyme which modulates the activities of sigma-E (RpoE)
spy-F	AGATCCGCGAAATCATGAAA	Encodes a periplasmic enzyme which decreases protein aggregation and helps protein refolding
spy-R	CTTTGCGCTGTTCTTCCATT	Encodes a periplasmic enzyme which decreases protein aggregation and helps protein refolding

Table 3. Primers used for qPCR analysis for gene expression.

2.14 Fluorescent labelling of oxidised glutathione (GSSG):

A fluorescent chemical, eosin isothiocyanate (Ei), was used to label GSSG. GSSG (100 μM) was incubated with 1 mM eosin isothiocyanate overnight in phosphate buffer (see Appendix A). One hundred μL of the mix was added to the Sephadex G25 column using PDI/DsbA buffer (see Appendix A). Different fractions (0.5 mL) were collected from the Sephadex G25 column. The fraction samples showing 70-fold increase in fluorescence when 10 mM DTT added were pooled together. This suggested the reaction was completed (i.e. the two eosin moieties were attached to two free amino termini of GSSG). The sample was stored at -80 ^{o}C.

2.15 Enzyme kinetic assay:

DsbA activity assay buffer was prepared that contained 0.1 M potassium phosphate buffer (pH 7.0) and 2 mM EDTA. After Di-E-GSSG had been prepared, 96 well plates were used for the DsbA inhibition assay. The reactions were prepared by making two mixes: mix A (150 nM Di-E-GSSG + 5 μM DTT + DsbA buffer) + mix B (40 nM DsbA +DsbA buffer). Each test compound was added to the mix A. The two reaction solutions were mixed, and enzyme activity monitored using UV Spectramax

microplate reader (Molecular Devices). The dynamic increase of fluorescence was monitored for 15 min, with excitation at 525 nm and emission at 545 nm. The inhibition of the DsbA was also monitored with using various test compounds in the reaction.

2.16 Evaluation of bacterial virulence using *Galleria mellonella* larva model:

Bacterial strains (AIEC and *Shigella sonnei*) were cultured O/N on LB agar plate at 37 ^{o}C. The O/N bacterial culture was subcultured and grown to OD600nm = 0.3. One mL of the culture was added in an Eppendorf tube and centrifuged for 4 min. The supernatant was removed, and the pellet was resuspended with 1 mL 1X PBS. The bacteria culture was diluted to 10^5 CFU per 10 µL (the maximal volume that can be used to inject a larva). Treatment doses of geraniol (10.9, 15.6, 21.9, 43.7 and 87.4 µg/larva) were administered in PBS mixed with live bacteria. Waxworms (*Galleria mellonella*) 15-25 mm are larvae used for this experiment (Livefoods UK). One group of larvae inoculated with PBS only was used as mock infection. Another group of larvae was inoculated with live *S. sonnei* with PBS as *S. sonnei* infection group. Ten

µL of the sample was taken using syringe and was injected it into larva. All larva samples were incubated in incubator (Desbois & Coote, 2011).

2.17 Use of acidic and nutrient-poor medium to assess inhibition of bacterial growth:

Bacteria (AIEC or *S. sonnei*) strains were cultured overnight. The overnight bacterial cultures were harvested and resuspended in the same volume of acidic and nutrient-poor medium. Cultures were then diluted 1:50 in the medium. The bacteria were grown at 37 °C with shaking. At different time intervals (0, 3 and 6 h), 50 µL of the culture was diluted in water and plated onto Mueller-Hinton agar plates to determine the number of CFU per millilitre (Bringer *et al.*, 2007).

2.18 Statistical analysis:

Results data were expressed as mean ± SD for different sets of experiments. Statistical significance between groups was calculated using the Bonferroni correction t test. A p value less than 0.016 was considered statistically significant. A p value less than 0.003 and 0.0003 were also used which were considered higher

statistically significant. Bonferroni correction was performed to reduce the chance of type 1 error in t test. Differences between untreated and treated groups were assessed using Bonferroni correction t test which is used for multiple comparisons and to reduce the chance of false positive result.

Bonferroni's multiple comparisons test was also used to compare the growth curves of the different *S. sonnei* strains. The multiple comparison test is used to compare and examine more than one pair of means at the same time and determine whether there is a significant difference among treatment means. The confidence interval (CI) is a type of interval estimate that tells how precisely the mean was determined. A 95% CI is the range of values that contain 95% of the true mean of the population. A 95% CI means that if population on the interval estimate are made for each sample, the resulting interval would support the population parameter in 95% of cases.

Chapter 3: *Shigella sonnei*-host interaction: the roles of septin cage and autophagy, and intervention of propolin D

This chapter aims to investigate the potential effect of propolin D to the septin cage formation and autophagy, two cellular processes. *Shigella sonnei* uses actin-based motility to spread within and between host cells. Host cells use septin and autophagy for self-protection. However, *Shigella sonnei* has many strategies to evade both septin cage formation and autophagy. As Xu *et al*. (2011) has shown that propolin D inhibits intracellular growth of *Shigella*, it was therefore of interest to investigate whether such activity occurs through the enhancement of the processes of septin cage formation and autophagy.

3.1 Construction and characterisation of *ΔicsA*, *ΔicsB* strains using red λ recombination system:

To control intracellular *Shigella*, host cells initiate autophagy and septin cage formation by targeting IcsA protein expression on the old bacterial pole (Introduction sections 1.4 and 1.5). Therefore, it would be of interest to delete *icsA* and *icsB* in order to investigate the fate of these mutants in terms of their behaviour in

autophagy and septin cage formation, and to investigate whether propolin D promotes these cellular defence mechanisms to inhibit intracellular growth of *Shigella*.

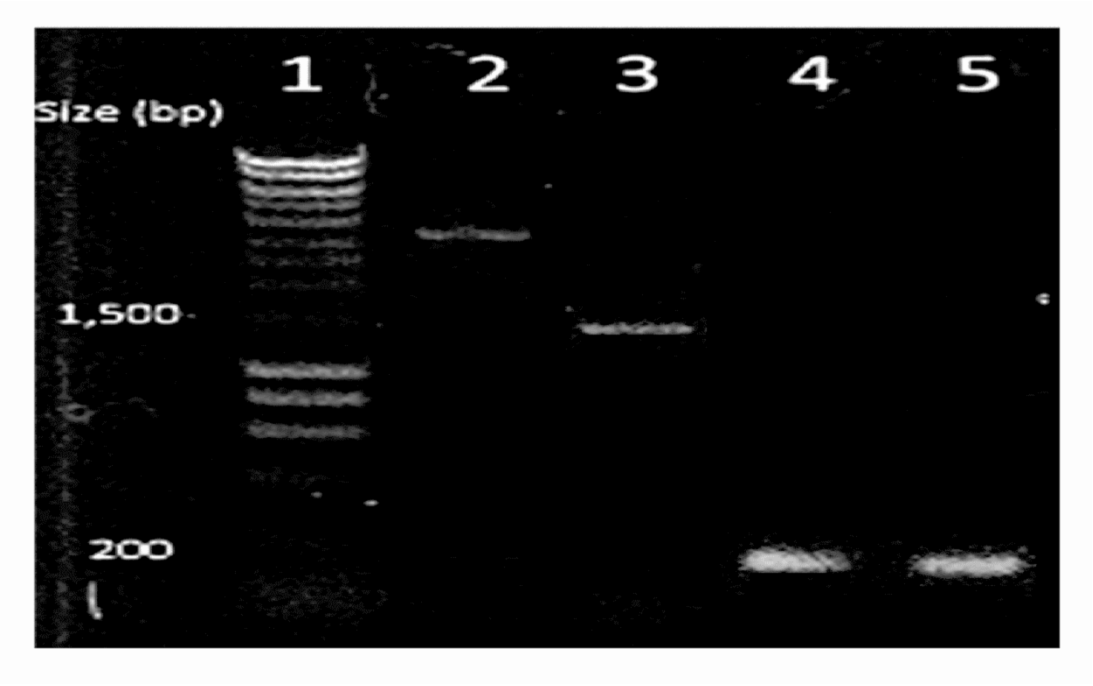

Figure 8. PCR verification of *icsA* and *icsB* gene deletions. Lane 1: DNA Hyperladder 1 (Bioline); Lane 2: full length of *icsA* coding sequence (3309 bp); Lane 3: full length of *icsB* coding sequence (1485 bp), Lane 4: scar of *ΔicsA* (102 bp); Lane 5: scar of *ΔicsB* (102 bp).

ΔicsA and *ΔicsB* mutants were successfully constructed using the *λ* red recombination system (Datsenko & Wanner, 2000). Plasmid pKD4 was used as DNA template to amplify the cassettes *icsA*-kan and *icsB*-kan. The two amplicons were purified using a Qiagen gel extraction kit. The Kan-cassettes were electroporated

into wild-type *S. sonnei* harbouring plasmid pKD46 which expresses *λ* red recombinase, the enzyme that mediates recombination between the Kan-cassettes and *icsA* and *icsB*, respectively. Full lengh of *icsA* coding sequence was 3308bp, while full length *icsB* coding sequence was confirmed to be verified as 1484bp (Fig. 8, lanes 2, 3). Selection on kanamycin-agar (50 µg/mL) at 37 ^{o}C overnight allowed selection of colonies whose *icsA* or *icsB* genes had been replaced by the respective kan-cassettes, and in which pKD46 which is temperature sensitive, had been eliminated. Plasmid pCP20, which expresses FLP recombinase, was then introduced into the *icsA*-kan and *icsB*-kan mutant strains to eliminate the Kan-cassette. The mutant bacteria were then cultured at 43 °C to eliminate pCP20. The majority of the transformants had lost the FRT-flanked Kan gene and the helper pCP20 plasmid following culture at 43 °C, resulting in a 102 bp scar fragment in *ΔicsA* and *ΔicsB* strains, respectively (Fig. 8, lane 4 and 5). In later stages of the study, a *ΔdsbA* mutant *S. sonnei* was also constructed using the same procedure. These results confirm that the *λ* recombination system is an efficient and rapid method for producing gene deletions in *S. sonnei*.

3.2 Actin-based motility is crucial for *S. sonnei* intracellular growth:

Since actin-based motility is the trigger for the initiation of septin cage formation and autophagy in host cells in order to restrict *Shigella* growth, mutant strains *ΔicsA* and *ΔicsB* were analysed to establish whether they were defective in intracellular growth as a result of impaired actin polymerisation, compared to wild-type *S. sonnei*. The gentamicin-killing assay was performed using HEK293 cells, which were infected with wild-type *S. sonnei* and the two mutant strains. Compared to wild-type *S. sonnei*, the *ΔicsA* mutant yielded significantly fewer intracellular CFUs 5 h post infection ($p < 0.003$), whereas the *ΔicsB* mutant yielded a modest, through statistically non-significant, decrease in the number of intracellular CFUs. This decrease in intracellular CFUs by the *ΔicsB* mutant had been observed previously, and was found to be the result of autophagy, which led to *Shigella* bacteria lacking IcsB becoming trapped (Ogawa *et al.*, 2005). However, the addition of 10 μM cytochalasin D, which effectively prevents actin polymerisation during infection result in all three strains yielding significantly fewer intracellular CFUs compared to

untreated *Shigella* infected wild-type cells (Fig. 9). Thus, actin-based motility is required for *S. sonnei* intracellular growth.

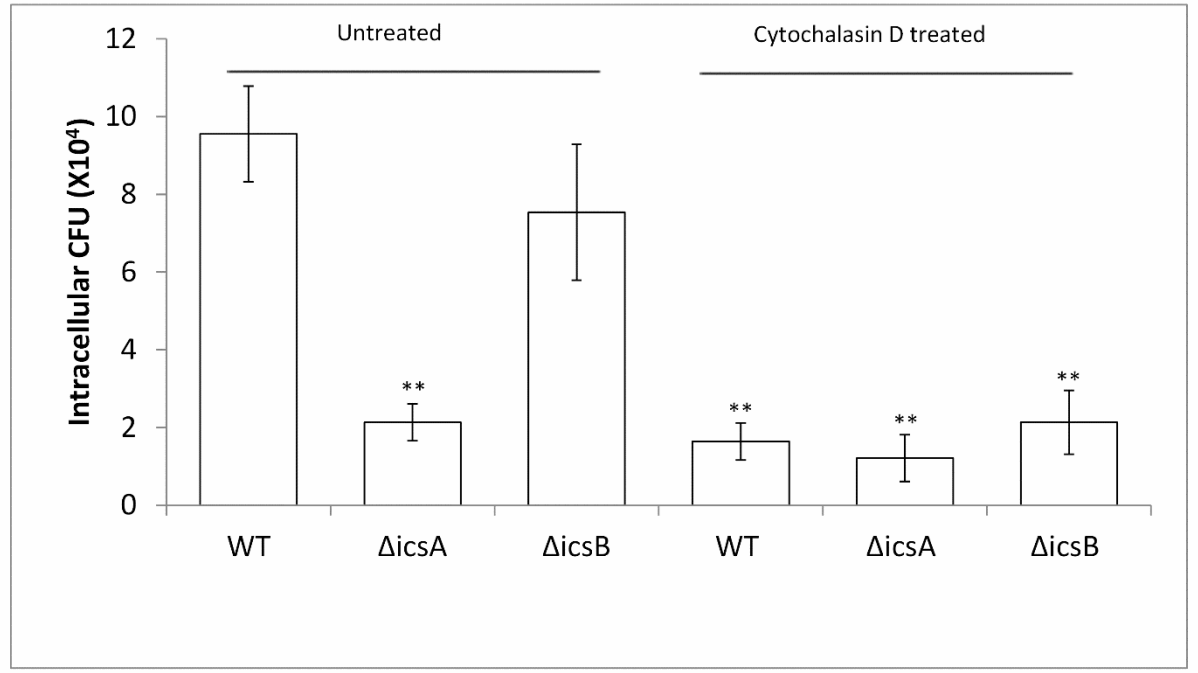

Figure 9. Impact of actin polymerisation to intracellular growth of *Shigella sonnei*. HEK293 cells infected with *S. sonnei* strains (WT = wildtype, *ΔicsA* and *ΔicsB*) for 5 hours with and without treatment of cytochalasin D. The experiments were carried out in triplicate 3 times. Pooled data were shown as means ± SD. Comparison was made between WT untreated and WT treated with cytochalasin D, and between WT untreated and the *ΔicsA* and *ΔicsB* mutants with or without cytochalasin D treatment. Differences between groups were assessed using the Bonferroni correction. Asterisks depict statistical significance (**: $p < 0.003$).

3.3 Microscopic analysis of actin polymerisation by intracellular bacteria and the effect of propolin D:

One possible explanation for the reduced intracellular growth of *ΔicsA* mutant could be that septin cages are more active against the mutant than wild-type *S. sonnei*. Septin cage formation is directly associated with actin polymerisation by intracellular *Shigella*. Since the autophagy machinery recognises IcsA and indirectly participates in septin cage formation (Mostowy et al., 2010), the participation of actin polymerisation in inhibiting *Shigella* spread in the presence and absence of IcsA and propolin D, respectively, was examined.

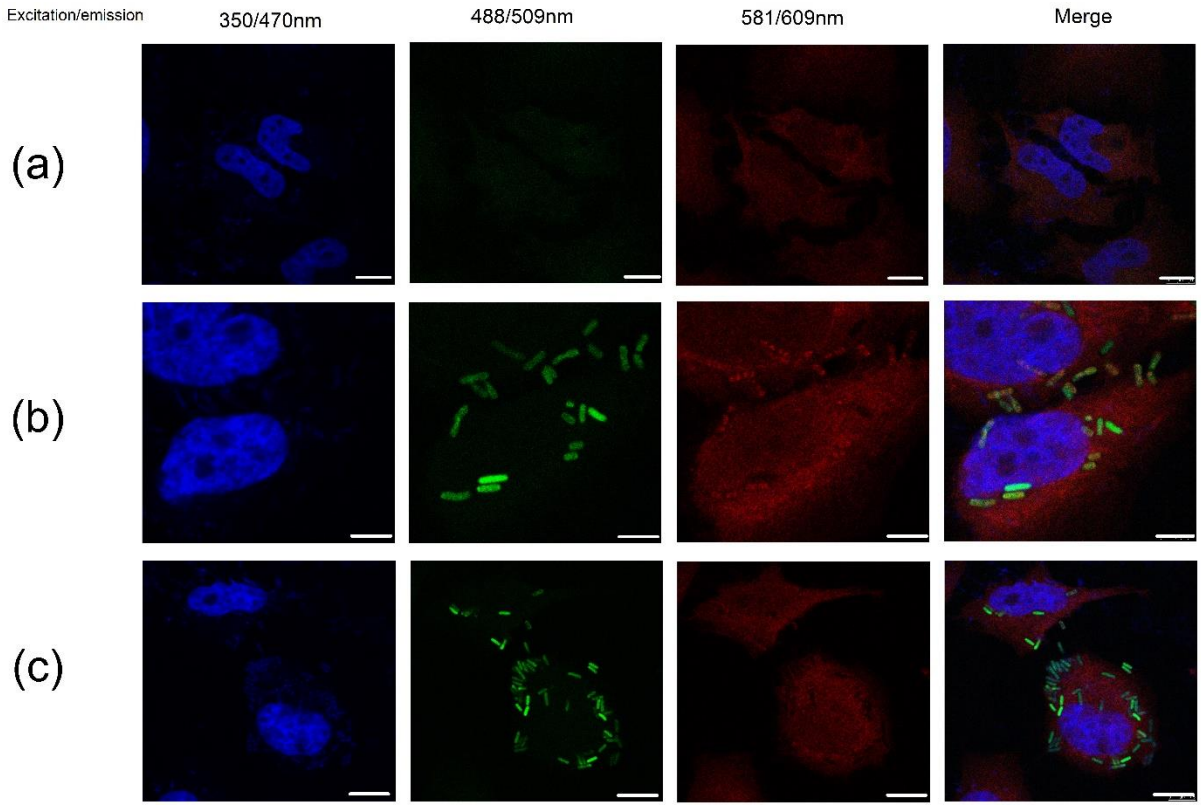

Figure 10. Confocal microscopy of HeLa cells and intracellular *ΔicsA* mutant. HeLa cells were mock infected (with PBS) or infected for 5 hours with *ΔicsA* which expressed GFP. Cells were fixed with paraformaldehyde and stained with DAPI. (a) mock infected cells; (b) cells infected with *ΔicsA* mutant expressing GFP protein (c) cells infected with *ΔicsA* mutant expressing GFP where Propolin D (42μM) was supplemented in the culture medium during infection. Size bars of the image for a, b and c are 10, 5 and 7.5 μm respectively.

HeLa cells were infected with the *ΔicsA* mutant that was carrying pEGFP, which expresses enhanced green fluorescent protein. The infected cells were examined under a confocal microscope. No actin tail formation behind the *ΔicsA* mutant bacteria was observed (Fig. 10). In contrast, the wild-type *S. sonnei* strain produced

actin tails behind the moving bacteria (Fig. 11). This result confirms that IcsA mediates actin polymerisation.

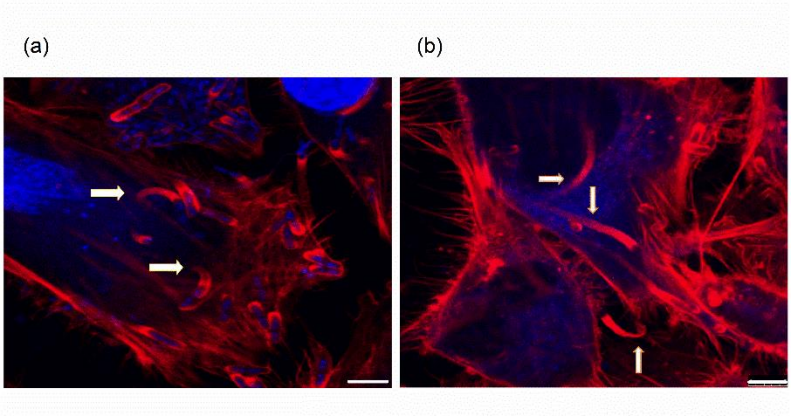

Figure 11: Confocal microscopy on HeLa cells infected with wild-type *S. sonnei*. Cells were infected for 5 hours, during (a) without supplementation of propolin D in the culture medium (DMEM) (b) with 42μM of propolin D supplemented in the culture medium (DMEM). Cells were fixed with paraformaldehyde and stained with Alexa Fluor® 594 phalloidin. Actin-tails are observed behind intracellular bacteria (arrows). Size bars of the image for (a) and (b) are 5 μm.

Furthermore, the image in Figure 11 (b) was generated in the presence of 42 μM of propolin D, which confirms that propolin D does not affect the ability of *Shigella* to polymerise host actin. Formation of septin cages is complex; the data obtained did not indicate whether propolin D promotes or inhibits septin cage formation. The

observed inhibition of intracellular *Shigella* growth by propolin D is presumably independent of septin cage formation.

3.4 Autophagy is a mechanism of innate defence against *S. sonnei* infection and natural products enhance autophagy activity:

To investigate whether autophagy plays a role in the innate defence against *Shigella* infection, an *ATG5*-knockout HEK293 cell-line was exploited; ATG5 encodes a crucial component of the autophagy process that is involved in the maturation of autophagosome. Both wild-type and *ATG5* KO cells were analysed in a gentamicin-killing assay. Four hour post-infection, the intracellular CFU was significantly higher in *ATG5* KO cells compared to wild-type HEK293 cells. This result confirms a previous report that autophagy is one of the host cell defence mechanisms that act against intracellular *Shigella* (Kayath *et al*., 2010). Prompted by the finding of a previous report by Xu *et al*. (2011), propolin D and other natural compounds were tested for activity in promoting autophagy for the control intracellular *S. sonnei*. The results were striking (Fig. 12). All the tested compounds significantly reduced intracellular CFU in wild-type HEK293 cells. However, none reduced intracellular

CFU in *ATG5* KO cells. Thus, these compounds help host cells control *Shigella* infection by promoting autophagy.

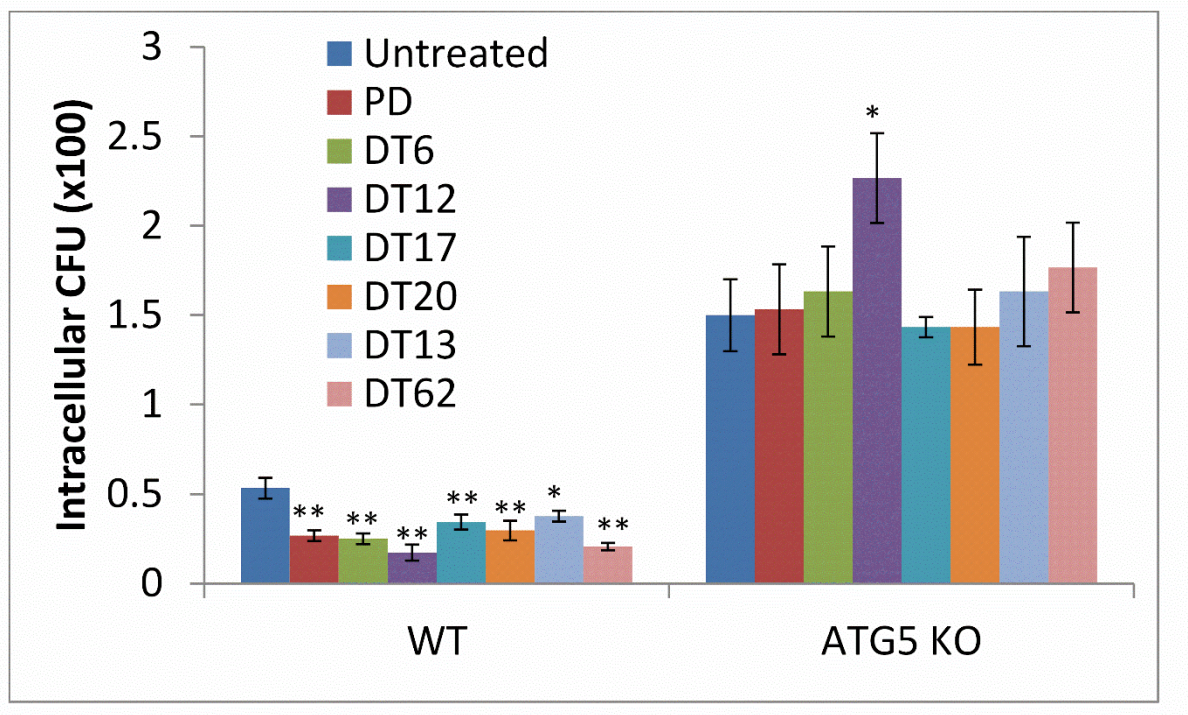

Figure 12. Autophagy is involved in the control of *Shigella* intracellular growth and natural compounds enhance autophagy. Wildtype and *ATG5*-knockout HEK293 cells infected with *S. sonnei* for 4 hours with and without treatment of 7 natural products. The experiments were carried out in triplicate 4 times (N=4, n=3). Pooled data are shown as means ± SD. Differences between groups were assessed using the Bonferroni correction test. Asterisks depict statistical significance (* : $P < 0.016$ and ** : $P < 0.003$).

It has been previously reported that IcsB binds a motif in IcsA to evade autophagy and that loss of IcsA results in complete evasion of autophagy (Kayath *et al.*, 2010). Hence, it would be informative to test whether these natural products work in the

ΔicsB genetic background. The results demonstrated that a number of these compounds, of which propolin D was the most potent, significantly reduced intracellular CFU of the *ΔicsB* mutant 5 h post-infection (Fig. 13). Propolin D is the most potent with a *p* value = 9.12679E-07. Thus, propolin D is more effective when *S. sonnei* is unable to evade autophagy.

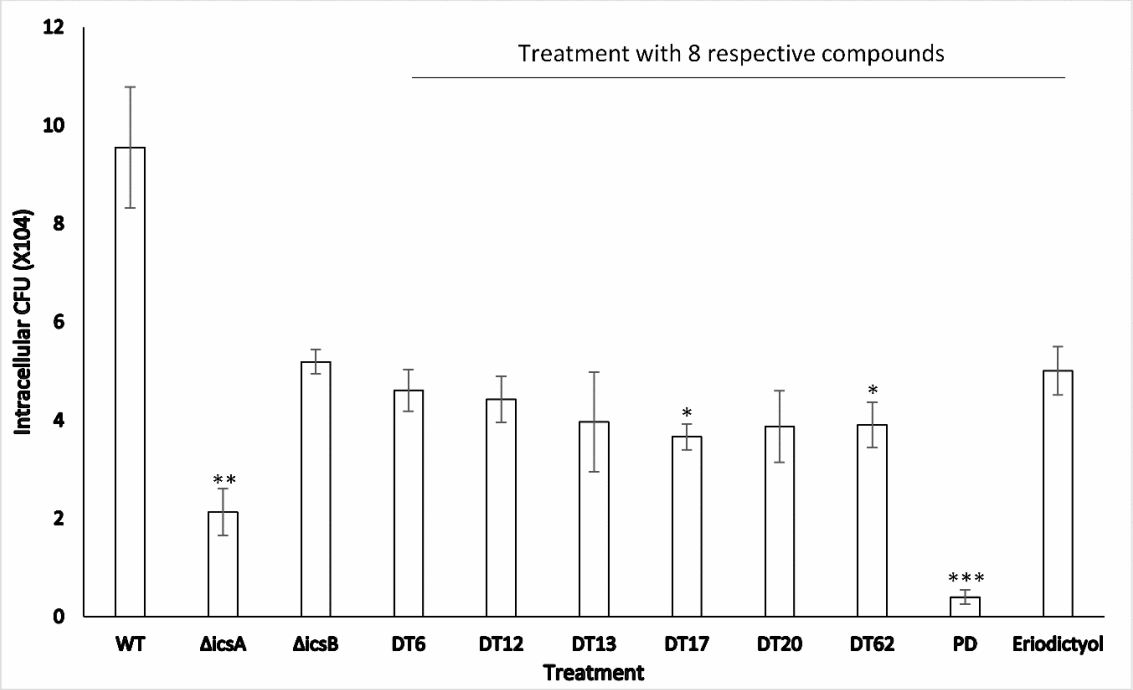

Figure 13. Impact of natural products to intracellular growth of *S. sonnei ΔicsB* mutant. HEK293 cells were infected with wild-type, *ΔicsA*, and *ΔicsB* strains for 5 h in DMEM containing gentamicin. DT6 to DT62 and PD and eriodictyol represent *ΔicsB*-infected cells with supplementary of 8 respective natural products. Experiments were carried out in triplicate 3 times (N=3, n=3). Data were collectively shown as means ± SD. Differences between untreated and treated groups were assessed using the Bonferonni correction t test. Asterisks depict statistical significance (*: $p < 0.016$) (**: $p < 0.003$) (***: $p < 0.0003$). Propolin D is most potent in inhibiting intracellular growth of the bacteria.

3.5 Cytotoxicity of the flavonoids by (MTT) assay on HEK293 cells:

Prior to further investigation of propolin D and other natural products for their therapeutic potential, it was necessary to test their cytotoxicity. The rationale behind this is that if these compounds are cytotoxic, intracellular bacteria may be killed by gentamicin that penetrated damaged host cell membranes. Cell cytotoxicity of the eight compounds was tested by MTT assay. The results showed that seven natural products exhibited no cytotoxicity. However, compound DT-6 reduced cell viability (Fig. 14). The results confirm that these seven compounds do not assist gentamicin-mediated killing of intracellular bacteria. The results also confirm that these compounds are able to help host cells control *Shigella* infection through their effect on autophagy.

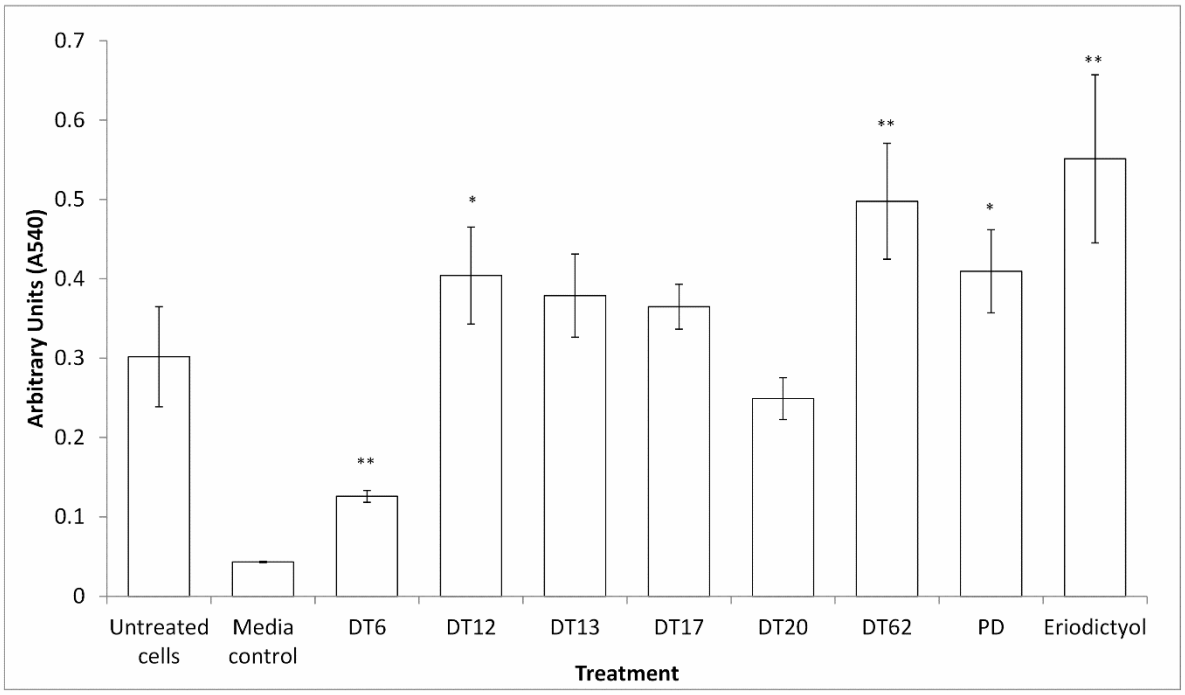

Figure 14. MTT assay for cytotoxicity of natural products to HEK293 cells. Cells were cultured in DMEM without or with supplementation of natural products (all 42 μM) overnight. Cells were washed with PBS and incubated with MTT solution (48 μM) for 40 min. Purple precipitates were solubilised with DMSO and absorbance was measured (540 nm) and expressed as arbitrary units (Y-axis). Experiments were carried out in triplicate 4 times (N=4, n=3). Pooled data were shown as means ± SD. Differences between untreated controls and treated groups were assessed using the Bonferroni correction t test. Asterisks depict statistical significance (*: $p < 0.016$; **: $p < 0.003$).

3.6 Microscopic detection of flavonoids in the cell:

As many of the compounds tested inhibit intracellular growth of *S. sonnei* (both wild-type and the *ΔicsB* mutant) by assisting host autophagy (Fig. 12 and 13), it is of interest to investigate whether they penetrate cells and directly act on intracellular bacteria. Flavonoids are known to be fluorescent, but the signals are too weak to be

detected by fluorescence microscopy. However, acridine orange can be used to enhance the intensity of the fluorescence (Myc *et al.*, 1991). Cells were first treated with various flavonoids, and then overlaid of the cell monolayer with acridine orange to detect flavonoids in the cells via fluorescence microscopy. The results showed that while propolin D accumulated at high levels in the host cells (Fig. 15), none of the other flavonoids tested were detected inside cells, except eriodictyol, which accumulated at low levels. These data suggest that propolin D may directly act on intracellular *S. sonnei* in addition to its role in promoting autophagy (Fig. 12). Other compounds may exert their anti-*Shigella* activity by interacting with the cell membrane; however, the underlying mechanisms remain to be determined. It is also important to note that eriodictyol, a compound that has the same structure as propolin D except that it lacks a terpene side-chain, accumulated at much lower level in the host cells (Fig. 15). Moreover, this compound does not promote autophagy (Fig. 13). Thus, the terpene side-chain in propolin D appears to be the key moiety to determine cell penetration and intracellular activity.

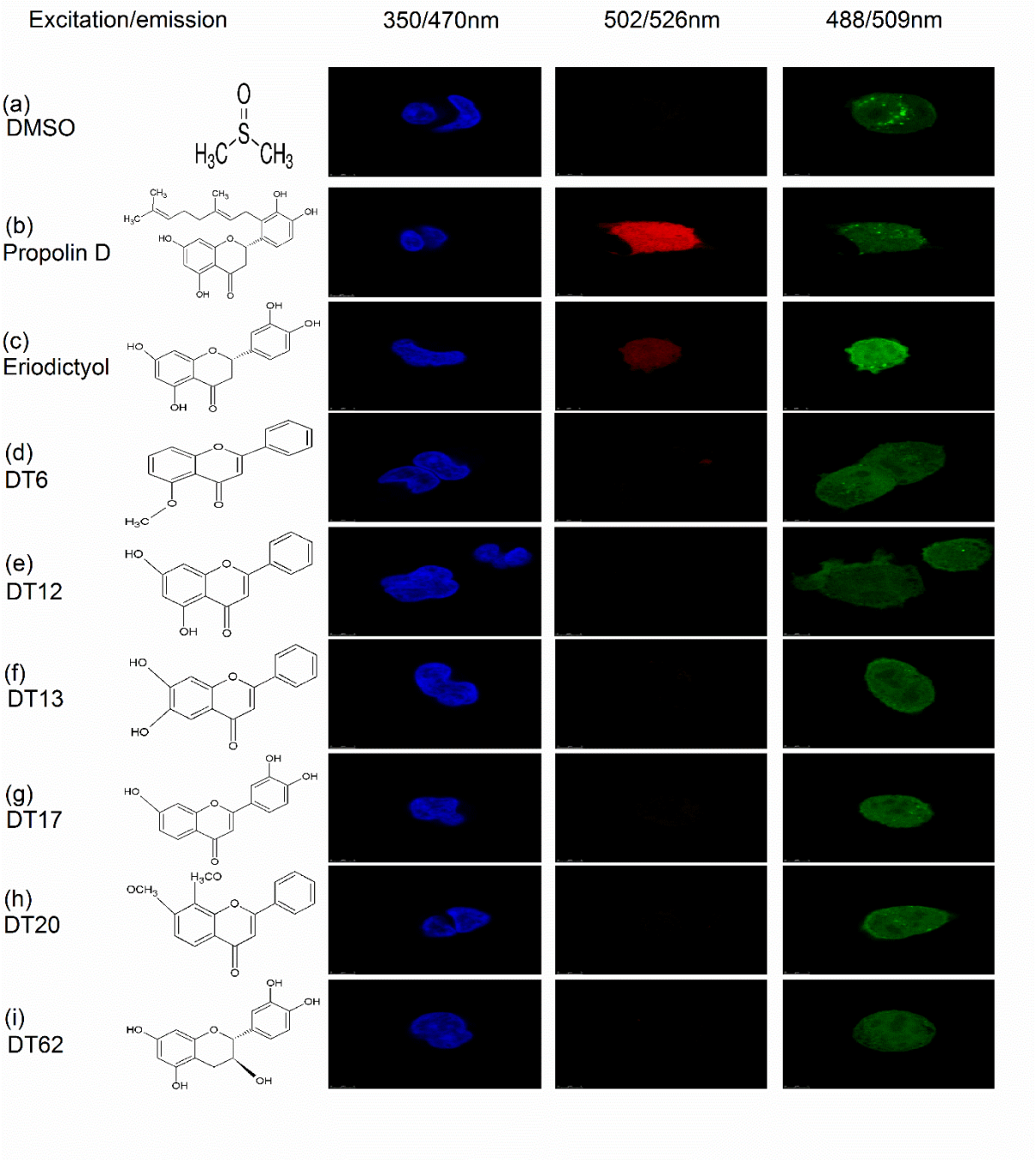

Figure 15. Detection of flavonoids in the cell. HEK293 cells were treated with various flavonoids for 5 hours at 37 °C, followed by acridine orange stain. (a) DMSO (127 μM); (b) Propolin D; (c) Eriodictyol; (d) 5-Methoxyflavone; (e) Chrysin (5,7-dihydroxylflavone) ; (f) 6,7-Dihydroxyflavone; (g) 3',4',7-trihydroxyflavone; (h) 7,8-dimethoxyflavone; (i) (-)-Catechin. Note: DMSO supplemented DMEM was used as controls because all the flavonoid were dissolved in DMSO and 127 μM DSMO was supplemented with each of the compounds. Acridine orange enhances fluorescence emission from flavonoids. Cell actin was stained with Alexa Fluor 488® phalloidin.

Chapter 4: The action of propolin D and monoterpenes on DsbA *in vitro*

The aim of this chapter initially was to investigate the activity of propolin D on growth of *S. sonnei* both *in vitro* and inside cultured host cells. As propolin D was anticipated to cause envelope stress on *S. sonnei*, the regulation of a set of genes involved in envelope stress responses was investigated. Consequently, a key gene, *dsbA*, which is responsible for envelope stress, was further investigated. This led to the hypothesis that the terpenoid side chain of the propolin D exerted inhibitory activity on the function of DsbA. DsbA protein and an active mutant derivative, DsbA33G, were purified and their enzymatic activity in reduction of oxidised glutathione (GSSG) was evaluated in the presence and absence of monoterpenes, including geraniol and geranyl acetate.

4.1 Propolin D inhibits growth of *S. sonnei in vitro* :

Since propolin D accumulated at high levels in cells (Fig. 15), it was hypothesised that propolin D may have direct anti-*Shigella* activities in the host cell cytosol. Previous demonstrations that propolin D does not have any direct activity against Gram-negative bacteria *in vitro* (Raghukumar *et al.*, 2010) suggest that propolin D only works

inside the host cell cytosol. Since the cell cytosol is a reducing environment (see introduction), it is possible that propolin D exhibits anti-*Shigella* activity under reducing conditions. To test this hypothesis, *S. sonnei* was adapted to M9 minimal medium, which can be conditioned by supplementing with reduced glutathione (GSH). Fig. 16 shows the growth of *S. sonnei* in M9 medium supplemented with propolin D or eriodictyol in the presence of 5 or 10 mM GSH. As can be seen, addition of propolin D significantly reduced bacterial growth in the presence of 5 mM GSH. Bacterial growth was further reduced when 10 mM GSH was added to the medium. In contrast, addition of eriodictyol and GSH made no difference to bacterial growth at all. The difference between propolin D and eriodictyol is that the former has a terpenoid side-chain whereas the latter does not. Hence, this terpenoid side chain seems to determine the properties of the compound with respect to the inhibition of *Shigella* growth in reducing M9 medium. These data led the speculation that propolin D might have a direct anti-*Shigella* activity inside the reducing host cell cytosol. The question to ask next is the mode of action, i.e. how propolin D acts on *Shigella* in the cell cytosol as well as in the reducing M9 medium.

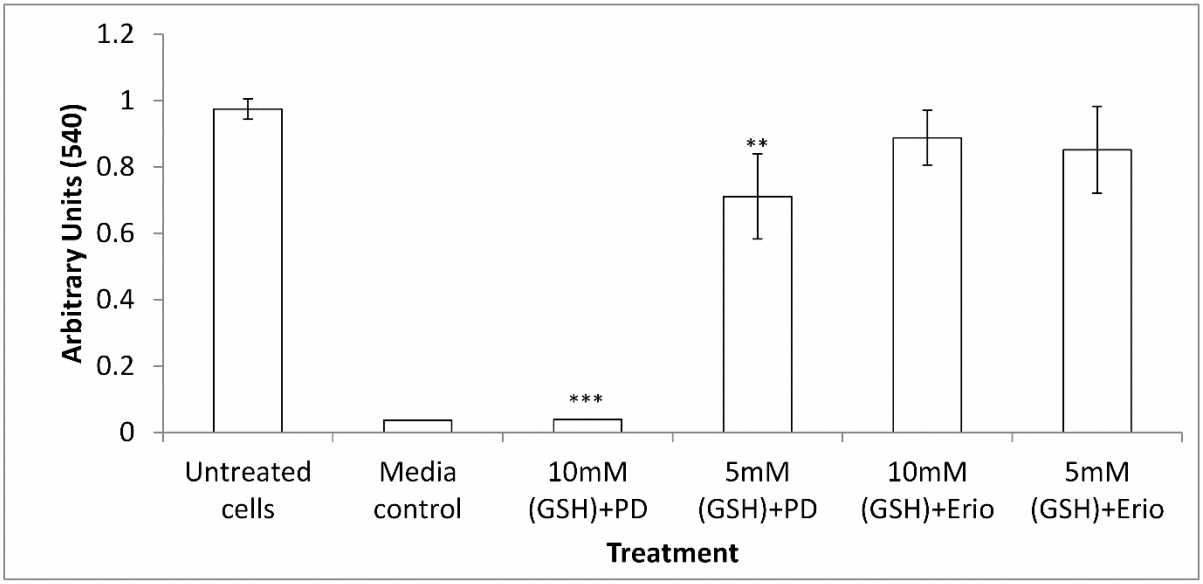

Figure 16. MTT assay for viability of *S. sonnei* in M9 medium. Bacteria were grown overnight at 37 °C in M9 without or with GSH and propolin D (PD) or eriodictyol (Erio). Experiments were carried out in triplicate and repeated 3 times. Pooled results were shown as means ± SD. Differences between untreated and treated groups were assessed using the Bonferonni correction t test. Asterisks depict statistical significance (**: $p < 0.003$; ***: $p < 0.0003$). 10mM GSH + propolin D is most potent in inhibiting intracellular growth of the bacteria.

4.2 Stress responses of *S. sonnei in vitro* :

Since *Shigella* DsbA protein is known to be important for *Shigella* growth in the cell cytosol (see introduction), propolin D was tested to establish whether it acts on DsbA. Therefore, a *dsbA* deletion mutant (*ΔdsbA*) was constructed and compared with wild-type *S. sonnei* under growth conditions in M9 medium. Fig. 17 shows the growth

curves of four different *S. sonnei* strains: wild-type *S. sonnei*, *S. sonnei ΔdsbA*, *S. sonnei ΔdsbA*/pDsbA, and *S. sonnei ΔdsbA*/pDsbA33G. DsbA33G is a mutant protein in which residue Cys33 in the active site has been substituted with a glycine (Charbonnier *et al.*, 1999). The *ΔdsbA* and *ΔdsbA*/pDsbA33G mutants displayed much longer lag phases. Furthermore, the growth rate of complemented strain *ΔdsbA*/pDsbA was comparable to wild-type *S. sonnei*. In contrast, the *ΔdsbA*/pDsbA33G mutant grew poorly compared to the other strains (Fig. 17). The doubling time for wild-type and *ΔdsbA*/pDsbA is one hour. The doubling time for *ΔdsbA* and *ΔdsbA*/pDsbA33G is one and a half hour. Differences between groups were assessed using Bonferroni's multiple comparisons test (Table 4). These data demonstrate that functional DsbA is required for *S. sonnei* survival in a reducing environment.

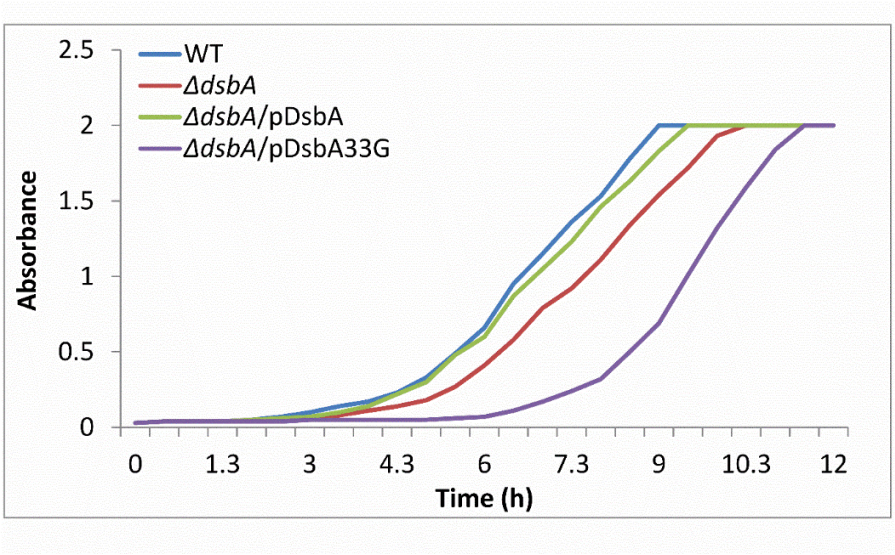

Figure 17. Growth curve of *S. sonnei*. All strains were grown in M9 broth at 37 °C with shaking (200 rpm). OD600nm was taken at time intervals shown in X-axis. WT: wild type; *ΔdsbA*: deletion mutant; *ΔdsbA*/pDsbA: the deletion mutant expressing wildtype DsbA protein from the plasmid; *ΔdsbA*/pDsbA33G: the deletion mutant expressing mutant DsbA33G protein from the plasmid.

Table 4.1 Bonferroni's multiple comparisons test of the growth curves in figure 17 using Graphpad Prism software.

Test pair	Mean	95% confidence interval (CI)	Statistical significance	*P* Value
WT vs. *ΔdsbA*	0.1496	0.06068 to 0.2385	**	0.0007
WT vs. *ΔdsbA*/pDsbA	0.0368	0.01023 to 0.06337	*	0.0047
WT vs. *ΔdsbA*/pDsbA33G	0.4304	0.1859 to 0.6749	**	0.0004

To demonstrate that DsbA is responsible for ameliorating adverse conditions to support the growth of *S. sonnei*, the wild-type strain and the *ΔdsbA* mutant were grown in M9 medium supplemented with salt (a general stress condition) or GSH (a specific

stress condition mimicking the reducing cell cytosol). Fig. 18a shows that the growth of wild-type *S. sonnei* was significantly reduced at a concentration of 250 mM NaCl and completely ceased in the presence of 500 mM salt. The doubling time was one hour without supplement but extended one and a half hour in the presence of 150 or 250 mM NaCl. Differences between the two strains were assessed using Bonferroni's multiple comparisons test (Table 5). Fig. 19a shows that wild-type *S. sonnei* grew equally well in the presence or absence of 5 mM GSH. However, when 5 mM GSH and 42μM propolin D were included together in the medium, the growth of the wild-type strain was significantly reduced (Fig. 19a). The doubling time was one hour in the presence of 5 mM GSH, but increased to one and a half hours in the presence of 5 mM GSH and 42 μM propolin D. These results suggest that propolin D completely inhibits *S. sonnei* strain 86 at that these concentrations (Fig. 19a).

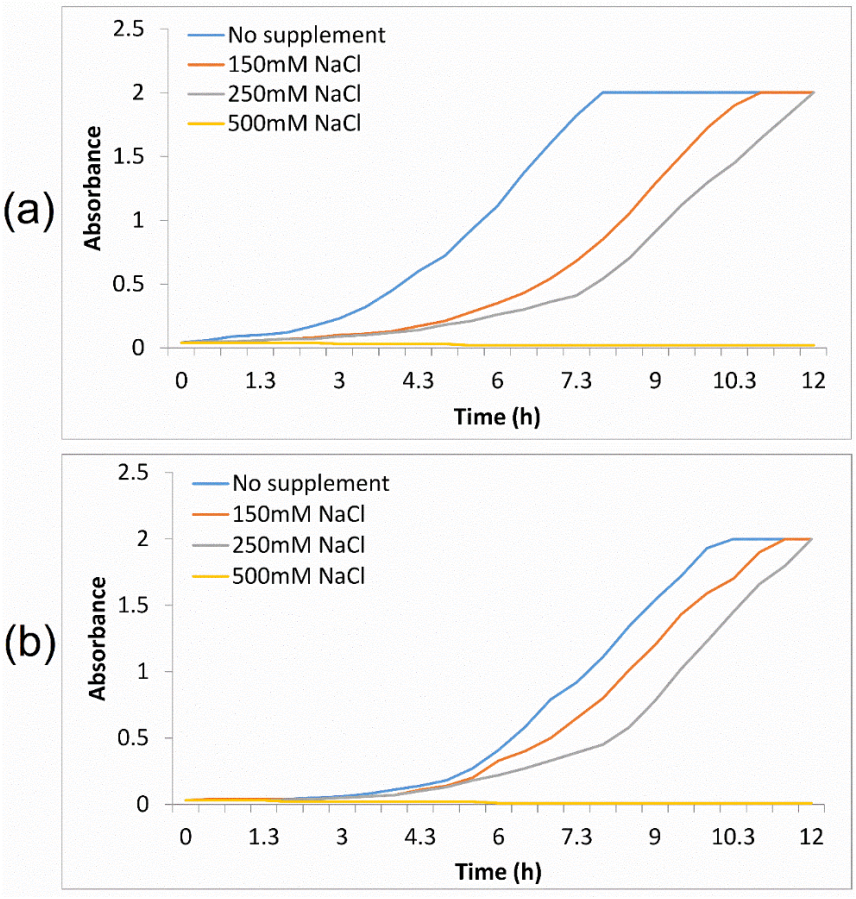

Figure 18. Growth curves of *S. sonnei* and *ΔdsbA* mutant under different growth conditions. Wild-type *S. sonnei* were grown in M9 media supplemented (a) without or with sodium chloride (NaCl), and (b) The *ΔdsbA* mutant was grown in M9 media supplemented without or with different concentrations of sodium chloride (NaCl).

Table 5: comparison of statistical significance of the growth curves in figure 18 using Graphpad Prism software.

Test pair	Mean.	95% confidence interval (CI)	Statistical significance	*P* Value
No supplement (WT) vs. 150mM NaCl	0.4016	0.1931 to 0.6101	***	0.0001
No supplement (WT) vs. 250mM NaCl	0.5492	0.2964 to 0.8020	***	< 0.0001
No supplement (*ΔdsbA*) vs. 150mM NaCl	0.1220	0.05124 to 0.1928	**	0.0005
No supplement(*ΔdsbA*) vs. 250mM NaCl	0.2580	0.1093 to 0.4067	**	0.0005

The growth curve of the *ΔdsbA* mutant was determined to compare with wildtype *S. sonnei*. In the presence of 100 mM and 250 mM NaCl, the growth was significantly (p value < 0.0001) slower than non-supplemented controls, with growth ceasing in the presence of 500 mM NaCl (Fig. 18b). Without supplement, the doubling time (Fig. 18b) was one and a half hours, but increased to two hours in the presence of 150 or 250 mM NaCl. In the presence of 5 mM GSH (Fig. 19b), the mutant grew as well as it did in medium without any supplement. However, the growth was significantly reduced when the 5 mM GSH medium was supplemented with 42 µM propolin D, with the doubling time of one and a half hours in supplemented-free of 5 mM GSH-supplemented medium (Fig. 19b) increasing to two hours in the presence propolin D. The *ΔdsbA* mutant also displayed a longer lag phase compared to that of the wild-type. Differences between the groups were assessed using the Bonferroni's multiple comparisons test (Table 6). The *ΔdsbA* mutant had a lag phase of ~5 h before entering the exponential phase under each of the stress conditions, while the lag phase of wild-type *S. sonnei* was ~3 h under the same conditions.

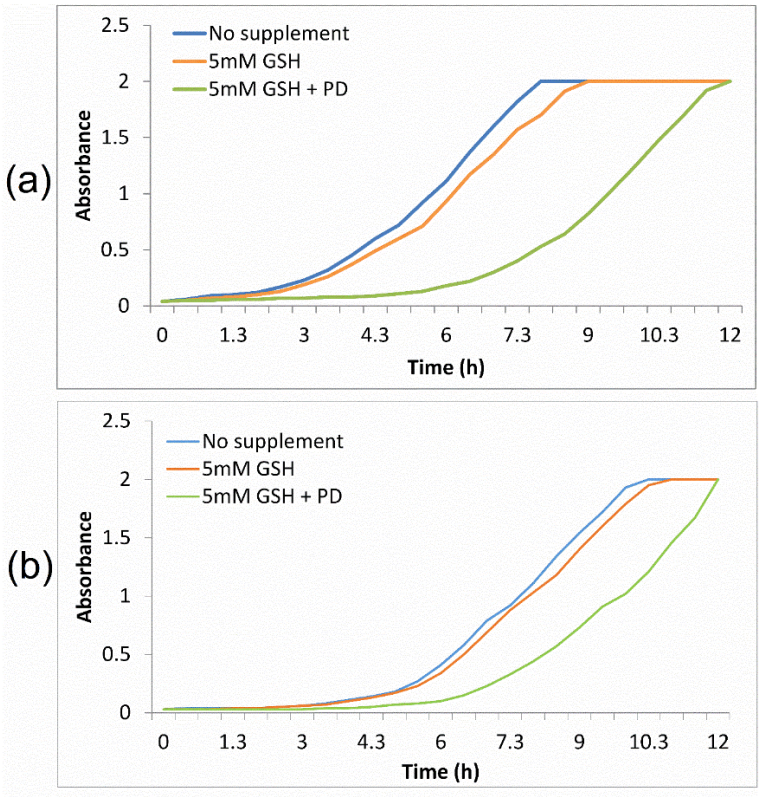

Figure 19. Growth curves of *S. sonnei* and *S. sonnei ΔdsbA* mutant under different conditions. Wild-type *S. sonnei* were grown in M9 media supplemented (a) without or with 5 mM GSH or 5 mM GSH + 42 µM propolin D (PD) and (b) The *ΔdsbA* mutant was grown in M9 media supplemented 5 mM GSH or 5 mM GSH + 42 µM propolin D (PD).

Table 6: Comparison of statistical significance of the growth curves in figure 19 using Graphpad Prism software.

Test pair	Mean.	95% confidence interval (CI)	Statistical significance	*P* Value
No supplement (WT) vs. 5mM GSH	0.08000	0.03415 to 0.1258	**	0.0007
No supplement (WT) vs. 5mM GSH + PD	0.5748	0.3277 to 0.8219	***	< 0.0001
No supplement (*ΔdsbA*) vs. 5mM GSH	0.0432	0.01802 to 0.06838	**	0.0008
No supplement (*ΔdsbA*) vs. 5mM GSH + PD	0.3244	0.1675 to 0.4813	***	< 0.0001

4.3 Envelope stress responses of wild-type *S. sonnei* and the *ΔdsbA*:

Since it is known that *dsbA* is one of the genes responsible for bacterial envelope stress (Raivio, 2005), the regulation of *dsbA* and other stress genes under the stress conditions shown in Fig. 18 and 19 was analysed. The purpose was to investigate whether propolin D in the presence of GSH causes a specific stress that contributes to the inhibition of bacterial growth, as compared to high osmotic stress.

Total RNAs were isolated from cultures at exponential phase under the stress conditions shown in Fig. 18 and Fig. 19. The quality of the RNA samples was adequate for qPCR, as shown in Fig. 20.

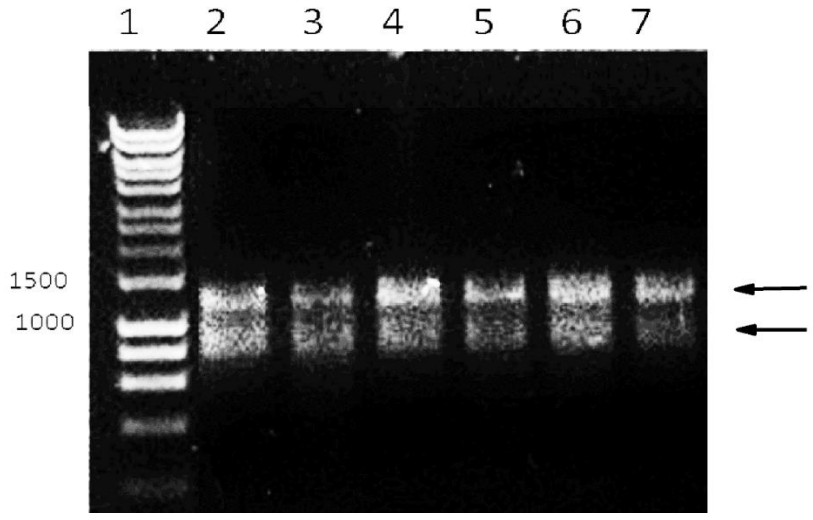

Figure 20: Total RNA isolated from WT (lanes 2-4) and the *ΔdsbA* strains (lanes 5-7) cultured in M9 without or with various supplements: Lane 1 Hyperladder 1 (Bioline); lanes 2 & 5 42 µM propolin D + 5 mM GSH; lanes 3 & 6 5 mM GSH; lanes 4 & 7 150 mM NaCl. Arrows indicate ribosomal 23S and 16S RNA bands.

Four periplasmic space genes (*dsbA, fkpA, resB and spy*) known to be involved in envelope stress responses were analysed by real-time quantitative PCR (Fig.21). *dsbA* encodes periplasmic DsbA, which is required for disulphide bond formation in periplasmic proteins. *fkpA* encodes a periplasmic enzyme the exhibits both cis/trans peptidyl-prolyl isomerase (PPIase) and chaperone activities. *rseB* encodes an enzyme that modulates the activities of sigma-E (RpoE), while *spy* encodes a periplasmic enzyme that decreases protein aggregation and helps protein refolding. cDNA was synthesised from total RNA and amplification curves of *dsbA*, *fkpA*, *resB* and *spy*, and house-keeping gene, *cysG*, were obtained using a Rotor-Gene 6000 instrument (Life Technologies). The expression of these genes in M9 without supplement was set as calibrator (zero) and changed expressions under various stress conditions is shown as $2^{(-\Delta\Delta C_T)}$ values in a natural log scale. Technical details are described in material methods and figure legend (Fig. 21). The first experiment was to assess osmotic stress response in response to high concentrations of NaCl.

All four genes were upregulated by the addition of NaCl to the cultures for both wild-type and *ΔdsbA* mutant strains. These results suggest that hyperosmotic stress imposes a general stress on the bacterial envelope and that bacteria respond by upregulating all four genes. Changes observed for all four genes were small and mostly insignificant in the presence of 5 mM GSH for both wild-type and mutant strains. These results were consistent with the data shown in Fig. 19, which shows that growth of the wild type and the mutant was not significantly changed in the presence of 5mM GSH. Wild-type *S. sonnei* responded to the addition of supplements 5mM GSH and 42μM propolin D with significant up- and downregulation of *dsbA* and *spy*, respectively ($p < 0.001$). These data suggest that propolin D and GSH together induced a specific response that was different to that induced by hyperosmotic stress. Upregulation of *dsbA* is a specific response to reducing conditions, as *Shigella* requires *dsbA* to survive in the host cell reducing cytosol (Yu, 1998). Downregulation of *spy* (Spheroplast protein y), however, is intriguing and requires further investigation. Spy is an ATP-independent periplasmic chaperone involved in decreasing protein aggregation and helping protein refolding. Spy overexpression is regulated by ESR systems (extracytoplasmic stress response), which play important roles by regulating

gene expression in response to stress (Kwon *et al.*, 2010). Cpx and Bae (two-component systems of ESR) in *E.coli* upregulate Spy expression when the bacterial cell wall undergoes spheroplast formation (Kwon *et al.*, 2010). *spy* was not downregulated in the *ΔdsbA* mutant, suggesting that the ESR system is not active in this strain. The response of the *ΔdsbA* mutant differed from that of the wild type. While *spy* was not downregulated, *resB* was significantly downregulated ($p < 0.016$). The *Δ dsbA* gene was also downregulated, although to a lesser significant level ($p < 0.016$). *ΔdsbA* mutant has scar of *dsbA* which is a DNA fragment of *dsbA*. This results in expression of the *dsbA* gene despite it deletion. Thus, deletion of *dsbA* probably incurs a global change in response to stress caused by the presence of GSH + propolin D.

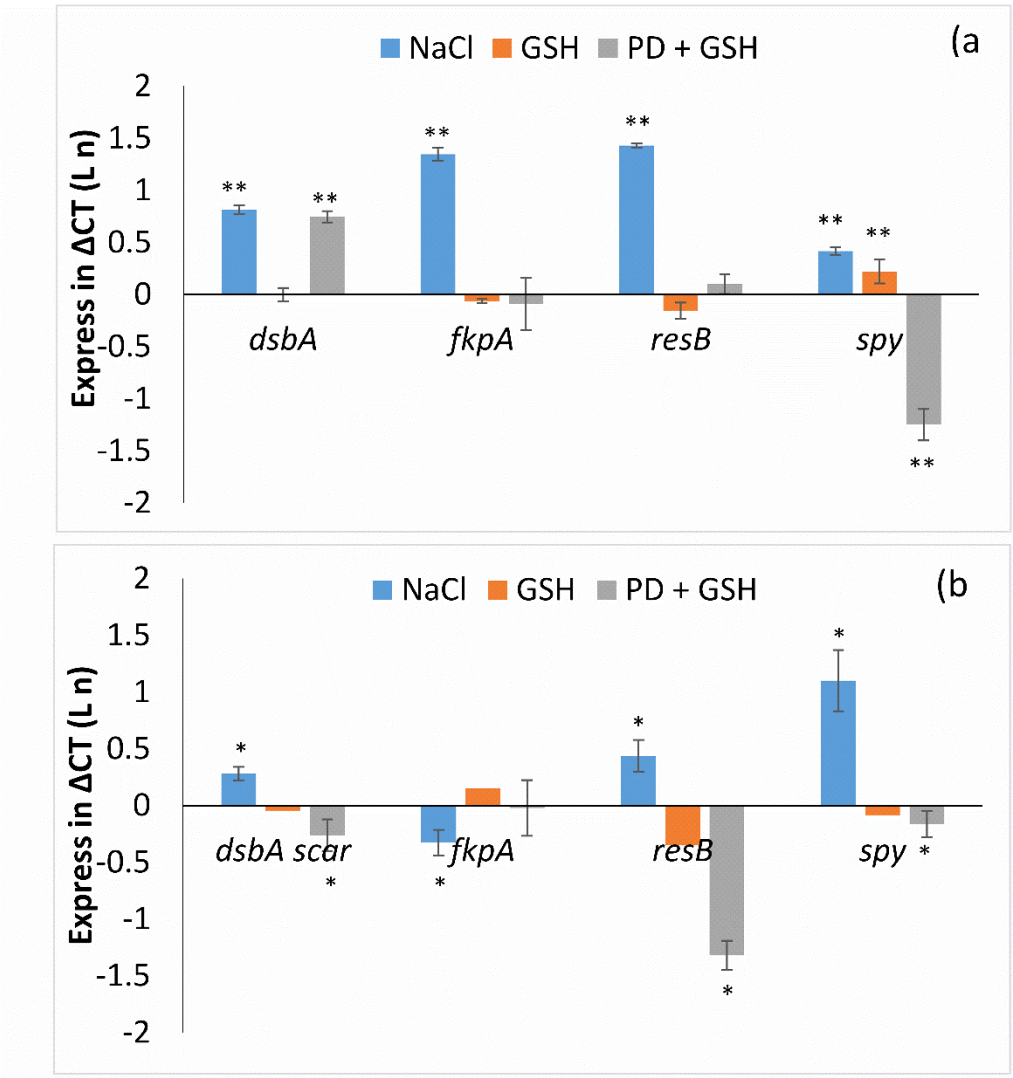

Figure 21. qPCR analysis of stress gene expression profiles of the wild-type *S. sonnei* (a) and the *Δ dsbA* mutant (b). Total RNA were isolated from bacteria grown under various growth conditions and four envelope stress genes *dsbA*, *fkpA*, *resB* and *spy* were subjected to the analysis. The house-keeping gene, *cysG*, was used as an internal control. The amplification curves of each of the genes were normalised with that of *cysG*, and quantification was calculated using the standard curves (see Materials and Methods). The levels of transcripts from bacteria grown without supplements were set as calibrator and levels of transcripts from bacteria grown with supplements were expressed as $2^{(-\Delta\Delta C_T)}$ values in natural log scale; values greater than and less than zero indicate higher and lower levels of gene expression in different growth conditions compared with bacteria grown without supplements. Differences between untreated and treated groups were assessed using the Bonferroni correction t test. Asterisks depict statistical significance (*: $p < 0.016$; **: $p < 0.003$).

4.4 DsbA purification:

The data obtained from sections 4.2 and 4.3 strongly suggests that propolin D may inhibit the function of DsbA in the reducing medium, resulting in slow *S. sonnei* growth. This result is consistent with the notion that propolin D accumulates in the host cells (Fig. 15), and the previous report that DsbA is required by *Shigella* to proliferate inside host cells (Yu, 1998). The interaction between propolin D and DsbA was therefore investigated. DsbA and mutant DsbA33G proteins were purified. Both proteins were tagged with 6X histidine and were isolated from periplasmic crude extracts followed His-tag purification, as outlined in Materials and Methods. Fig. 22 shows the purified proteins following SDS-PAGE and Western blot detection.

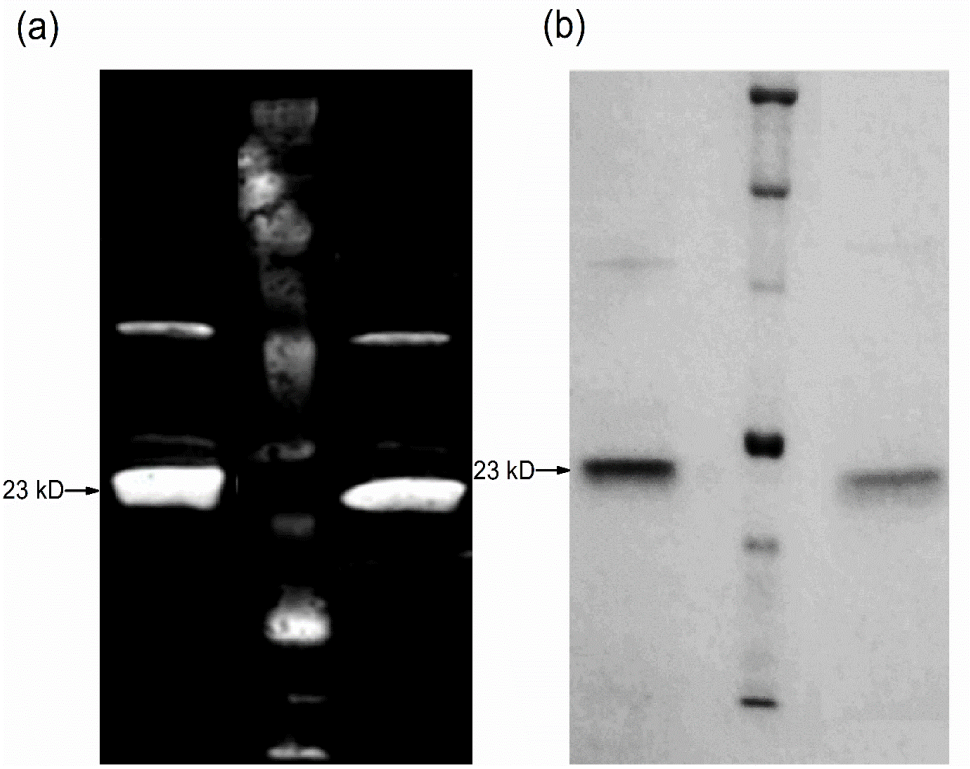

Figure 22. (a) Detection of DsbA-6XHis and DsbA33G 6XHis proteins by Western blot. Lane1: DsbA-6Xhis; Lane 2: protein marker; lane 3: DsbA33G-6XHis. The arrow on the left indicates DsbA protein on 10% polyacrylamide gel. 25 µL of purified protein sample (2.5 µg/mL of DsbA or DsbA33G) with 5 µL of protein loading buffer (BIORAD) were loaded in the gel. Proteins were transferred to a polyvinylidene difluoride (PVDF) membrane, and the membrane was incubated at 23 °C for 1 h with mouse anti-His primary antibody (Thermo Scientific). The membrane was washed with TBS and incubated Alexa flour 680 anti-mouse secondary antibody at 4°C for 2 h with (Thermo Scientific). Fluorescent signals were detected with an Odyssey infrared imaging system western blot scanner (LI-COR). (b) SDS-PAGE for purified DsbA and DsbA33G. Purified proteins (2.5µg each) were separated in 10% SDS-PAGE, and proteins were stained with the Coomassie staining solution. Lane1: DsbA-6XHis protein, Lane 2: protein marker, lane 3: DsbA33G-6XHis protein.

4.5 Reduction of GSSG by PDI, DsbA and DsbA33G *in vitro* :

DsbA is known to share a catalytic domain with mammalian disulphide isomerase (PDI). PDI from the ER of eukaryotic cells can effectively reduce fluorescently labelled Di-E-GSSG *in vitro* (Raturi & Mutus, 2007). This method was used to analyse the enzymatic activity of DsbA *in vitro* and to assess the function of propolin D in the inhibition of DsbA *in vitro*.

For kinetic analysis of DsbA proteins, Di-E-GSSG was prepared as described in Material and Methods. 1 mM eosin isothiocyanate was incubated with 100 µM glutathione disulphide at pH 8.8 to enable the conjugation of the two free amino groups of GSSG to two molecules of eosin, forming Di-E-GSSG. Fluorescence self-quenching (FSQ) occurs when eosin molecules are in close proximity, which makes the molecule weakly fluorescent (Fig. 23a). When the reducing agent dithiothreitol (DTT) is added to the solution, reduction of Di-E-GSSG occurs, leading to the separation of the two eosin molecules. This abolishes FSQ, resulting in the highly fluorescent molecule E-GSH (Fig. 23a). Complete reduction of Di-E-GSSG results in a 70-fold increase in fluorescence at emission 545 nm within 15 minutes (Fig. 23b).

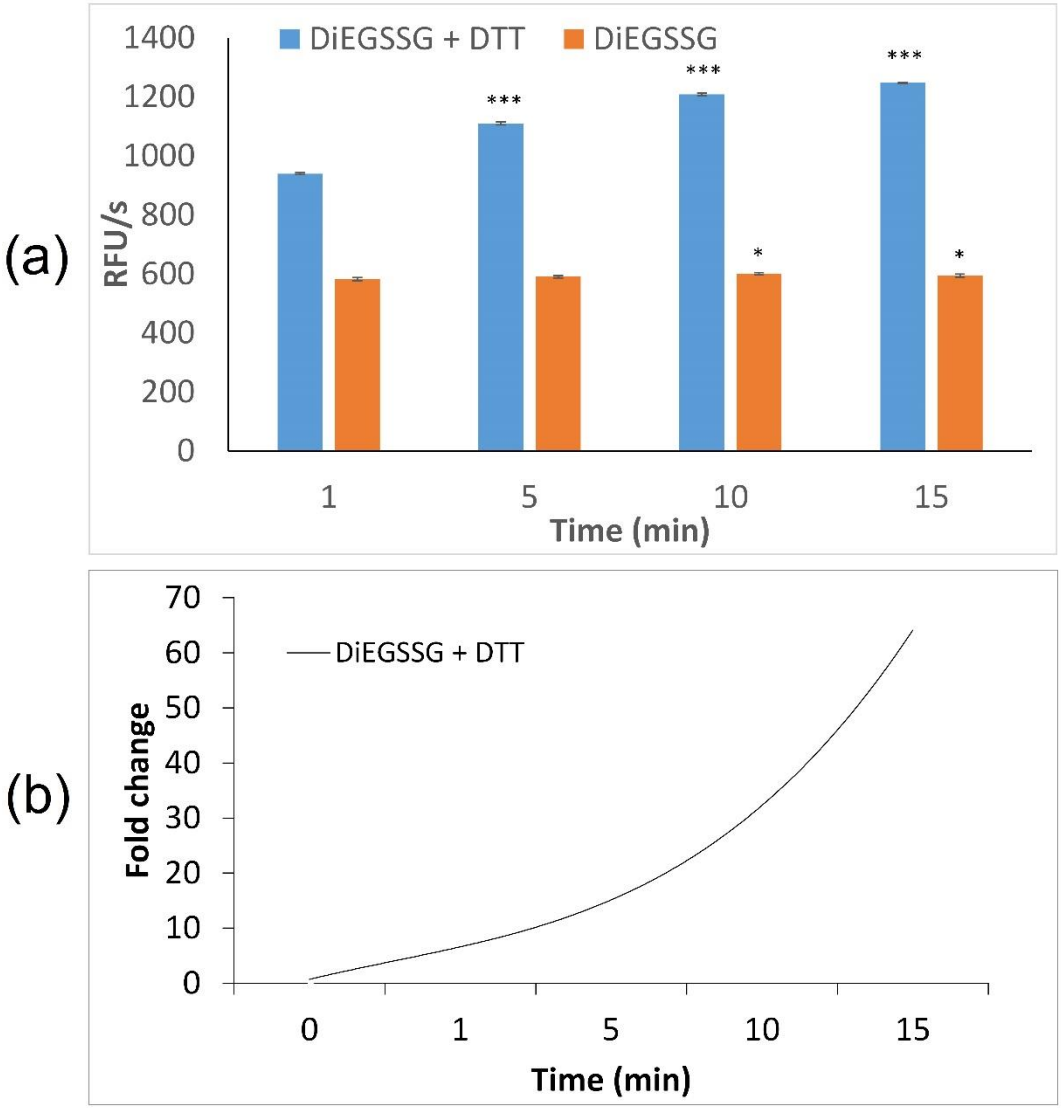

Figure 23. Reduction of Di-E-GSSG by DTT (10 mM). (a) Reduction of Di-E-GSSG by DTT. (b) Fold increase of Di-E-GSSG fluorescence by DTT. Buffer containing 150 nM Di-E-GSSG used as controls. Reduction of Di-E-GSSG was measured using a Spectamax plate reader (Molecular Devices); excitation 525 nm and emission 545 nm and expressed as Relative Fluorescent Units per second (RFU/s). There was no reduction of the Di-E-GSSG dilution buffer. 10 mM DTT converted Di-E-GSSG to EGSH in 15 min. 70 fold increase of fluorescence by 10 mM DTT was achieved in 15 min (b). Experiments were carried out in triplicate 3 times (N=3, n=3). Pooled results were shown as means ± SD. Differences between untreated and treated groups were assessed using the Bonferroni correction t test. Asterisks depict statistical significance (*: $p < 0.016$; ***: $p < 0.0003$).

Before testing DsbA, conditions for mammalian protein isomerase (PDI) in the reduction of Di-E-GSSG were tested (Raturi & Mutus, 2007). In order to determine the Vmax and Km values for PDI, various concentrations of Di-E-GSSG (50 nM-5 μM) were incubated with 40 nM PDI in PDI/DsbA buffer at room temperature for relative fluorescent unit per second (RFU/s) (Fig. 25a). Vmax (6.5s) and Km (600 nM ± 40 nM) were estimated for PDI using the Lineweaver-Burk plot (Prism) (Fig. 25b). The assay condition for PDI included 5μM DTT, which alone did not cause any reduction of Di-E-GSSG (controls in Fig. 24a & b). Following the addition of PDI (5, 10, 20 nM), a rapid increase in fluorescence as a function of time was observed (Fig. 24a). The Vmax values of the reaction were concentration dependent (5-20 nM) (Fig. 24b). These results demonstrate the disulphide reductase activity of PDI.

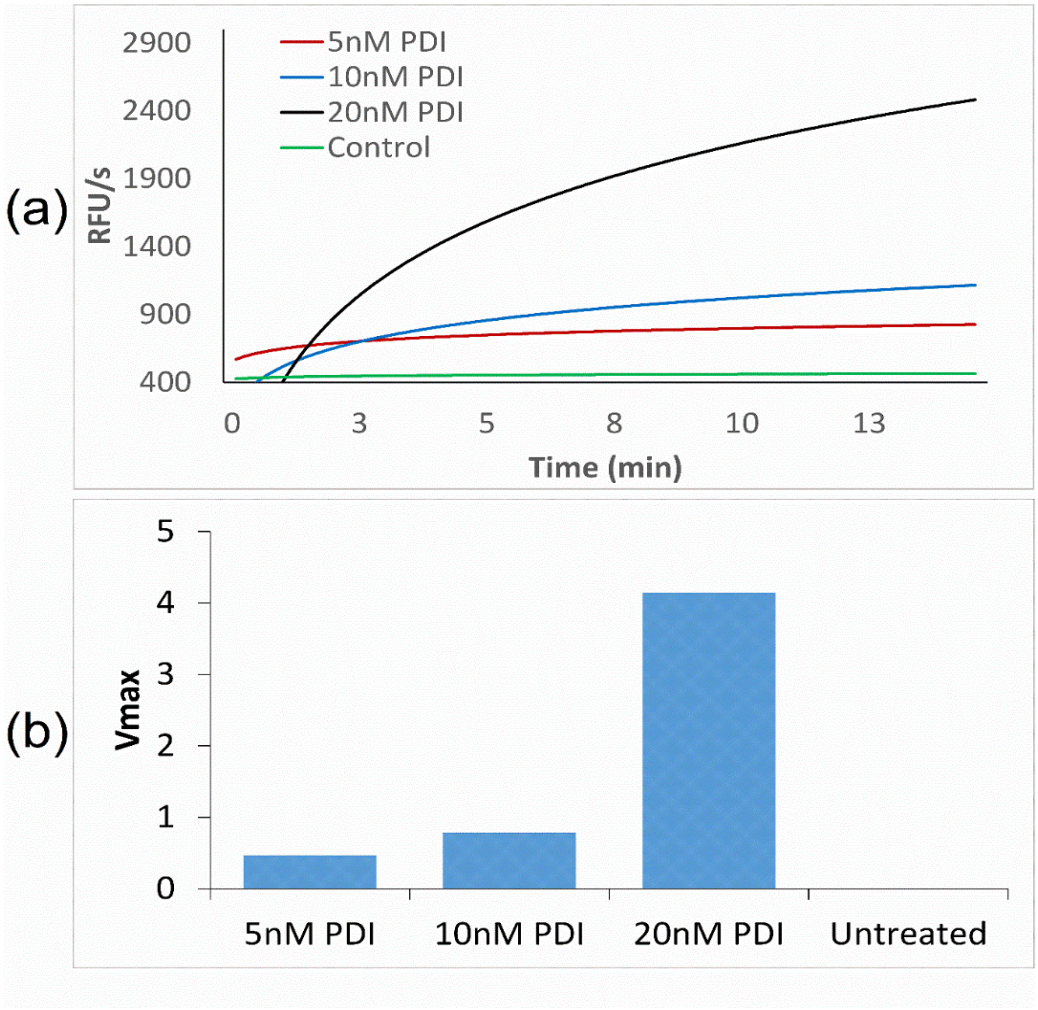

Figure 24. Reduction of Di-E-IGSSG by PDI. (a) Time course of PDI reduction of Di-E-GSSG. Buffer containing 150 nM Di-E-GSSG was incubated with 5 μM DTT in PDI/DsbA assay buffer at room temperature in the absence of PDI or in the presence of 5 nM, 10 nM and 20 nM PDI. Fluorescence was measured with excitation at 525 nm and emission at 545 nm using a Spectramax microplate reader (Molecular Devices). Reduction of Di-E-GSSG was expressed as relative fluorescent units per second (RFU/s). (b) Vmax increases accordingly with increasing PDI concentrations. Experiments were carried out in 3 times (N=3).

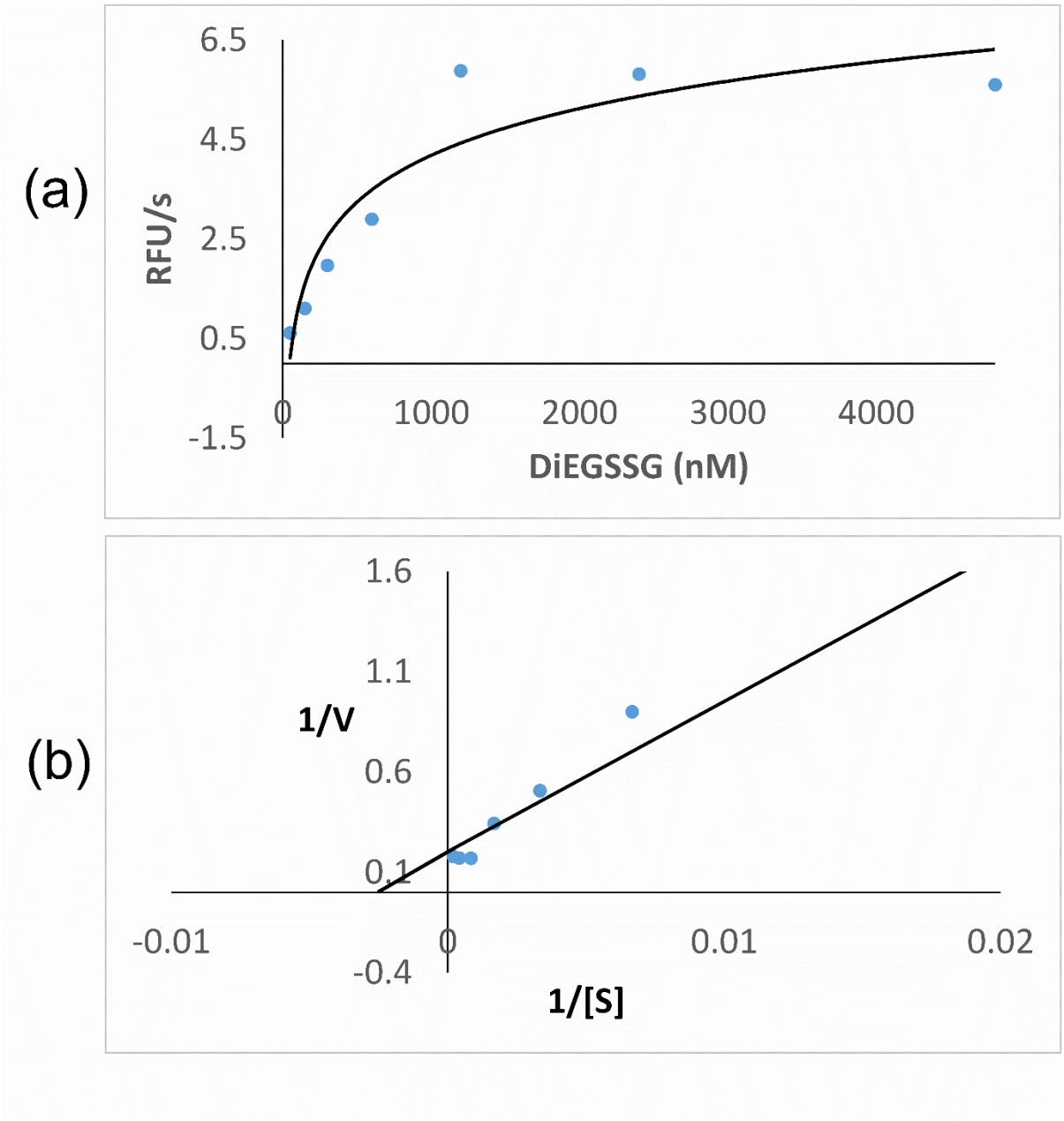

Figure 25. Estimation of Vmax and Km value for PDI. (a) 40 nM of PDI was incubated with various concentrations of Di-E-GSSG (50 nM – 5 μM) in PDI/DsbA assay buffer at room temperature. Fluorescence was measured with excitation at 525 nm and emission at 545 nm using a Spectramax microplate reader (Molecular Devices). The rates of EGSH formation were expressed as relative fluorescent units per second (RFU/s). (b) Km value was estimated using Lineweaver-Burk plot (Prism). 1/V was plotted against 1/[S] to determine Vmax (6.5 s) and Km (600 nM ± 40 nM). Experiments were carried out in 3 times (N=3).

DsbA has been reported to display similar reduction activity to PDI. Therefore, DsbA was tested for its activity in the reduction of Di-E-GSSG using the same conditions shown in Fig. 24. As shown in Fig. 26, incubation of Di-E-GSSG with 5 μM DTT did not result in any reduction (controls in Fig. 26a&b). Incubation of Di-E-GSSG with DsbA and 5 μM DTT resulted in a rapid increase in fluorescence as a function of time, and in a dose-dependent manner (Fig. 26a). Incubation of Di-E-GSSG with DsbA33G also showed an increase of fluorescence as a function of time (Fig. 26b) but to a lesser degree Vmax 14.97 RFU/s and Km as 222 nM for DsbA (Fig. 29a) and Vmax 10.14 RFU/s and Km as 537.6 nM for DsbA33G (Fig. 29a).

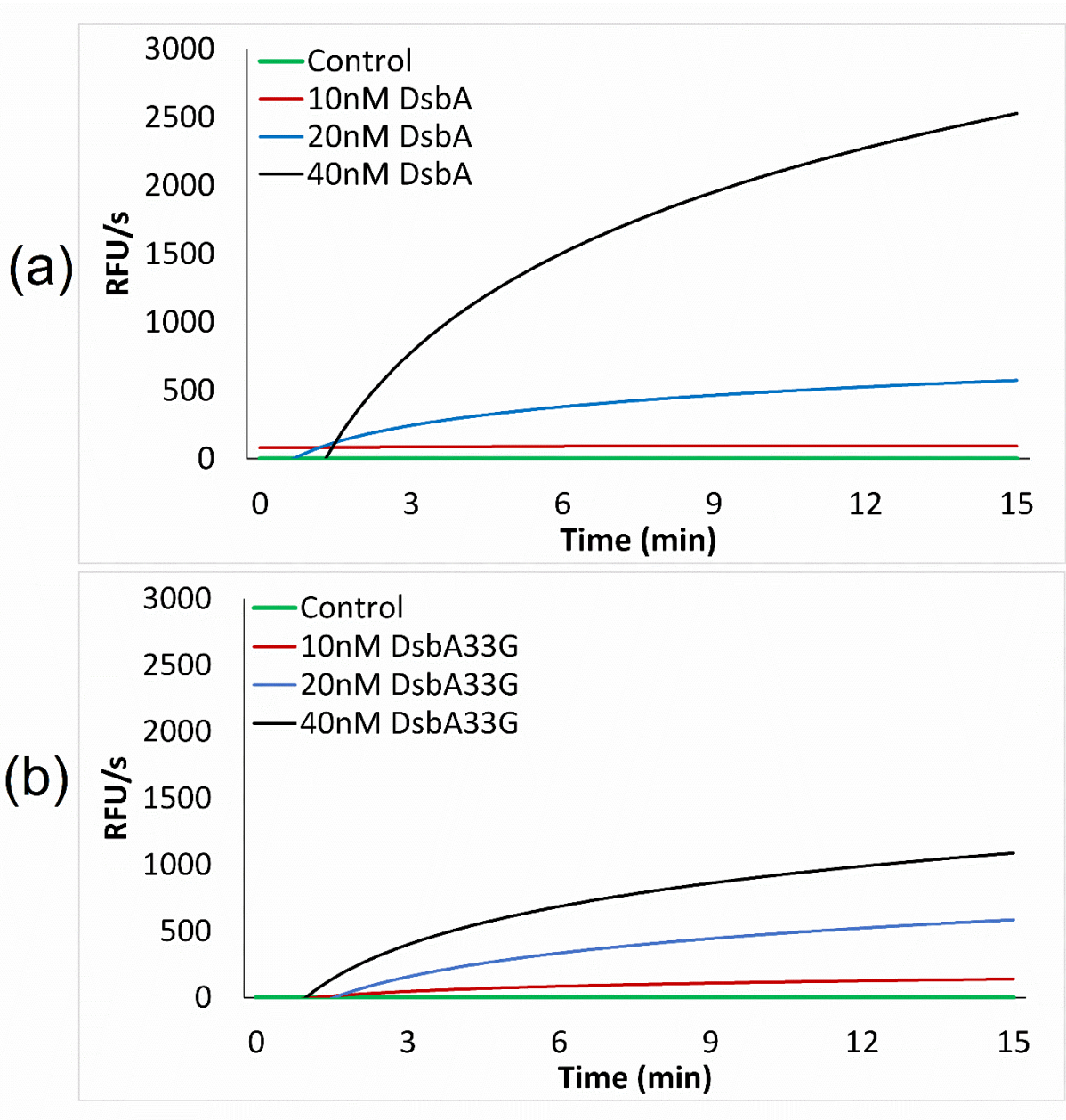

Figure 26. Reduction of Di-E-GSSG by DsbA-6XHis (a) and DsbA33G-6XHis (b). 150 nM of Di-E-GSSG was incubated with 5 μM DTT in PDI/DsbA assay buffer at room temperature in the absence of DsbA-6XHis/DsbA33G-6XHis or in the presence of 10 nM, 20 nM and 40 nM of DsbA6XHis protein or DsbA33G-6XHis protein. Fluorescence spectrum was measured with excitation at 525 nm and emission at 545 nm in a Spectramax microplate reader (Molecular Devices). Conversion of Di-E-GSSG was expressed as relative fluorescent unit per second (RFU/s). Experiments were carried out in 3 times (N=3).

4.6 Inhibition of DsbA in reduction of Di-E-GSSG by monoterpenes

As has been previously mentioned, the monoterpenes group of natural compounds, including geraniol and geranyl acetate, have a similar structure to the terpenoid side-chain of propolin D. Therefore, these monoterpenes may exhibit anti-DsbA activity. They were therefore analysed to determine whether they inhibited the reduction of Di-E-GSSG by DsbA. Geraniol and geranyl acetate are natural products found in essential oils. Inhibition of Di-E-GSSG reduction by DsbA in the presence of geraniol or geranyl acetate was determined. As shown in Fig. 27, Di-E-GSSG reduction by DsbA was inhibited in the presence of both geraniol and geranyl acetate, respectively, in a concentration-dependent manner. Thus, geraniol and geranyl acetate may physically interact with DsbA to prevent its GSSG-reduction activity.

Next, DsbA33G was used to determine the inhibition function of geraniol and geranyl acetate. As mentioned previously, DsbA33G bears a 33G substitution for cysteine in the active site of DsbA. Di-E-GSSG reduction by DsbA33G was approximately half that of DsbA (Fig. 28). DsbA33G activity was also inhibited by geraniol or geranyl acetate in a dose-dependent manner. These results suggest that DsbA33G is able to

interact with geraniol and geranyl acetate despite loss of the cysteine residue at position 33 in the active site. According to structural analysis, Cys30 in the active site is more exposed to the solvent, and Cys30 first reacts with substrate to form a folding intermediate (Kishigami *et al.*, 1995). Once Cys30 receives a hydrogen element from the substrate, DsbA becomes reduced, and the intramolecular disulphide bond is transferred from DsbA to the substrate (Fig. 4). However, Cys30 must be reduced in DsbA33G, and this reduced Cys30 is still capable of interacting with a substrate, resulting in reduction of GSSG, likely causing transfer of a hydrogen element from DTT to GSSG.

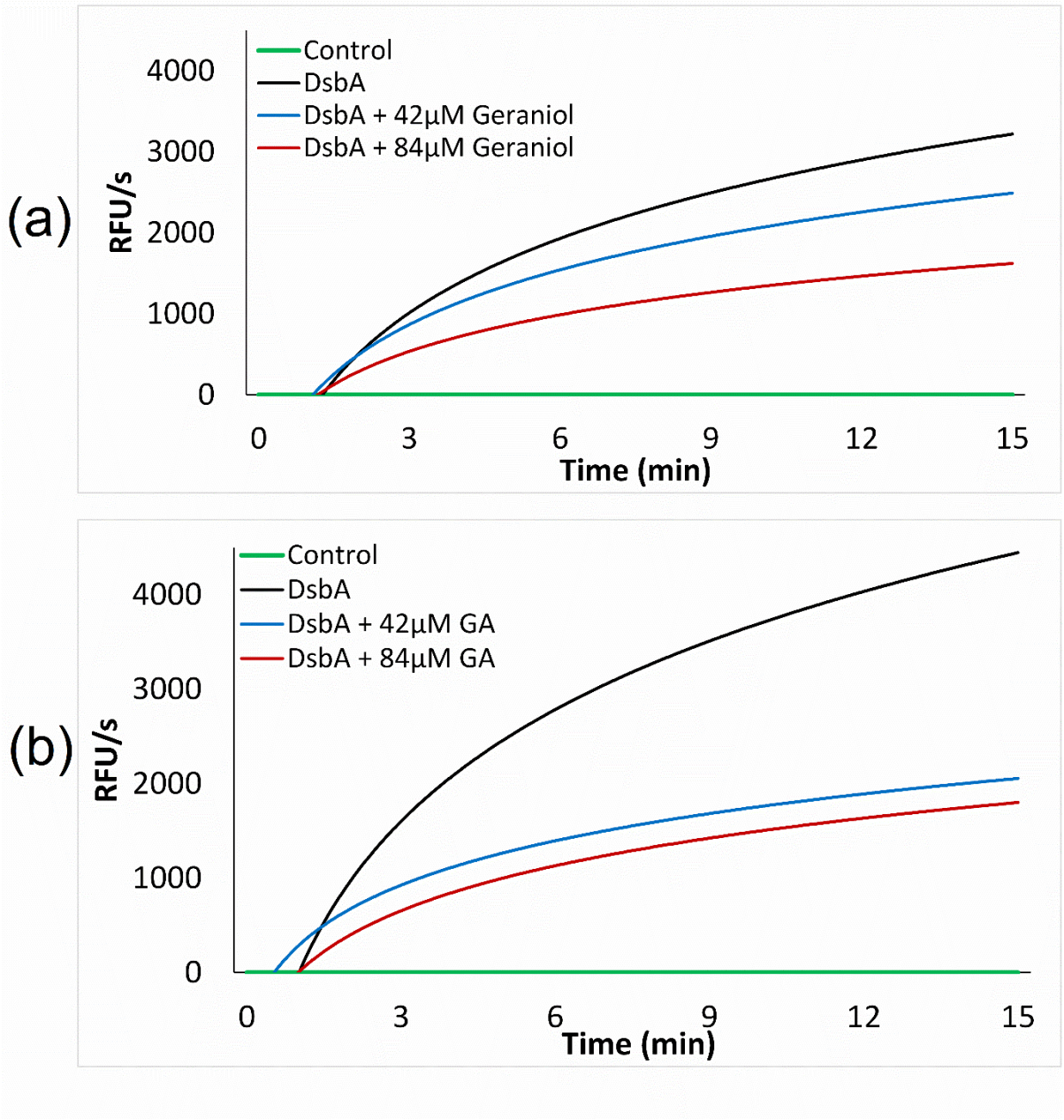

Figure 27. Reduction of Di-E-GSSG by DsbA in the presence of geraniol (a) or geranyl acetate (b). Di-E-GSSG (150 nM) was incubated with 5 µM DTT in PDI/DsbA assay buffer at room temperature in the absence of DsbA (control) or in the presence of 40 nM DsbA-6XHis protein without or with geraniol (42 µM and 84 µM) (a) or without and with geranyl acetate (42 µM and 84 µM) (b). Fluorescence was measured with excitation at 525 nm and emission at 545 nm using a Spectramax microplate reader (Molecular Devices). Conversion of Di-E-GSSG was expressed as relative fluorescent units per second (RFU/s). Experiments were carried out in 3 times (N=3).

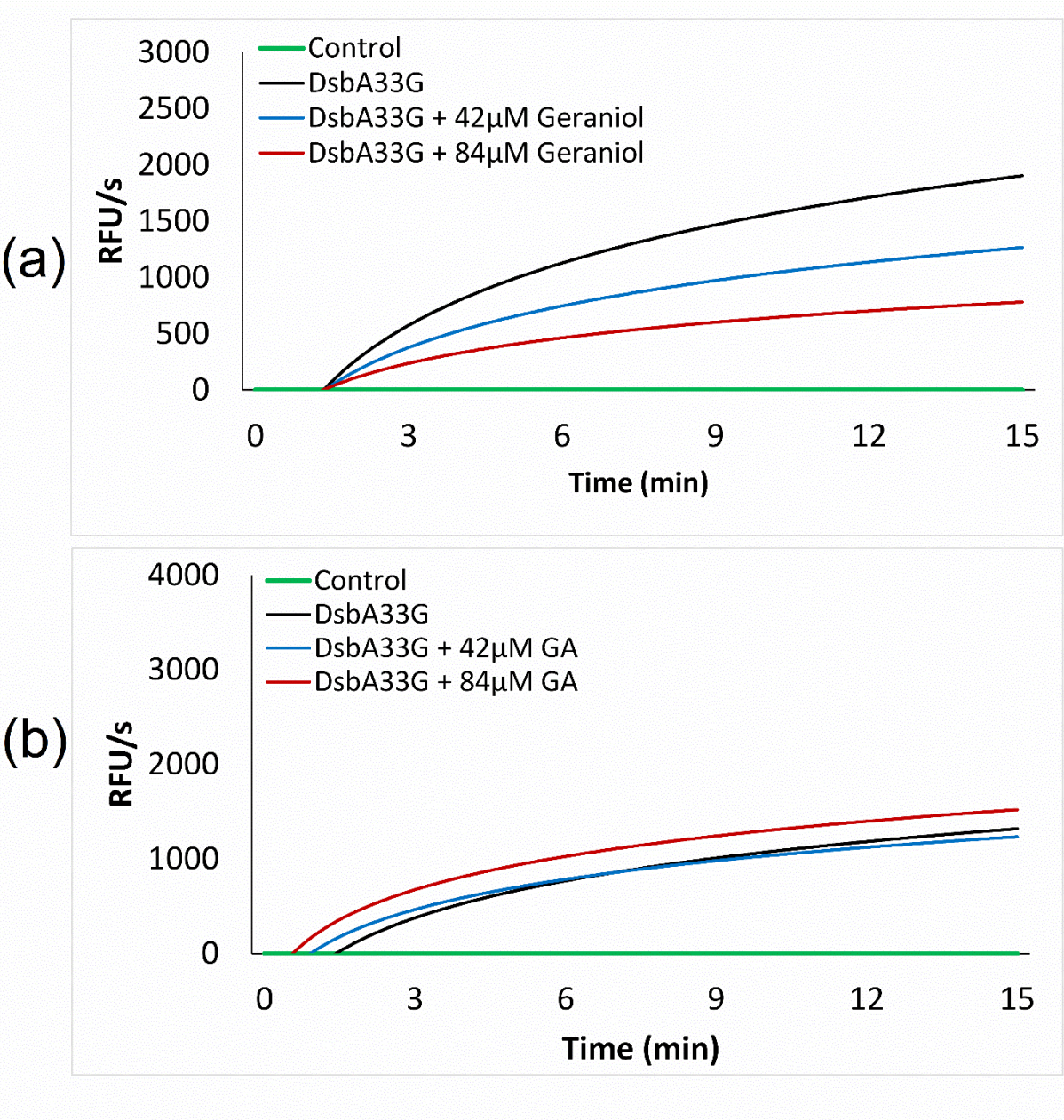

Figure 28. Reduction of Di-E-GSSG by DsbA33G in the presence of geraniol (a) and geranyl acetate (b). Di-E-GSSG (150 nM) was incubated with 5µM DTT in PDI/DsbA assay buffer at room temperature in the absence of DsbA33G (control) or in the presence of 40 nM DsbA33G with and without geraniol (42 µM or 84 µM) (a) or without and with geranyl acetate (42 µM or 84 µM) (b). Fluorescence was measured with excitation at 525 nm and emission at 545 nm using a Spectramax microplate reader (Molecular Device). Conversion of Di-E-GSSG was expressed as relative fluorescent unit per second (RFU/s). Experiments were carried out in 3 times (N=3).

There are two major mechanisms for the inhibition of enzymatic activity: competitive or non-competitive. In competitive inhibition, the substrate and inhibitor compete for binding to the same active site. Non-competitive inhibition occurs when the inhibitor binds to another site on the enzyme molecule, resulting in conformational change, with the result that the enzyme can no longer interact with its substrates. Geraniol was shown to be a more effective natural product than geranyl acetate in inhibiting Di-E-GSSG reduction by DsbA33G (Fig. 28). Subsequent experiments were performed to determine whether geraniol was a competitive or non-competitive inhibitor. First, the Vmax of DsbA with and without geraniol was determined (Fig. 29). The Vmax of DsbA with geraniol was lower compared to DsbA alone. The Vmax of DsbA33G was approximately the same in the presence and absence of geraniol. Km values were then determined in order to assess whether geraniol was a competitive inhibitor. Km is defined as the Michaelis constant at which the substrate concentration is at ½ maximum velocity (Vmax). The variation in Km value directly determines whether the inhibitor is competitive or non-competitive. The reductase activity of DsbA was monitored as function of Di-E-GSSG with an apparent Km value of 200 ± 40 nM (black curve in Fig. 29a). Following the addition of geraniol in the reaction, the Km value

increased to 331.7 ± 40 nM (Fig. 29b blue curve), which means DsbA displayed reduced affinity to the substrate, i.e. more substrate was required to achieve the same rate of reaction. These results suggest that substrate (GSSG) and geraniol compete for binding to the same active site of DsbA (Fig. 29b).

The reductase activity of DsbA33G was significantly slower with a Vmax of 10.14RFU/s, and was exacerbated by the addition of geraniol with Vmax of 9.03 RFU/s. The Km value for DsbA33G was 537.6 ± 40 nM (Fig. 29c), which was double that of DsbA, suggesting that affinity of substrate to DsbA33G is very low. Thus, DsbA33G is less efficient than DsbA in the reduction of GSSG. With the addition of geraniol, the Km value of DsbA33G became 331.8 ± 40 nM (Fig. 29c). These data were unexpected and unexplainable. The reasons for geraniol making the affinity of DsbA33G to GSSG higher requires further investigation.

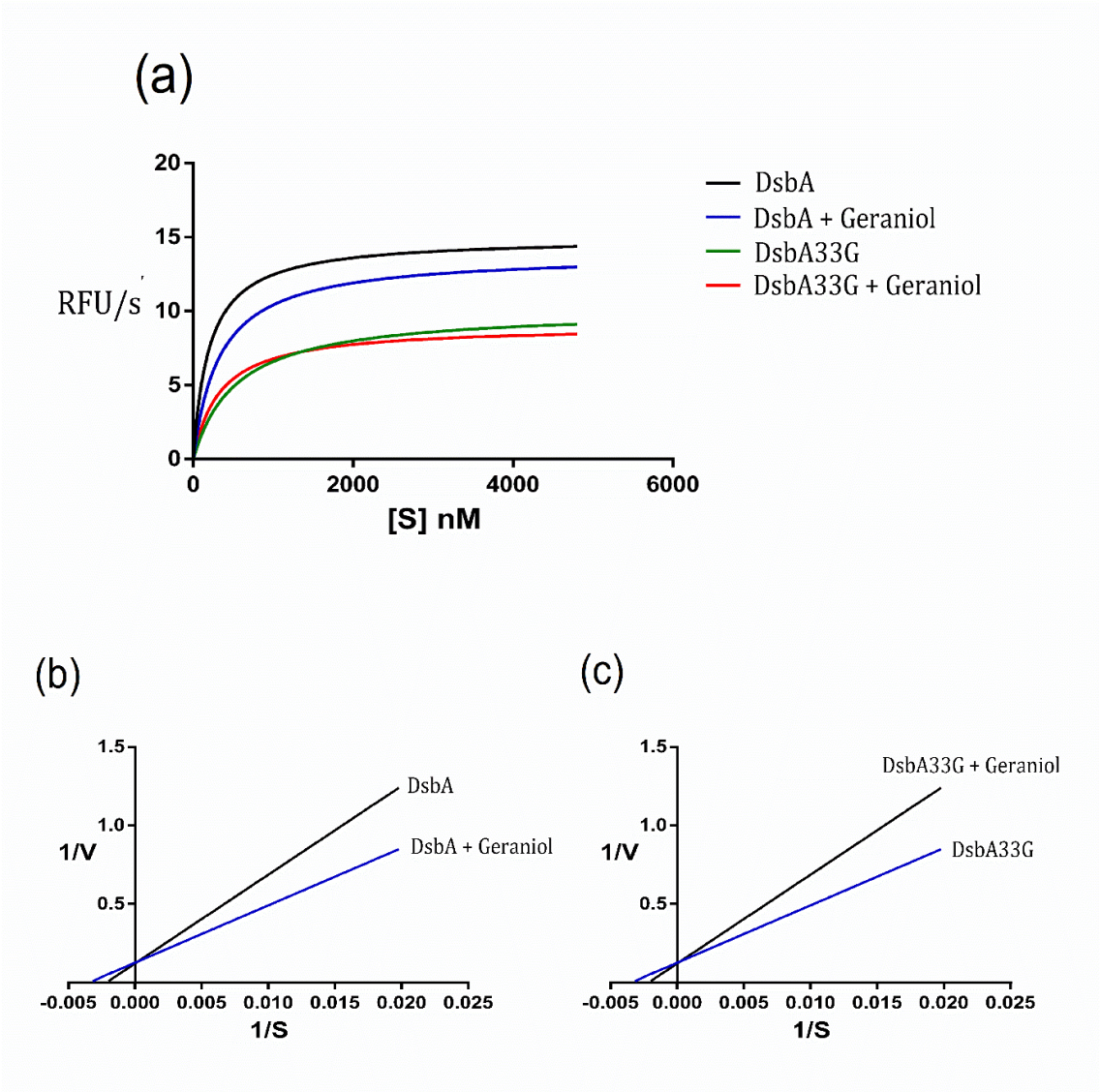

Figure 29: Estimation of Vmax and Km. (a) 40nM of DsbA or DsbA33G without and with various concentrations of Di-E-GSSG (50 nM – 5 µM) in PDI/DsbA assay buffer at room temperature. Fluorescence was measured with excitation at 525 nm and emission at 545 nm using a Spectramax microplate reader (Molecular Device). Conversion of Di-E-GSSG was expressed as relative fluorescent unit per second (RFU/s). Theoretical hyperbolic curves allowed estimation of Vmax for DsbA (14.97 RUF/s) and DsbA + geraniol (13.89 RFU/s). Vmax for DsbA33G and DsbA33G + geraniol were 10.14RUF/s and 9.03 RFU/s, respectively. Estimation of Km using Lineweaver-Burk plot for DsbA (b) and DsbA33G (c). Km was estimated as 222 nM and 331.8 nM for DsbA without and with 42 µM geraniol, respectively. Km was estimated as 537.6 nM and 331.8 nM for DsbA33G and DsbA33G + 42 µM geraniol, respectively. Experiments were carried out in 3 times (N=3).

In summary, it has been successfully demonstrated that propolin D exhibits anti-*Shigella* activity under reducing conditions. The terpenoid side chain of propolin D appear to be responsible for the accumulation of propolin D inside host cells, where it exerts direct anti-*Shigella* activity in the reducing host cell cytosol. The cytosol is where *Shigella* DsbA plays an important part in *Shigella* growth. The *ΔdsbA* mutant shows significantly impaired growth compared to wild-type *S. sonnei*. A specific stress is caused on the *dsbA* gene by GSH + propolin D, which contributes to the inhibition of bacterial growth compared to high osmotic stress. *dsbA* is one of the periplasmic space genes (*dsbA, fkpA, resB and spy*) involved in envelope stress responses, and can be quantified by real-time quantitative PCR. Following successful purification of DsbA, it was demonstrated that it reduces Di-E-GSSG to E-GSH *in vitro*. This reduction of GSSG by DsbA can be inhibited by natural monoterpene products such as geraniol. Geraniol appears to be a competitive inhibitor that competes with GSSG in binding the active site of DsbA. Finally, anti-DsbA activity is a novel finding that could potentially represent a new strategy in the treatment of dysentery.

Chapter 5: Geraniol as a lead candidate for the treatment of *Shigella* infection

Chapter 4 presented evidence that the terpenoid side chain and monoterpenes were biologically functional in inhibiting the enzymatic activity of DsbA. Since geraniol and geranyl acetate are more readily available from commercial sources than propolin D, and since geraniol exhibits better DsbA inhibiting activity than geranyl acetate (Fig. 27), it was analysed for its action on *Shigella* infection *in vitro* and *in vivo*. Furthermore, geraniol has been shown to induce interleukin 10 (IL-10) production in macrophages (Murbach *et al.*, 2014). IL-10 suppresses inflammation, which is a desirable for treating shigellosis, which is characterised by hyperinflammation. Moreover, geraniol also works synergistically with certain antibiotics (Lorenzi *et al.*, 2009). Lorenzi *et al.* 2009 found that geraniol increased the susceptibility of a number of bacteria to β-lactams, quinolones and chloramphenicol. Therefore, additional experiments were conducted to further compare geraniol with geranyl acetate.

First, the growth curves of *S. sonnei* were determined in the presence or absence of equal concentrations (42 μM) of propolin D, geraniol and geranyl acetate (Fig. 30). All three supplements were able to inhibit *S. sonnei* growth in M9 minimal medium in the

presence of 5 mM GSH. The doubling time was estimated to be 1 hour in the absence of any supplement but increased to one and a half hours when M9 was supplemented with propolin D, or geraniol, or geranyl acetate. Differences between groups were assessed using Bonferroni's multiple comparisons test (Table 7). As geraniol has additional useful properties, i.e. inducing IL-10 in macrophages and displaying synergistic effects with antibiotics, further experiments conducted hereon focused on the characterisation of geraniol alone.

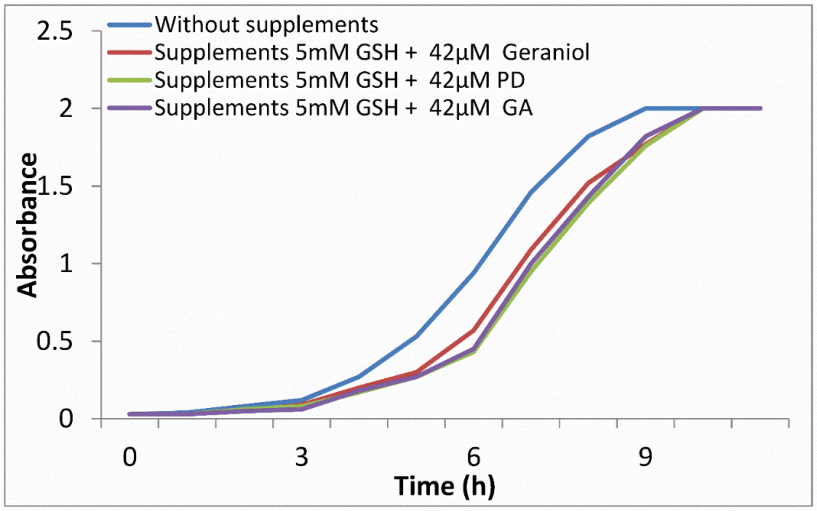

Figure 30. Growth curves of *S. sonnei* WT under different conditions. Bacteria were grown in M9 media containing 5 mM of GSH, which was further supplemented with 42 µM geraniol, or 42 µM propolin D, or 42 µM geranyl acetate. OD600nm was taken each hour. The doubling time is one hour in the absence of supplements, and the doubling time is one hour and half in the presence of 5mM of GSH plus 42 µM propolin D, or 42 µM geraniol, or 42 µM geranyl acetate. Experiments were carried out in 3 times (N=3).

Table 7. Comparison of statistical significance of the growth curves in figure 30 using Graphpad Prism software.

Test pair	Mean	95% CI	Statistical significance	P Value
WT vs. WT + 5mM GSH + 42µM Geraniol	0.1262	0.01063 to 0.2417	*	0.00311
WT vs. WT + 5mM GSH + 42µM PD	0.1631	0.006245 to 0.3199	*	0.00407
WT vs. WT + 5mM GSH + 42µM GA	0.1515	0.007669 to 0.2954	*	0.00380

5.1 Cytotoxicity of geraniol on RAW 264 macrophage cells and HEK293 cells:

Cytotoxicity is an important consideration for therapeutic application. A good agent must possess selective cytotoxicity, i.e. it must be toxic to pathogens but not to host cells. Therefore, an MTT assay was performed to test geraniol cytotoxicity in RAW 264 macrophage cells and HEK293 cells. The results showed that the minimal concentration of geraniol to cause cytotoxicity in RAW 264 macrophage was 336 µM of geraniol (Fig. 31).

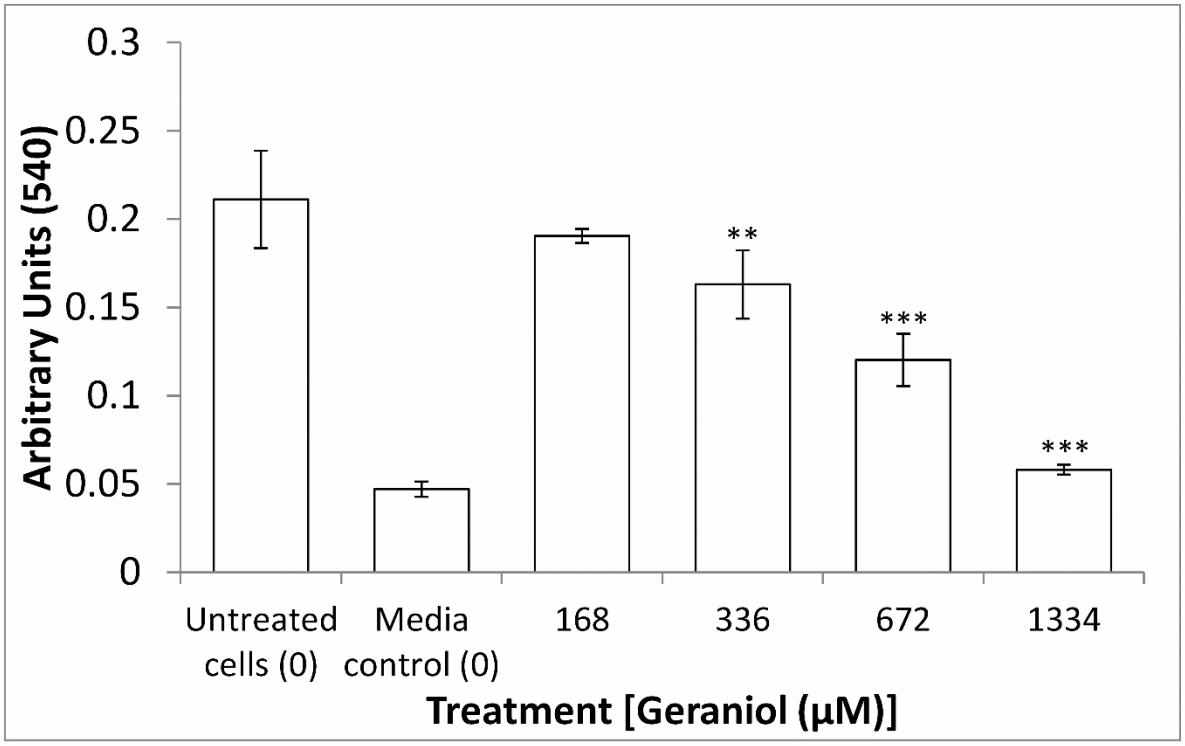

Figure 31. MTT assay for cytotoxicity of geraniol on RAW 264 macrophage cells. Experiments were carried out in triplicate 3 times. Pooled data were shown as means ± SD. Differences between untreated and treated groups were assessed using the Bonferroni correction t test. Asterisks depict statistical significance (**: $p < 0.003$) (***: $p < 0.0003$). 336 µM of geraniol is the minimal concentration to cause cytotoxicity.

Next, MTT assay was performed to test for geraniol cytotoxicity on HEK293 cells. The results showed that 672 µM was the minimal concentration of geraniol to cause cytotoxicity on HEK293 cells (Fig. 32). Lower concentrations of geraniol showed no cytotoxicity in either RAW 264 macrophage cells or HEK293 cells.

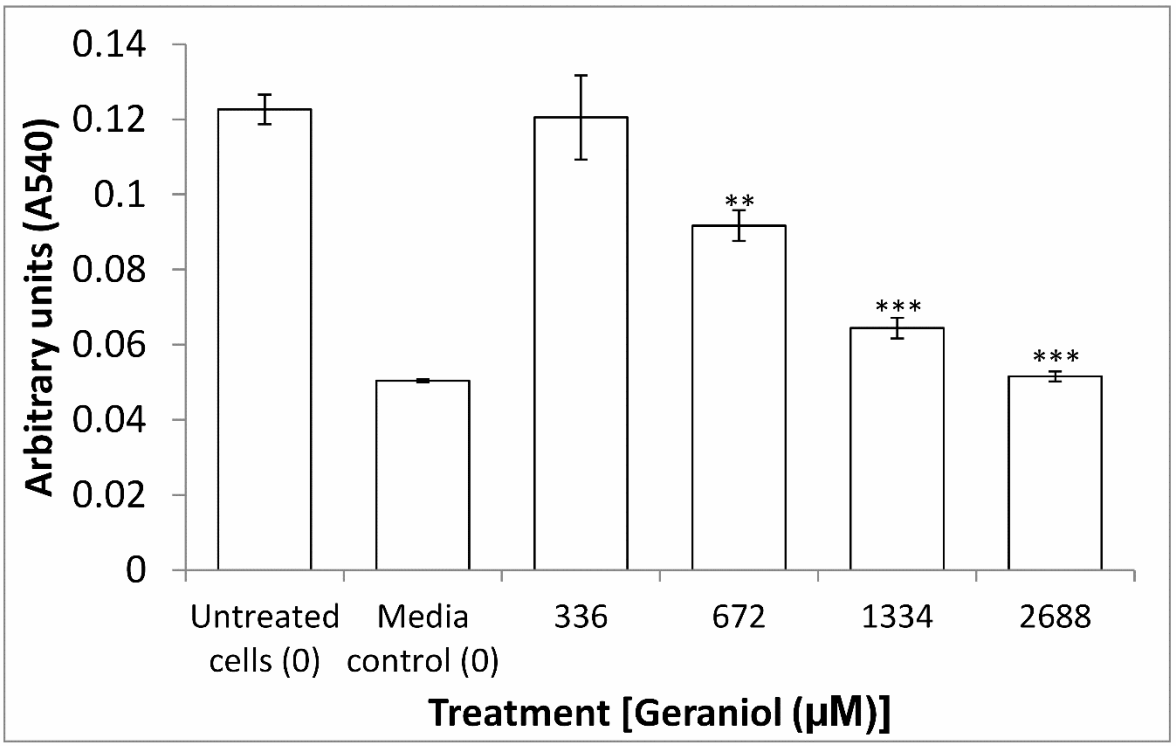

Figure 32. MTT assay for cytotoxicity of geraniol on HEK293 cells. Experiments were carried out in triplicate and repeated 3 times. Pooled data are shown as means ± SD. Differences between groups were assessed using the Bonferroni correction t test. Asterisks depict statistical significance (***: $P < 0.0003$). 672 µM is the minimal concentration of geraniol to cause cytotoxicity.

5.2 Protection of geraniol in *Galleria mellonella* larva infected with *S. sonnei*:

The greater *Galleria mellonella* larva model has become an increasingly utilised *in vivo* model for assessing pathogen virulence and for drug discovery (Desbois & Coote, 2011). Hence, this larva model was used to determine the suitability of geraniol in the treatment of *S. sonnei* and AIEC infections (Chapter 6).

First, this model was used to determine the cytotoxicity of geraniol in the larvae. Larvae were separated into 6 groups, with 10 larvae per group. Larvae in each group were injected with indicated concentrations of geraniol or mock infected with PBS (Fig. 33a). One control group of larvae were injected with 10^5 CFU of *S. sonnei*, which is the concentration required to kill a larva in one day. Larvae were observed for 5 days to estimate the survival rate. As shown in Fig. 33a, all larvae in groups that received 8.74 µg, 87.4 µg and 874 µg of geraniol survived while all larvae in groups infected with *S. sonnei* or that received 8740 µg geraniol died within one day. Hence, larvae can tolerate at least 874 µg of geraniol, and possibly higher levels if experiments were conducted to titrate concentrations of geraniol between 874 µg and 8740 µg.

Next, the protection efficacy of geraniol in larvae infected with *S. sonnei* was tested (Fig. 33b). As seen in Fig. 33b, larvae infected with 10^5 CFU of *S. sonnei* all died in one day. However, mock infected larvae and those treated with 87.4µg of geraniol all survived. Administration of geraniol at concentrations as low as 15.6µg resulted in 40% of larvae surviving for 5 days.

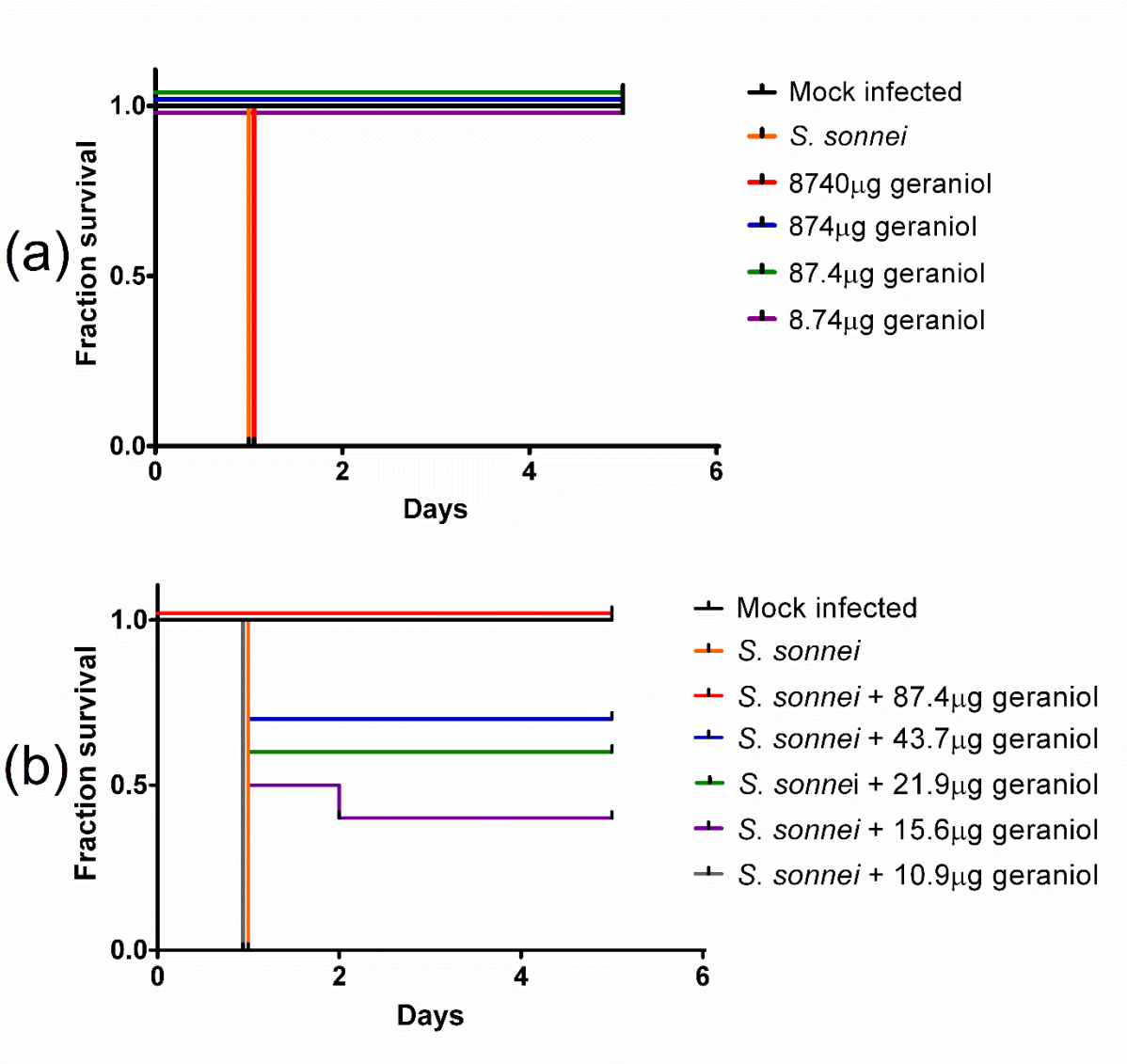

Figure 33. *Galleria mellonella* larva model for geraniol cytotoxicity and protection of larva by geraniol from *S. sonnei* infection. (a) Cytotoxicity of geraniol. Note: *S. sonnei* infected larvae and 8740μg geraniol treated larvae all died in one day, and larvae in all other treated groups survived for 5 days; curves were overlapped with that of the mock infected group. (b) Treatment of *S. sonnei* infected larvae with geraniol. Wild-type *S. sonnei* was administered 10^5 CFU per larva with indicated concentrations of geraniol. Insects were observed for 5 days. Note: Larvae that received 87.4μg of geraniol all survived for 5 days and the curve was overlapped with that of mock infected group.

5.3 Geraniol inhibits *S. sonnei* growth in RAW 264 mouse macrophage and HEK 293 cells:

In the *Galleria mellonella* larva model, infection of the larval haemocytes is one of the underlying mechanisms that cause larval death (Harding *et al.*, 2013). As haemocytes possess properties similar to vertebrate macrophages, a gentamicin-killing assay was conducted to test whether geraniol inhibits *S. sonnei* growth in mouse RAW 264 macrophages. Since geraniol also inhibits *S. sonnei* growth in epithelial cells, HEK293 cells were also used in the same assay.

A range of concentrations of geraniol were used to test inhibition of *S. sonnei* growth in RAW 264 macrophage cells. CFU of intracellular *S. sonnei* was reduced by addition of 42, 84 and 168 μM of geraniol in comparison to medium without supplement, suggesting that geraniol effectively inhibited proliferation of intracellular *S. sonnei*. Geraniol at concentration of 84 and 168 μM reduced intracellular CFU approximately 3 fold (Fig. 34).

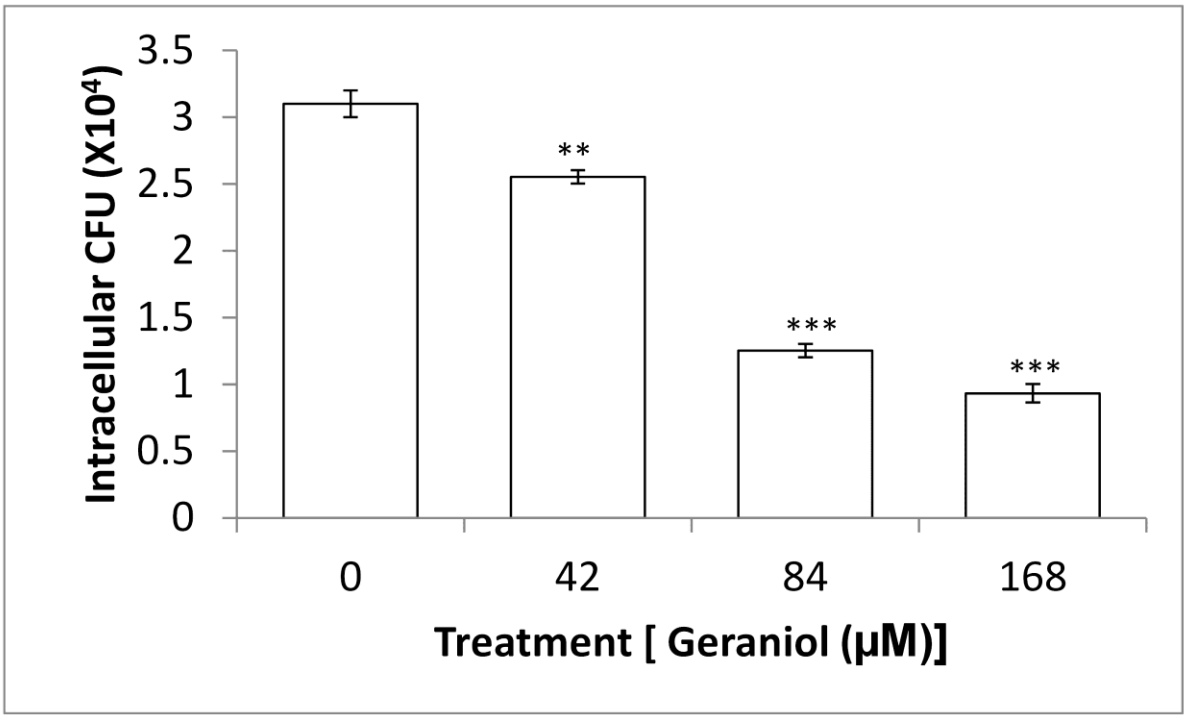

Figure 34: Geraniol inhibits *S. sonnei* growth inside RAW 264 mouse macrophages. Cells infected with wild-type *S. sonnei* for 3 hours with indicated concentrations of geraniol. The results were carried out in triplicate 3 times and repeated 3 times. The results are shown as means ± SD. Differences between groups were assessed using the Bonferroni correction t test. Asterisks depict statistical significance (**: $p < 0.003$ and ***: $p < 0.0003$).

Next, different concentrations of geraniol were used to test inhibition of *S. sonnei* growth in HEK293 cells. Geraniol at concentrations of 42 and 84 µM significantly inhibited intracellular *S. sonnei* growth in the host cells approximately 5 fold (Fig. 35).

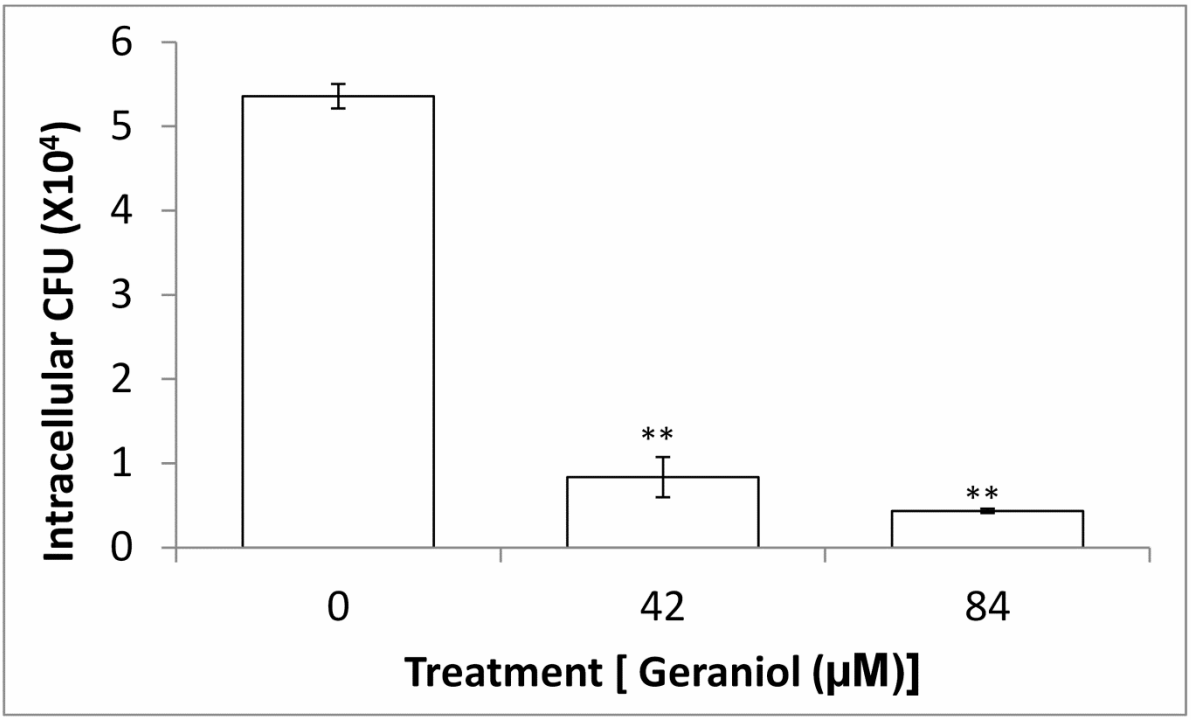

Figure 35. Geraniol inhibits *S. sonnei* growth inside HEK293 cells. Cells infected with wild-type *S. sonnei* for 3 hours without or with 42 or 84 µM of geraniol. The results were carried out in triplicate 3 times and repeated 3 times. The results shown as means ± SD. Differences between groups were assessed using the Bonferroni correction t test. Asterisks depict statistical significance (***: $p <$ 0.0003).

5.4 Growth and survival of *S. sonnei* are inhibited in acidic and nutrient-poor medium:

As part of host defence mechanism, phagosomes mature into phagolysosomes, inside which invading pathogens are killed (Bringer *et al.*, 2006). Phagolysosomes have a low pH and are poor in nutrients, a cellular niche unfavourable for bacterial survival.

Hence, an acidic, nutrient-poor medium was formulated to mimic phagolysosome conditions and characterise the virulence properties of bacteria (Bringer *et al.*, 2006). This medium was used to test the inhibition activity of geraniol on *S. sonnei* growth.

Fig. 36 shows growth of *S. sonnei* in the acidic, nutrient-poor medium with and without supplementation of geraniol. In the absence of geraniol, *S. sonnei* grew to 33 x 10^7 CFU in 3 h, and to 5 x 10^7 and 1 x 10^7 CFU in the presence of 42 μM and 84 μM geraniol, respectively, in the same time. After 6 h, *S. sonnei* grew to 65 x 10^7 and 20 x 10^7 CFU without or with 42 μM geraniol respectively. The growth of *S. sonnei* in the presence of 84 μM geraniol was further reduced, as shown in Fig. 36. These results suggest that geraniol may inhibit *S. sonnei* in cell phagolysosomes to enhance host cell innate immunity.

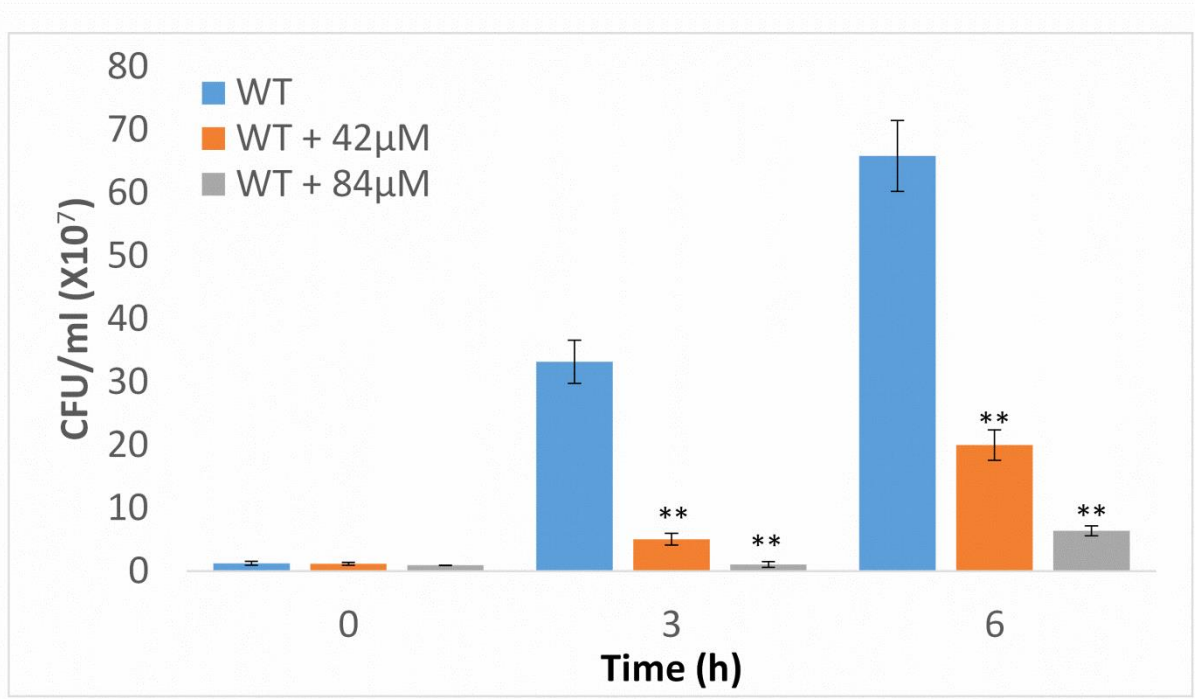

Figure 36. Growth of the wild-type *S. sonnei* (WT) strain in acidic, nutrient-poor medium. The results were carried out in triplicate 3 times. Pooled data are shown as means ± SD. Differences between groups were assessed using the Bonferroni correction t test. Asterisks depict statistical significance (**: $p < 0.003$).

In summary, geraniol protected *Galleria mellonella* larvae infected with *S. sonnei*. In addition, geraniol also significantly inhibited intracellular *S. sonnei* growth in both epithelial cells and macrophages. It is also inhibited intracellular *S. sonnei* growth and survival in acidic nutrient-poor environments.

Chapter 6: Geraniol as a lead candidate for the treatment of AIEC infection

In chapter 5, it was shown that geraniol has potential in treating shigellosis. In this chapter, the potential of geraniol in the treatment of Crohn's disease (CD) is examined. AIEC infection is one of the contributing factors in CD (Boyapati *et al.*, 2015). AIEC are able to adhere and invade intestinal epithelial cells and can also replicate extensively in macrophages within large vacuoles (Glasser *et al.,* 2001; Bringer *et al.*, 2006; Mpofu *et al.,* 2007; Subramanian *et al.,* 2008). Geraniol was therefore analysed for its activities in the control of AIEC infection *in vivo* and *in vitro*. The *G. mellonella* larva model is a commonly used *in vivo* model for assessing the efficacy of antimicrobial agents and therapeutics for infection (Desbois & Coote, 2011). The protection of AIEC-infected *Galleria mellonella* larvae by geraniol was examined. Macrophages engulf bacteria within phagosomes, leading to the degradation of the bacteria. However, AIEC are able escape the degradation process and grow within macrophages (Flanagan *et al.*, 2015). Geraniol was therefore investigated for its activity in inhibiting AIEC growth in the RAW 264 macrophage cell line. Since AIEC are able to survive in the acidic, nutrient-poor

environment of phagolysosomes (Bringer *et al*., 2006), geraniol was tested for its inhibition of AIEC growth in acidic nutrient-poor medium, which mimics the conditions within the phagolysosomes.

6.1 Protection of geraniol in *Galleria mellonella* Larva infected with AIEC:

Since *S. sonnei* growth was shown to be significantly inhibited by geraniol, the *G. mellonella* larva model was exploited to analyse the potential of geraniol to inhibit AIEC growth *in vivo*. AIEC bacteria were injected into each larva, which were monitored for 5 days. Fig. 37 shows the protection of geraniol of *G. mellonella* larvae infected with AIEC strains: LF82 (Darfeuille Michaud *et al*., 1998), HM427, HM605 and HM615 (Martin *et al*., 2004; Subramanian *et al*., 2008). At 10^5 CFU, the ileal CD AIEC strain LF82, and all three of the colonic CD mucosa-associated AIEC HM427 HM605 and HM605 strains, killed all 10 larvae within the first or second day of infection. Using 43μg geraniol per larva, 70% of larvae infected with AIEC strain LF82 survived to the fifth day of infection. Using 87μg geraniol per larva, all larvae infected with AIEC strains survived 5 days. Thus, geraniol is able to protect *G. mellonella* larvae infected with AIEC strains. The results are highly encouraging, since they suggest geraniol has the potential to counter AIEC infection (Fig. 37).

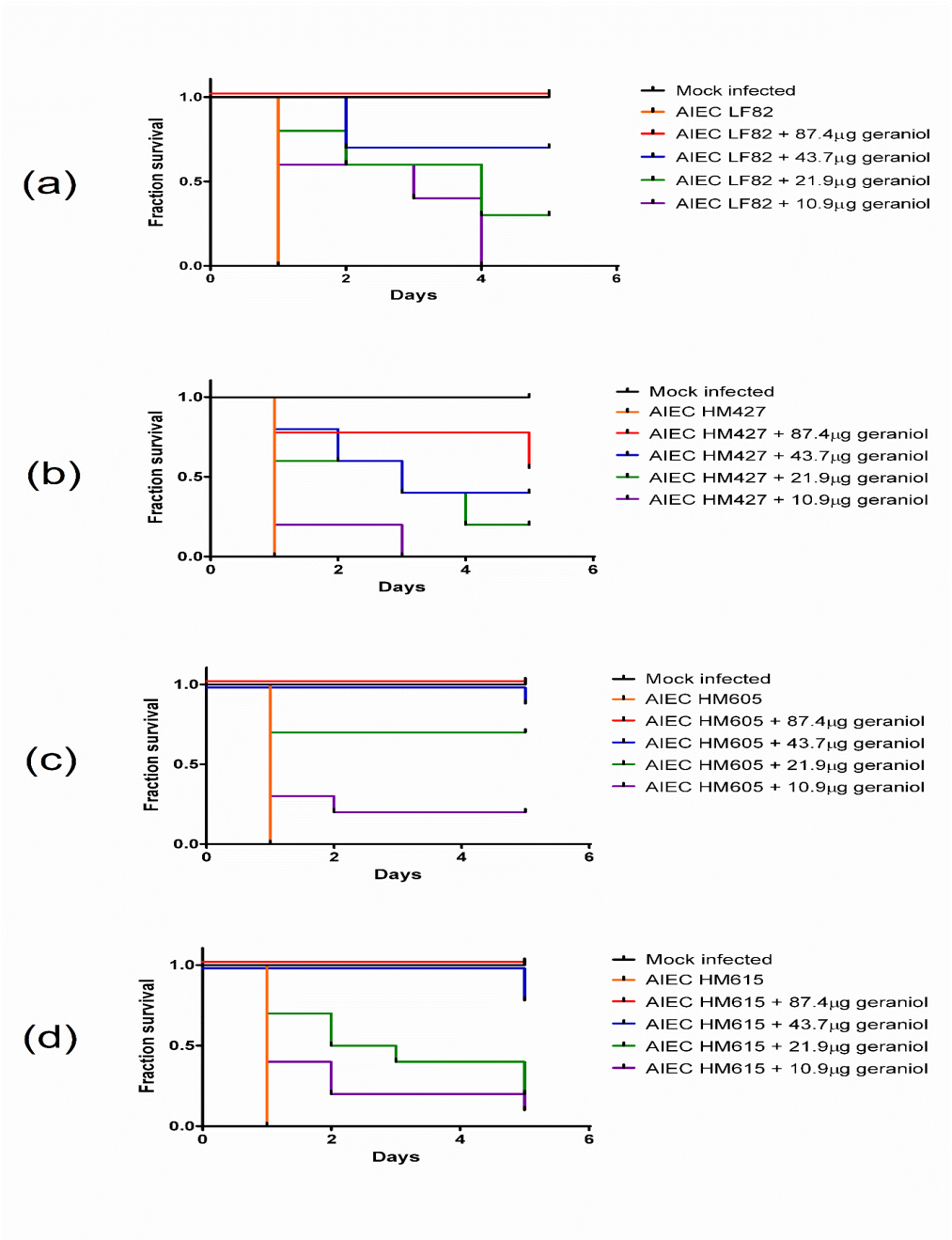

Figure 37. Protection of *G. mellonella* larva by geraniol from AIEC infection. Indicated AIEC strains were administrated,10^5 CFU per larvae; ileal CD AIEC strain LF82 (a) and colonic CD AIEC strains HM427 (b), strains HM605 (c) and HM615 (d) per larva, 10 larvae per group., Geraniol concentrations used for protection are indicated. Larvae were observed for 5 days.

6.2 Intracellular growth of AIEC is inhibited in mouse RAW 264 macrophage cells treated with geraniol

G. mellonella haemocytes are the major mediator of cellular defences against many bacterial pathogens (Harding *et al.*, 2013). These haemocyte cells act as professional phagocytes, performing similar functions to vertebrate macrophages. Here, different concentrations of geraniol were tested on human RAW 264 macrophage cells infected with AIEC strains. Intracellular CFU of AIEC strains were reduced by approximately 2 fold by 84μM geraniol (Fig. 38a). Previous results showed that *G. mellonella* larvae infected with AIEC strains are protected by geraniol. In addition, it has been found that AIEC can replicate and survive inside macrophages (Glasser *et al*., 2001; Bringer *et al*., 2006; Mpofu *et al.,* 2007; Subramanian *et al.,* 2008). An acidic environment is essential for replication of AIEC bacteria such as LF82 within macrophages where it is exposed to degradative activity of cathepsin D and to low pH (Bringer *et al.,* 2006). Colonic mucosa-associated AIEC strains such as HM427, HM605 and HM615 are able to replicate effectively inside macrophages (Mpofu *et al.,* 2007; Subramanian *et al.,* 2008; Subramanian *et al.,* 2008 b). Thus, geraniol is able to reduce intracellular CFU of

AIEC strains in macrophages. In the previous chapter, it was shown that *Shigella* growth was reduced in macrophages cells by geraniol. It is possible to speculate that geraniol reduces AIEC in similar way as it does *Shigella*. DsbA may be targeted by geraniol in macrophages infected with AIEC.

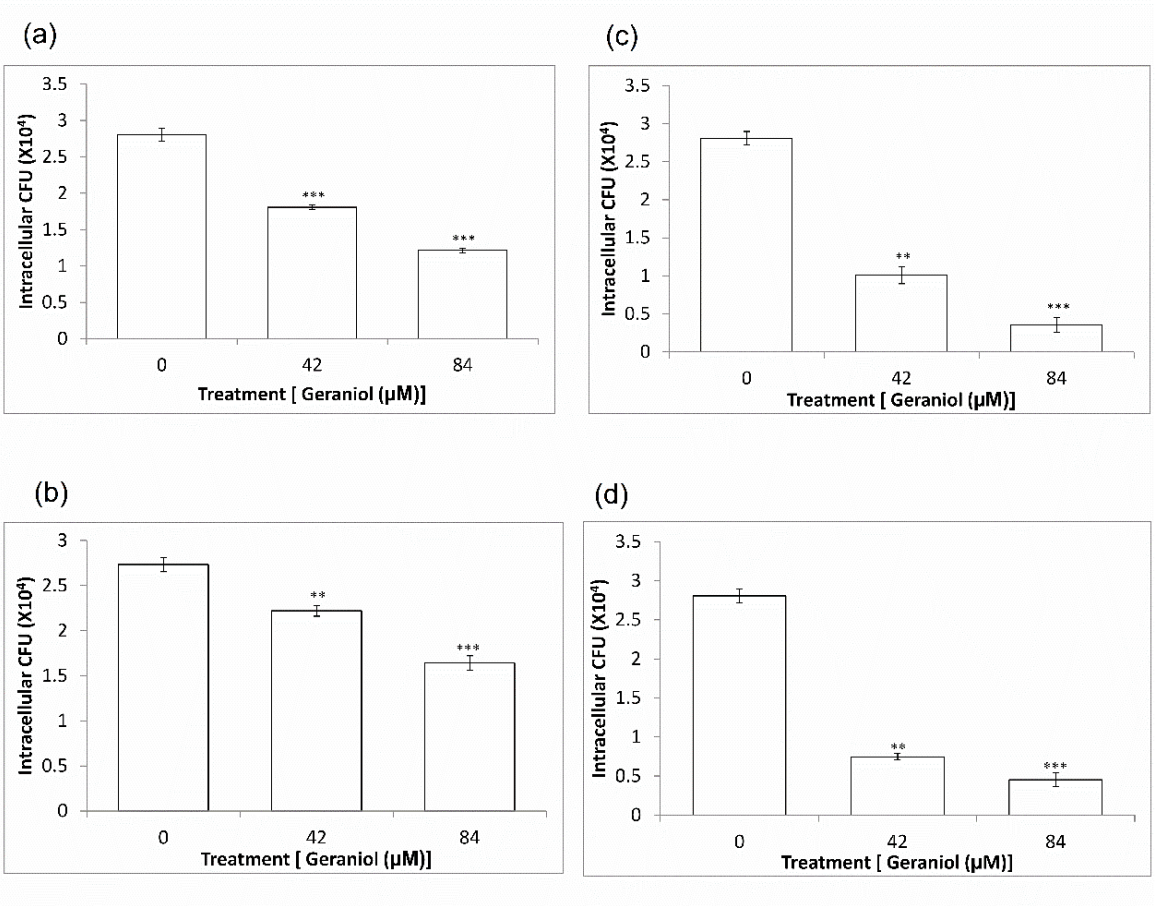

Figure 38. Geraniol inhibits AIEC growth inside RAW 264 mouse macrophages. Cells infected with wild-type AIEC strain for 3 hours with different concentrations of geraniol: 42, 84 and 168µM. (a) strain LF82; (b) strain HM427; (c) strain HM605; (d) strain HM615. The results were carried out in triplicate 3 times and repeated 3 times. The results are shown as means ± SD. Differences between groups were assessed the Bonferroni correction t test. Asterisks depict statistical significance (**: $p < 0.003$; ***: $p < 0.0003$).

6.3 Survival of AIEC bacteria in acidic and nutrient-poor medium:

In the macrophages, AIEC bacteria are internalised into phagosomes which mature into phagolysosomes. These phagolysosomes are the niche where bacteria such as AIEC are exposed to acidic pH with poor nutrient supply. Geraniol was tested to determine its effect on AIEC strains growth in acidic, nutrient-poor medium, which mimics phagolysosome condition. Fig. 39 shows growth of the AIEC strains (LF82, HM427, HM605 and HM615) in acidic, nutrient-poor medium with and without treatment of geraniol. As shown, the growth of AIEC LF82 was increased to 20 x 10^7 CFU in 3 hours. After 6 hours of growth, the growth of AIEC LF82 in the presence of 42μM geraniol was approximately 430 X 10^7 CFU compare to control 610 x 10^7 CFU. The growth of AIEC LF82 in the presence of 84μM geraniol was further reduced. Similar to results of AIEC LF82, the growth of AIEC HM427 in the presence of 42 and 84μM geraniol was reduced compare to control in the same time. These results suggest that geraniol inhibits the growth of AIEC LF82 and HM427 strains in acidic, nutrient-poor medium.

As shown in Fig. 39b, the growth of another isolate AIEC HM605 was increased to 20 x 10^7 CFU in 3 hours. After 6 hours, the growth of AIEC HM605 in the presence of 42μM geraniol was about 350 x 10^7 CFU compared to control 700 x 10^7 CFU. The growth of AIEC HM605 following in the presence of 84μM geraniol was very similar to the seen with a lower dose of reduction to 42μM geraniol, as shown in Fig. 39b. The growth of AIEC strain HM615 in the presence of 42 and 84μM geraniol was also reduced compared to control. These results suggest that geraniol inhibits the growth of AIEC HM605 and HM615 strains in acidic, nutrient-poor medium. These results suggest that geraniol is able to accumulate in the phagolysosomes and inhibit the growth of AIEC in this cellular niche. As previous studies showed that DsbA is vital for AIEC to survive in this cellular niche (Bringer *et al.*, 2006), and that geraniol inhibits DsbA activity, it could be speculated that geraniol may also inhibit DsbA activity in this cellular niche in addition to the cytosol, as shown in previous chapters. However, questions remain. In the cytosol, DsbA is required for *Shigella* to survive, since excessive GSH must be converted to GSSG. It is not known whether phagolysosomes also contain excessive GSH. Thus, converting GSH to GSSG may or may not be the underlying mechanism for AIEC survival in the phagolysosomes.

Additionally, in the acidic, nutrient-poor phagolysosomes, specific virulence or accessory factors may be required for AIEC survival; DsbA may be required to catalyse these factors for proper folding in order to gain biological functions. These accessory factors required for intramacrophage AIEC survival include HtrA, Hfq, glutamaic acid decarboxylase (Gad) and GipA. High temperature requirement A protein (HtrA) supports Crohn's AIEC survival and replication within host macrophages (Bringer *et al.,* 2005; Tawfik *et al.,* 2014). Hfq may play also a role supporting AIEC survival within macrophages as stress tolerance factor, which mediates bacterial adaptation to chemical stress (Simonsen *et al.,* 2011; Tawfik *et al.,* 2014). *E. coli* also survive high acid stress encountered in the macrophage phagolysosome by GadA and GadB decarboxylases, which are part of an efficient acid resistance system, as they are components of glutamate-dependent acid response (Castanie-Cornet *et al.,* 2010; Tchaptchet *et al.,* 2013). GipA is another key factor required for survival within macrophages by AIEC and for optimal colonisation of mouse PPs (Vazeille *et al.,* 2016).

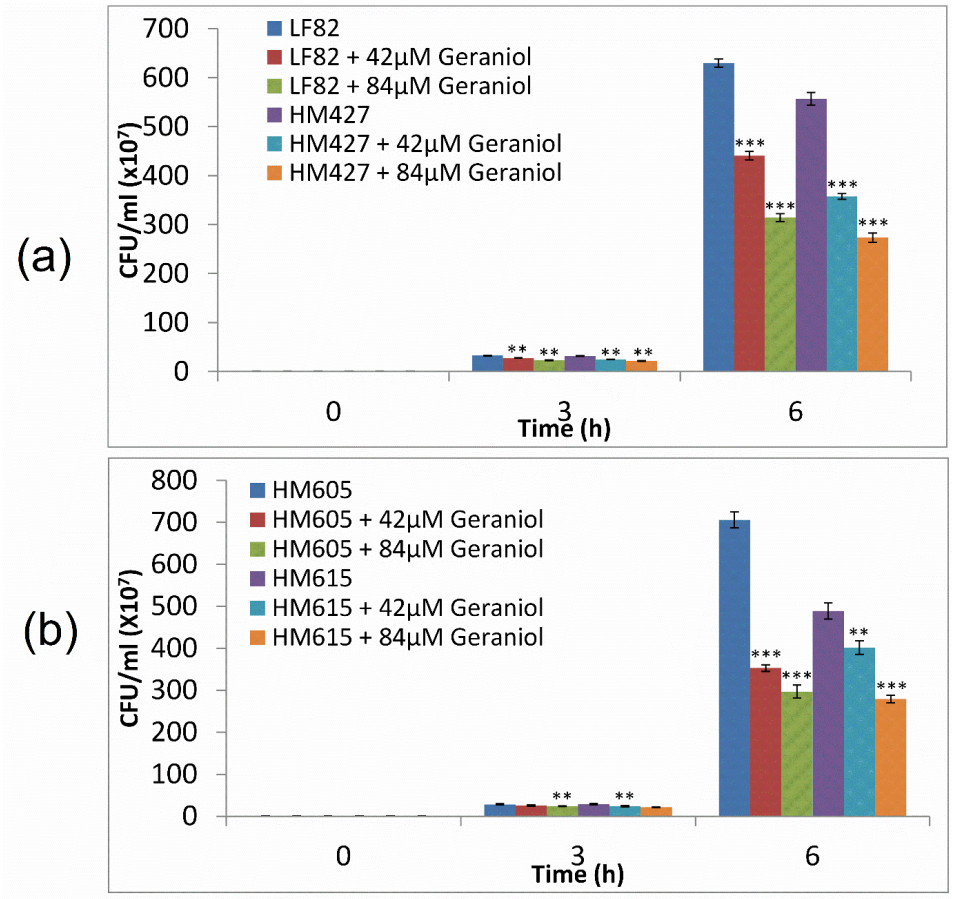

Figure 39. Growth of the AIEC strains [(a) LF82 and HM427, (b) HM605 and HM615] in acidic, nutrient-poor medium with and without treatment of geraniol. Data shown are pooled means ± SD from three independent experiments. Differences between groups were assessed using the Bonferroni correction t test. Asterisks depict statistical significance (**: $p < 0.003$; ***: $p < 0.0003$).

In summary, geraniol has been shown to successfully protect *Galleria mellonella* larvae infected with AIEC. Geraniol has also been shown to inhibit AIEC growth in RAW 264 macrophages cell-line and to inhibit the survival of AIEC in acidic and nutrient-poor medium.

Chapter 7: Discussion

7.1 *Shigella sonnei*-host interaction: the roles of septin cage and autophagy, and intervention of propolin D

Shigella invades epithelial host cells where it escapes from phagosomes and replicates in the cytoplasm. Autophagy and formation of septin cages are initiated in infected host cells to control *Shigella* replication. *Shigella* IcsA and IcsB are key components in triggering autophagy and formation of septin cages. Therefore, it would be of interest to delete both *icsA* and *icsB* in *Shigella* in order to study their roles in host cells. *Shigella ΔicsA* and *ΔicsB* mutants were constructed using a λ red recombination system, as described in chapter 3. This method uses homologous recombination and was used to delete genes *Shigella icsA* and *icsB* (Fig. 8).

Shigella, as an intracellular bacterial pathogen, induces actin polymerisation at its surface. *Shigella* promotes actin polymerisation by exploiting the host protein Arp2/3 complex, which is activated by N-WASP. *Shigella* IcsA binds to N-WASP, enabling motility of *Shigella* within the cell (Gouin *et al.,* 2005). This actin-based motility is targeted by autophagy and septin cage formation (Mostowy & Cossart, 2011).

Therefore, *S. sonnei* actin-based motility was tested by using the two constructed *Δ icsA* and *ΔicsB* mutants in order to test whether they were defective in intracellular growth compared to wild-type *S. sonnei*. The *Shigella ΔicsA* mutant was found to be defective in intracellular growth compared to the wild type. IcsA is a 120-kDa outer membrane protein which is necessary for actin-based motility of *Shigella* (Goldberg & Theriot, 1995). As detailed in chapter 3, *icsA* was deleted using the *λ* recombination system in *Shigella* strain, which was successfully verified by PCR to test for the presence of specific-sized fragments of *icsA* (Fig. 8). Deletion in the gene encoding IcsA produces a mutant defective in actin polymerisation, formation of protrusions, cell-to-cell spread (Goldberg *et al*., 1994). Actin-based motility can be prevented in *Shigella*-infected host cells by compartmentalising bacteria inside septin cages, the formation of which is initiated through recognition of IcsA (Mostowy *et al*., 2010). The IcsA protein then induces autophagy by binding to ATG5. This process leads to protective autophagy, and septin cages assemble around *Shigella*. However, these processes are inhibited by *Shigella* IcsB, which binds to IcsA. *Shigella* defective in IcsB exhibits impaired growth in host cells (Campoy & Colombo, 2009). Deletion of *icsA* causes defective binding of IcsB to IcsA. Therefore, deletions

in *icsA* cause defects in the intracellular growth of *Shigella*. In addition, wild-type *Shigella*, and the *ΔicsA* and *ΔicsB* mutant strains were found to be defective in intracellular growth in the presence of cytochalasin D (Fig. 9). Cytochalasin D, an agent that inhibits actin polymerisation, was used as an inhibitor of actin polymerisation that disrupts actin microfilaments formation. These results show that defective *icsA* prevents intracellular growth and actin polymerisation.

Intracellular growth of *Shigella ΔicsA* was reduced in host cells. *Shigella* IcsA is also involved in the formation of actin tails for cell-to-cell spread. The *ΔicsA* mutant strain was tested for its ability to form actin tails by microscope analysis. No actin tails were observed forming in *Shigella ΔicsA* carrying pEGFP (Fig. 10). This result suggests that the lower intracellular cell-to-cell spread observed was due to the absence of actin polymerisation (Fig. 10). One study showed that *Shigella* can either become compartmentalized in septin cage-like structures, or form actin tails (Mostowy *et al*., 2010). However, septin cages are not active in the presence of the *ΔicsA* mutant due to the removal of IcsA and consequent absence of actin polymerisation. In contrast, wild-type *S. sonnei* produced actin tails (Fig. 11). In addition, the increased number

of *Shigella* bacteria with no actin tails is caused by the functions of myosin II. Mostowy *et al.,* in their 2010 study, compared the number of *Shigella* septin cages and actin tails in SiRNA-treated cells. They found that myosin II-depleted cells had significantly more actin tails (2.3 ± 0.4-fold) compared to control cells (Mostowy *et al.,* 2010).

Propolin D is a natural compound that can inhibit *Shigella* growth inside host cells (Xu *et al.,* 2011). The presence of propolin D in infected host cells has no effect on the ability of wild-type *S. sonnei* to form actin tails (Fig. 10 and 11). Although propolin D has no role in inhibition of actin tail formation, it does play a role in promoting autophagy (Fig. 12). However, our results did not indicate whether propolin D promotes or inhibits septin cage formation. More research is required in order to determine whether propolin D promotes septin cage formation. Additionally, propolin D may promote expression of TNFα, which stimulates septin cage formation in response to *Shigella* infection.

The septin cages that compartmentalize intracellular *Shigella* are then targeted by autophagy (Mostowy *et al.*, 2010). In the absence of IcsA, all *Shigella* were caged by septin, leading to autophagy for degradation. Autophagy is a conserved process in host cells with different functions, including nutrient cycling, degradation of defective proteins and organelles, and microbial recognition in innate defence against pathogens such as *Shigella* (Kayath *et al.*, 2010). Wild-type and *ATG5*-knockout HEK293 cell lines were used to test the role of autophagy against intracellular *Shigella*. Intracellular CFU significantly increased in *ATG5*-knockout cells compared to wild-type HEK293 cells. Results showed that intracellular growth is prevented in strain with defective *icsA*. Moreover, ATG5 recognises *Shigella* IcsA in order to trigger the formation of autophagic isolation membranes (Ogawa *et al.*, 2005). Thus, a defective ATG5 in host cells increases intracellular growth and exhibits actin polymerisation promotion by preventing autophagy. Propolin D and other compounds were screened for their activities in enhancing autophagy in the control of intracellular *S. sonnei*. All the compounds significantly reduced intracellular CFU in wild-type HEK293 cells. However, none of these compounds reduced intracellular CFU in *ATG5*-knockout cells. ATG5 is essential for autophagy. ATG5 is induced by

the binding of *Shigella* IcsA and this binding is prevented by IcsB. Propolin D inhibited intracellular growth of *S. sonnei ΔicsB* mutant (Fig 13). In addition, propolin D inhibited *Shigella* growth in host cells lacking ATG5 protein, which prevents autophagy initiation (Fig 12). In contrast, intracellular *Shigella* growth in wild-type host cells was not inhibited by propolin D or other compounds. Therefore, propolin D and other compounds enhance autophagy. Intracellular CFU was not reduced following deletion in the autophagy *ATG5* gene which causes defects in the control of intracellular *Shigella*. Propolin D and other compounds appear to play a mechanistic role in enhancing the autophagy pathway to control intracellular *Shigella* growth.

The release of the T3SS effector IcsB in epithelial cells supports the ability of *Shigella* to evade autophagy. IcsB plays essential roles in *Shigella* transmission and survival, with IcsB involved in binding to IcsA. IcsB is not only involved in actin polymerisation, but also binds to ATG5, which results in *Shigella* destruction by autophagosomes. This destruction is prevented by IcsB binding to IcsA (Kayath *et*

al., 2010). Here, natural compounds have been examined for their effect on HEK293 cells infected with *ΔicsB* strains. Evasion of the autophagy pathway is inhibited by *Shigella ΔicsB* strain. Intracellular *Shigella ΔicsB* CFU in HEK293 cells were significantly reduced by treatment of natural compounds and propolin D (Fig. 13). This demonstrates that propolin D significantly inhibits *S. sonnei* growth in cells lacking autophagy evasion. IcsB inhibits the interaction between IcsA and ATG5 by binding IcsA, which is required for autophagy evasion (Ogawa *et al.*, 2005). Results showed that flavonoid compounds have no effect on cells lacking ATG5 (Fig. 12), and confirmed that propolin D also enhances autophagy in the control intracellular *Shigella* growth. Propolin D functions better in the presence of *ΔicsB* mutant strains, suggesting that propolin D may enhance autophagy. Since autophagy and septin cage formation contribute to the same process, propolin D may also have an effect on septin cage formation. These natural products seem to have important mechanisms that enable them to control bacterial intracellular survival. Flavonoids such as propolin D play important roles in protecting against intracellular bacterial pathogens. Importantly, MTT assays showed that these flavonoids displayed insignificant cytotoxicity on HEK293 cells, except compound DT-6 (Fig. 14). An MTT

assay for host cell cytotoxicity also verified that the highest concentration of the seven compounds (42 μM) used did not decrease intracellular CFU.

It is clear that propolin D penetrates host cells (Fig. 15). The side chain of propolin D seems to be the structure that determines intracellular accumulation, as eriodictyol (which lacks this side-chain) hardly penetrated the cell cytosol (Fig. 15). Thus, it is possible that propolin D acts directly on intracellular *S. sonnei* in addition to its role in promoting autophagy (Fig. 12). Actin tails were observed behind intracellular *Shigella* in the presence of propolin D (Fig. 11), which suggests that this compound has no impact on septin cage formation, and therefore no effect on reducing intracellular growth of *S. sonnei* through this mechanism, since septin cages are known to reduce actin polymerisation of intracellular *Shigella* (Mostowy *et al.*, 2010).

Different types of propolin can be isolated from propolis, including A, B, C, E, F, G and H. Propolin A, B and C are inducers of apoptosis in human melanoma cells (Chen *et al.,* 2004). Propolin G can induce caspase–dependent apoptosis in brain

cancer cells (Huang *et al.,* 2007), and Propolin H can induce G1 arrest in human lung carcinoma cells (Weng *et al.,* 2007). Propolins are isolated from propolis, which contains approximately 50% of resin and balsam, 30% of wax, 10% of essential and aromatic oils, 5% of pollen and 5% of impurities. The variability of plant species growing around any hive causes variability of the chemical composition of propolis. In addition, propolis composition depends on seasonality, illumination, altitude, collector type and food availability (Toreti *et al.,* 2013). To date, there are more than 300 chemical constituents identified in propolis from different regions. This difference affects biological activities of propolis. The chemical composition of bee glue is also determined by the composition of the plant sources which again depends on geographical location. The biological activities of propolis depends too on the site of collection. Thus, there is an issue related to the diversity of the chemical composition of propolis. This inevitably leads to problems of standardisation of preparation of test and future use as a medicinal product. For example, the chemical composition of propolis varies with the plant source collection. This is important for dealing with reliable criteria for chemical standardisation of different propolis types (Toreti *et al.,* 2013).

Since DsbA has previously been demonstrated to be crucial in *Shigella* intracellular survival (Yu, 1998), it was logical therefore to investigate whether propolin D could inhibit the activity of *S. sonnei* DsbA. Since the cell cytosol is a reducing environment and DsbA has been demonstrated to be crucial in *Shigella* survival in this cellular niche (Yu, 1998), it was also logical to determine whether propolin D could inhibit *Shigella* DsbA within the cell cytosol.

7.2 The action of propolin D and monoterpenes to DsbA *in vitro*

The host cell cytosol is a reducing environment that contains high levels of GSH for cell protection. It has been demonstrated that propolin D reduces *Shigella* growth in the presence of GSH in M9 medium. Previous results showed that propolin D penetrates host cells, and GSH plays a role in protecting host cells from generating oxidative stress (Mari *et al*., 2009). It was therefore of interest to determine if propolin D could interact with *Shigella* in the cytosol, and to which *Shigella* protein it interacted with. DsbA is a prime candidate, as previous studies had shown that

Shigella requires this periplasmic protein to survive within the reducing cell cytosol (Yu, 1998). Most Gram-negative pathogens contain the DsbA protein which is a periplasmic disulphide oxidoreductase, catalysing disulphide bond formation in exported proteins.

Growth curves of *Shigella* in M9 medium were constructed to determine the inhibition of *S. sonnei* growth by propolin D. The results show that this compound indeed reduces *S. sonnei* growth (Fig. 19a). In the presence of 42 μM propolin D and 5 mM GSH, *S. sonnei* growth was significantly inhibited. Results indicating that *Shigella* number are reduced in the presence of both propolin D and GSH, and that propolin D is able to penetrate host cells, show that propolin D interacts with certain *Shigella* proteins. In addition, GSH is a reducing agent that reduces disulphide bonds formed within cytoplasmic proteins. GSH reduced oxidised DsbA, which is essential for *Shigella* survival. Moreover, the growth of wild-type *S. sonnei* was much faster compared to that of the *ΔdsbA* mutant strain. These results show the importance of DsbA in *Shigella* and propolin D activities in host cells.

Hyperosmotic M9 medium (addition of NaCl) causes slow growth of *S. sonnei*. The growth of the *ΔdsbA* mutant strain was much slower compared to that of wild-type *S. sonnei* in this hyperosmotic medium, suggesting that inactivation of *dsbA* renders *S. sonnei* more vulnerable to general stress. Analysis of the transcription of key genes responsible for envelope stress responses confirmed this notion. Transcription of *dsbA, fkpA, rseB* and *spy* genes differ in hyperosmotic conditions compared to medium supplemented with 5 mM GSH, and 5 mM GSH + propolin D. It seems that there is interaction between certain flavonoid compounds such as propolin D, and DsbA. Data obtained from qPCR clearly showed that *S. sonnei* in the absence of propolin D expresses low levels of *dsbA* compared to *S. sonnei* with propolin D treatment (Fig. 21). *S. sonnei dsbA* is an important gene which encodes a periplasmic oxidoreductase enzyme for disulphide bond formation. This ensures *S. sonnei* survival in reducing environments such as the cytosol. Previous data showed that propolin D penetrates host cells and reduces *S. sonnei* growth. This strongly suggests that propolin D has an impact on the upregulation of *dsbA* expression.

A fluorescence probe was created by attaching two eosin molecules to the free amino group of glutathione disulphide, generating Di-E-GSSG. This Di-E-GSSG is relatively non-fluorescent due to fluorescence self quenching (FSQ). By adding 10 mM DTT to Di-E-GSSG, a 70-fold increase in fluorescence was observed, suggesting that Di-E-GSSG was converted to EGSH (Fig. 23). A previous study demonstrated the sensitivity of this assay in determining reductase activity (Raturi & Mutus, 2007). The results obtained here confirm the speed and sensitivity of the assay in determining reductase activity. Studies by Raturi & Mutus (2007) also showed a rapid increase in the fluorescence of Di-E-GSSG as a function of time in samples containing 5-20 nM PDI (Raturi & Mutus, 2007). Similar results were obtained for the fluorescence of Di-E-GSSG in samples containing 5-20 nM PDI in the presence of a minimal concentration of 5 μM DTT (Fig. 24). PDI is a redox protein found in the lumen of the endoplasmic reticulum (Khan & Mutus, 2014). Raturi & Mutus (2007) also showed PDI reductase activity increases as a function of Di-E-GSSG, with a Km of 650± 40nM (Raturi & Mutus, 2007). These results are

similar to those obtained here, in which the Km was estimated, as shown in Fig. 25. These results demonstrate the reductase activity of PDI.

Next, the reduction of Di-E-GSSG by DsbA and DsbA33G as a function of time was determined (Fig. 26). DsbA and DsbA33G proteins were purified from periplasmic space by SDS-PAGE and western blot as per Wunderlich & Glockshuber, 1993. Large amounts of DsbA and DsbA33G protein were produced by *S. sonnei* cells upon induction with IPTG (Fig. 22a and b). A rapid increase in fluorescence of DI-E-GSSG (150 nM) was observed as a function of time in samples containing 10-40 nM of DsbA or Dsba33G (Fig. 26). This result shows that DsbA reduces Di-E-GSSG to EGSH. Previous results demonstrated that PDI reduced Di-E-GSSG to EGSH, while one study showed that DsbA has redox properties similar to those of eukaryotic PDI (Wunderlich & Glockshuber, 1992). However, it is still not known whether the oxidation properties of DsbA are similar to its reduction properties. In addition, it was interesting to determine whether the catalytic mechanisms of DsbA differ from those of other proteins. DsbA may have roles in promoting glutathione reductase, which

reduces GSSG to GSH. DsbA33G, in which the Cys33 residue at the active site is replaced with a glycine residue, was analysed. Reduction of Di-E-GSSG by DsbA33G was half that of DsbA, at approximately 2500 RFU/s and 1250 RFU/s for DsbA and DsbA33G, respectively. The DsbA protein was successfully shown to reduce Di-E-GSSG to EGSH. However, DsbA can also oxidise cysteines on a substrate protein (Kishigami & Ito, 1996). These results show that DsbA33G is less active than DsbA, since the cysteine residue in DsbA33G has been changed.

Inhibition of disulphide reduction was determined following treatment with the natural products geraniol and geranyl acetate. Propolin D is a flavonoid compound which causes stress on the *dsbA* gene, as shown previously (Fig. 21a). Geraniol and geranyl acetate were used to determine Di-E-GSSG inhibition by DsbA and DsbA33G. These two natural products have a similar chemical structure to the side-chain of propolin D. However, their inhibitory activity has not previously been tested. Here, the inhibitory activity of geraniol and geranyl acetate on the catalytic activities of DsbA and DsbA33G were determined. Reduction of Di-E-GSSG was inhibited by

geraniol and geranyl acetate (Fig. 27). Previous results showed that propolin D penetrate inside host cell and inhibited *Shigella* growth with GSH *in vitro*. The inhibition of geraniol is likely to be caused by its structure which is similar to the side chain of propolin D. However, it is unknown where geraniol interacts with DsbA, substrate or other proteins.

The DsbA enzyme can be inhibited either competitively or non-competitively. Vmax and Km values were estimated to determine the specific mechanism of inhibition. Competitive inhibition occurs when the substrate and inhibitor compete for binding to the same active site. Vmax of DsbA with and without geraniol was determined. In the presence of geraniol, the Vmax of DsbA was lower compared to that seen without geraniol (Fig. 29a). However, the Vmax of DsbA33G with geraniol was similar to that seen without geraniol. Km values were estimated in order to specify whether inhibition was competitive. DsbA had a Km value of 200 ± 40 nM (Fig. 29b). When adding geraniol as an inhibitor, the Km value was reduced to 331.7 ± 40 nM (Fig.

29b). These results suggest that the substrate and geraniol compete for binding to the same active site of DsbA.

The Km value of DsbA33G was also estimated in the absence and presence geraniol. The reductase activity of DsbA33G increased as a function of Di-E-GSSG, with an apparent Km value of 537.6 ± 40 nM, (Fig. 29c) which suggested that affinity of the substrate to DsbA33G was very low. The Km value of DsbA33G increased to 331.8 ± 40 nM (Fig. 29c) in the presence of geraniol, a result that was unexpected and unexplainable. Why geraniol should induce DsbA33G to have a higher affinity with GSSG requires further investigation.

One study found DsbA could be amenable to the development of novel antibacterial compounds (Adams *et al.,* 2015). Screening of fragments that bind to *E. coli* /DsbA, identified phenylthiazole compounds that inhibited DsbA activity *in vitro*. A bacterial motility assay was used to test these compounds for ability to inhibit DsbA. These compounds inhibited *E. coli* motility with no effect on growth of *E. coli* in liquid

culture, thus demonstrating selectivity for DsbA activity. The study also found that the binding of inhibitors occurred near the active site of DsbA (Adams *et al.,* 2015). Another study tested nineteen dimedone derivatives using a peptide oxidation assay and identified two strong inhibitors including one brominated compound (Halili *et al.,* 2015). This study also confirmed that inhibitors could bind near the active site of DsbA. Duprez and colleagues (2015) also showed that some inhibitors showed selectivity as they did not bind to or inhibit human thioredoxins that share a similar active site to DsbA.

7.3 Geraniol as a lead candidate for the treatment of *Shigella* infection

After determining the effect of geraniol on the reductase function of DsbA, the effect of geraniol on the inhibition of *Shigella* growth was determined in M9 minimal medium in the presence of GSH. It has been shown that geraniol significantly increases the level of GSH in animal cells (Khan *et al*., 2013). Geraniol had not previously been tested on *S. sonnei* growth. Here, the effect of geraniol on the growth curve of *S. sonnei* in M9 minimal medium was analysed. The growth curve of *S. sonnei* in M9 minimal medium was determined as shown in Fig. 30. Reduction in

S. sonnei growth in the presence of 5 mM GSH with 42 μM geraniol was observed. Moreover, the growth of *S. sonnei* in the presence of 5 mM GSH with 42 μM geraniol was observed to be similar to the growth of *S. sonnei* seen in the presence of 5mM GSH with 42μM propolin D (Fig. 30). Previous results showed that geraniol inhibits DsbA reduction of Di-E-GSSG to GSH, and that propolin D reduces *S. sonnei* growth in the presence of 5mM GSH. Therefore, it can be concluded that it is likely that propolin D inhibits DsbA reduction of Di-E-GSSG to GSH in *S. sonnei* growth. In addition, geraniol has a similar side chain to that of propolin D. These structures seem to determine the activities of propolin D. These results suggest that geraniol treatment acts similarly to propolin D on *S. sonnei* growth in the presence of 5 mM GSH.

The *G. mellonella* larva model is a useful model for assessing the effect of antimicrobial agents on infected larvae (Desbois & Coote, 2011). The *G. mellonella* larva *in vivo* model was used in this study to test geraniol. Since the effect of geraniol on *G. mellonella* larvae infected with *S. sonnei* was previously unknown, the *G.*

mellonella larva model was employed to determine the effect of geraniol. Geraniol was found to protect *S. sonnei*-infected *G. mellonella* larvae. Previous results (Fig. 27) showed that geraniol inhibited reduction of DsbA by Di-E-GSSG and also inhibited *Shigella* growth. Therefore, geraniol inhibited *Shigella* growth in *G. mellonella* larvae. In addition, geraniol exhibits no cytotoxicity in *G. mellonella* larvae, with all larvae treated with geraniol surviving for 5 days, except larvae treated at the highest amount tested, (i.e. 8740µg geraniol) (Fig. 33a). All larvae infected with *S. sonnei* and treated with geraniol also survived for 5 days (Fig. 33b). Additionally, previous results showed that geraniol displays no cytotoxicity in both RAW 264 macrophage cells and HEK293 cells. A good antimicrobial agent must possess selective cytotoxicity on bacterial cells (Fig. 31 & 32). These results suggested that geraniol is a safe effective a lead candidate in the potential treatment of *Shigella* infection.

Shigella, the agent that causes bacillary dysentery, invades epithelial cells and macrophages. HEK293 epithelial cells were used to determine the effect of geraniol

on *Shigella*. Results showed that geraniol inhibits *S. sonnei* growth in HEK293 cells (Fig. 35). A 5-fold reduction of intracellular *S. sonnei* in the host cells was seen with 42 μM geraniol (Fig. 35). We also observed that geraniol reduced *S. sonnei* growth in reducing environment in the presence of GSH; moreover, geraniol inhibited DsbA reduction of GSSG to GSH. Therefore, *S. sonnei* growth in epithelial cells can be inhibited by geraniol. In addition, propolin D has an impact on *dsbA*. These results demonstrate the effect of geraniol on *S. sonnei*.

Geraniol was examined for its effect on macrophages infected with *S. sonnei*. Geraniol inhibited *S. sonnei* growth in RAW 264 mouse macrophages cells (Fig. 34). At 84 μM, geraniol led to a ~50% reduction in intracellular CFU from 31 x 10^3 (control) to 12.5 x 10^3 CFU. Further intracellular reductions in CFU were seen using 168 μM geraniol. In line with previous results, showing that geraniol inhibits *S. sonnei* growth in host epithelial cells and that it inhibits DsbA reduction, it is likely that geraniol also inhibits DsbA within macrophages. It is also known that *Shigella* induces apoptosis in macrophages, which results in the release of IL-1β and IL-18

pro-inflammatory cytokines (Schroeder & Hilbi, 2008). It is not known, however, whether geraniol causes release of TNF-α. In addition, *Shigella* strains can induce rapid and significant release of IL-1β and IL18 (Zychlinsky *et al.*, 1994). The induction and release of IL-1 may be inhibited by geraniol. It was also confirmed that geraniol may prevent *S. sonnei* bacteria from inducing apoptosis in infected macrophages. It also suggests that the release of IL-1 may be prevented upon treatment with geraniol.

S. sonnei was grown in acidic, nutrient-poor medium with and without treatment of geraniol. It is known that some Gram-negative bacteria such as *Salmonella* can survive and replicate in active phagolysosomes where they are exposed to extreme conditions (e.g. low pH) (Bringer *et al.*, 2007). *Salmonella enterica* serovar typhimurium can invade intestinal macrophages, survive, replicate and spread throughout host cells (Achouri *et al.*, 2015). As shown in Fig. 36, *S. sonnei* bacteria were able to grow and survive in acidic, nutrient-poor medium. Moreover, geraniol was shown to inhibit the growth of *Shigella* (and perhaps other Gram negative

pathogens) in acidic, nutrient-poor medium. These results demonstrate that geraniol could potentially be used against *S. sonnei* infection *in vivo.*

7.4 Geraniol as lead candidate for the treatment of AIEC infection

Crohn's disease is an inflammatory bowel disease, and AIEC infection is a key aetiological factor in the disease and its progression. The disease pathogenesis includes aphthous ulceration of the mucosa, transmural abscesses and macrophage and epithelioid cell granulomas (Bringer *et al.*, 2006). The current treatment of AIEC infection focusses on combating Crohn's disease and/or preventing relapse and maintaining patients in remission. Hydroxychloroquine (HCQ) has been shown to enhance intramacrophage killing of AIEC in murine and human macrophages (Flanagan *et al.*, 2015). HCQ can also increase phagolysosomal pH and alter intracellular iron metabolism, which affects the killing of AIEC. The antimicrobial effect of antibiotics such as ciprofloxacin and doxycycline against AIEC replication in macrophages was also enhanced by treatment with HCQ (Flanagan *et al.*, 2015).

Other treatments involve the use of combination antibiotic therapy targeting intramacrophage AIEC. Antibiotics such as ciprofloxacin, rifampin, tetracycline, clarithromycin, sulfamethoxazole, trimethoprim and azithromycin can effectively kill HM605 CD AIEC in macrophages (Subramanian *et al*., 2008). Vitamin D is another compound which enhances killing of intramacrophage AIEC (Flanagan *et al*., 2015). Another approach to prevent relapse and combat Crohn's disease is the use of *Saccharomyces cerevisiae* yeast, which can prevent AIEC-induced colitis in mice. It has been shown that *S. cerevisiae* has the ability to inhibit AIEC LF82 adhesion to and invasion of, intestinal epithelial cells (Sivignon *et al*., 2015). AIEC adheres to intestinal epithelial cells through type-1 pili by binding to mannose residues on glycoproteins (Sivignon *et al*., 2015). *S. cerevisiae* inhibits FimH-CEACAM6 interaction to prevent AIEC colonisation. *S. cerevisiae* can also prevent AIEC adhesion to enterocytes isolated from patients with CD. *S. cerevisiae* can control disease activity and decreases AIEC LF82 gut colonisation (Sivignon *et al*., 2015). Levels of cytokines IL6 and IL1-β released by the colonic mucosa in LF82 infected mice are decreased by treatment with the yeast. In addition, *S. cerevisiae* can maintain barrier integrity in mice infected with AIEC (Sivignon *et al*., 2015). These

properties of *S. cerevisiae* show it to be a potential target treatment of CD-associated AIEC.

Geraniol exhibits antimicrobial activity against several bacterial pathogens (Solorzano-Santos & Miranda-Novales, 2012). Since the *Galleria mellonella* larva model can be used to determine the virulence of various human pathogens (Desbois & Coote, 2011), it was exploited here to investigate the *in vivo* potential of using geraniol in the treatment of AIEC infection. Larvae infected with AIEC strains (LF82, HM427, HM605 and HM615) were protected with geraniol treatment (Fig. 37). Data in Fig 27 showed that geraniol inhibited the reduction of Di-E-GSSG via DsbA, and moth larvae infected with *S. sonnei* were protected by geraniol; it is possible to speculate therefore that geraniol interacts with DsbA in infected moth larvae. In addition, previous results also showed that geraniol displays no cytotoxicity in moth larvae. The results of the *G. mellonella* larva model showed protection of geraniol in larvae infected with AIEC strains, which suggests that geraniol can be used as a lead structure in the treatment of AIEC infection. Since larvae can tolerate high

concentrations of geraniol, and since geraniol is widely used in skin beauty products, the safety of using geraniol is not of significant concern. The FDA (Food and drug administration) classified geraniol as generally safe. Geraniol is a compound of low toxicity which is widely used as an ingredient in fragrances, shampoos, soaps and other cosmetics (Lapczynski *et al.*, 2008; Fazio *et al.,* 2016). *In vitro* studies have shown too that geraniol has low skin absorption rates (3.5%), which suggests that geraniol has a low ability to induce allergenicity and other skin issues (Gilpin *et al.*, 2010).

A further study has tested the immunomodulatory and non cytotoxic activity of geraniol (Andrade *et al.,* 2014). Andrade and colleagues evaluated the immunomodulatory action of *Cymbopogon martinii* essential oil and geraniol with regard to secretion of pro and anti-inflammatory cytokines (TNF-α and IL-10) by human monocytes *in vitro*. The research found that geraniol had no cytotoxic effect on monocytes. Anti-inflammatory IL-10 levels were also significantly increased from

monocytes incubated with geraniol at concentration as low as 0.057 μg/mL (Andrade *et al.,* 2014).

The activity of geraniol in RAW 264 mouse macrophages was investigated. RAW 264 mouse macrophage cells were infected with AIEC in the presence of different concentrations of geraniol (42, 84 and 168 μM). At a concentration of 84 μM, geraniol was found to inhibit intracellular CFU of various AIEC strains (Fig. 38), suggesting that geraniol assists macrophages in killing bacteria. In addition, geraniol may reduce intracellular CFU by interacting with TNF-α. Geraniol may protect host cells from AIEC infection in a similar way as *Shigella*.

AIEC strains (LF82, HM427, HM605 and HM615) were grown in acidic, nutrient-poor medium with and without treatment with geraniol. It is known that AIEC bacteria can survive and replicate in active phagolysosomes where they are exposed to stress by the extreme conditions (low pH and poor nutrient supply) (Bringer *et al.*, 2007). AIEC bacteria were found to grow and survive in acidic, nutrient-poor medium. These

results suggest that AIEC bacteria can survive and replicate in active phagolysosomes. Using natural products such as geraniol, the growth of AIEC can be inhibited in acidic, nutrient-poor medium. The results (Fig. 39) confirm that the growth of AIEC strains was reduced by geraniol treatment. Studies have shown that DsbA oxidoreductase is important for AIEC bacteria in resisting death in the phagocytic vacuole environment (Bringer *et al.*, 2007). Since DsbA is essential in acidic, nutrient-poor environments for bacterial growth, the likely mechanism for geraniol in reducing intracellular CFU (Fig. 39) may be that it can kill AIEC in phagocytic vacuoles by inhibiting the function of DsbA. These results demonstrate that geraniol is an effective lead candidate against AIEC bacteria.

AIEC are affected by geraniol in an acidic culture environment, but it is unknown how geraniol inhibition of AIEC might occur in an acidic environment, such as within the macrophage phagolysosome. One study has shown that geraniol oxidation activity is increased as pH increases from 7.0 to 7.5, whereas the activities decreased sharply beyond pH 10.0 (Noge *et al.,* 2008). Geraniol may be changed by the pH within

phagolysosome, which results in killing of the bacteria. The structure of geraniol may be changed by the pH of the media and geraniol could be metabolised in the phagosome by host metabolism. One study showed that geraniol was metabolised to methyl geranate in *Achyranthes bidentata* after it conjugated with glucose (Tamogami *et al.,* 2016).

One of the key environmental factors within the phagolysosome is the presence of reactive oxygen species (ROS) which can impair many cellular components such as proteins, nucleic acids and polyunsaturated fatty acids. Hydroxyl and superoxide radicals, as well as non-radical oxidants such as hydrogen peroxide (H_2O_2), hypochlorous acid and peroxynitrite are some examples of ROS generated in organisms (Ozkaya *et al.,* 2017). Ozkaya *et al.,* 2017 observed that hepatic fatty acid alterations following H_2O_2 induced oxidative stress in male rats can be attenuated by geraniol. Another study also showed geraniol act as a cardeoprotective agent increasing cardioprotective AMP-activated protein kinase (AMPK) levels and

decreasing cardiotoxic signals, e.g. (ERK1/2 and ROS) in neonatal rat ventricular cardiomyocytes (Crespo *et al.,* 2017).

One study has also interestingly investigated the role of geraniol in amelioration of dextran sulfate sodium (DSS)-induced colitis (Fazio *et al.,* 2016). A geraniol dose at 30 and 120 mg/kg was orally administered to mice. They have found that orally and enema administered geraniol was able to prevent colitis-associated dysbiosis and decrease systemic inflammation of DSS-treated mice (Fazio *et al.,* 2016). In addition, geraniol was able to significantly reduce COX-2 expression in colonic tissue and improve the clinical colitis activity score (Fazio *et al.,* 2016). This study showed that geraniol might be safely used orally for treatment of intestinal human inflammation and dysbiosis.

AIEC can survive and replicate in macrophages without resulting in apoptosis. These infected macrophages release high levels of TNF-α (Glasser *et al.*, 2001). Geraniol has some effect in the inhibition of production of cytokines such as TNF-α, IL-6 and

IL1-β (Khan *et al*., 2013). A further study also showed that geraniol reduces TNF-α and IL1-β levels in fructose-induced metabolic syndrome (MetS) in mice (Ibrahim *et al*., 2015). Therefore, geraniol could be used to inhibit production of cytokines such as TNF-α in macrophages infected with AIEC. Application of 12-O-tetradecanoylphorbol 13-acetate (TPA), a phorbol-type tumour promoter, can induce the development of oedema, hyperplasia, ROS and inflammatory responses, including expression of cyclooxygenase-2 (COX-2) in mouse skin (Chaudhary *et al*., 2012). All these inductions can be inhibited by treatment with geraniol (Chaudhary *et al*., 2012), suggesting that geraniol could be used for inducing a pro-apoptotic state via inhibition of inflammation and oxidative stress response.

7.5 Geraniol's activities to host gene regulation

Geraniol possesses activities in host gene regulation. Chaudhary *et al* (2012) showed that geraniol significantly suppressed the Ras/Raf/ERK1/2 signalling pathway and reduced expression of Bcl-2 in skin tumour. The Ras/Raf/ERK1/2 signalling pathway is composed of three proteins which play important roles in cell survival. Ras has a role in transducing cell proliferation signal to the nucleus, while

Raf activates ERKs and phosphorylates target proteins. These ERKs then trigger many transcription factors which are necessary for cell proliferation (Chaudhary *et al* 2012). The Ras/Raf/ERK1/2 signalling pathway is suppressed by geraniol. *Bcl-2* gene encodes a protein which is a key regulator of apoptosis (Korsmeyer, 1999). Bcl-2 is involved in cell survival through inhibition of apoptosis. Bax interacts with Bcl-2, which exerts its anti-apoptotic role. Downregulation of Bax protein was found in certain diseases, including metastatic breast adenocarcinoma and oral cancers (Vinothkumar *et al*., 2012). The expression of anti-apoptotic Bcl-2 is decreased by geraniol, while it increases the expression of pro-apoptotic Bax (Chaudhary *et al* 2012). Therefore, geraniol induces apoptosis and inhibits tumorigenesis.

The tumour suppressor gene (*p53*) and *Bcl-2* and *Bax* genes regulate the apoptotic pathway. p53 protects against DNA damage by inducing apoptosis and prevents inflammatory response by inhibiting the expression of *COX-2* gene. It has been found that *p53* gene can be dysregulated in 7,12-dimethylbenz[α]anthracene (DMBA)-induced oral carcinogenesis (Vinothkumar *et al*., 2012). Geraniol also

downregulates the expression of *PCNA* and *Bcl-2* in rat colon carcinogenesis. Moreover, geraniol downregulates p53 and NF-κB expression, and upregulates caspases 3, 8 and 9 in renal carcinogenesis (Vinothkumar *et al.*, 2012). The dysregulation in the expression of cell proliferative, inflammatory and apoptotic genes in the buccal mucosa of hamsters treated with DMBA can be prevented by oral administration of geraniol (Vinothkumar *et al.*, 2012). These mechanisms reveal the potential additional benefits of using geraniol to treat *Shigella* and AIEC.

Both shigellosis and Crohn's disease are characterised by inflammation. Combination of geraniol and geranium oil with vaginal washing has protective activity, suppressing *Candida* cell growth and infiltration of neutrophils to improve vaginal inflammation in vaginal candidiasis in mice (Maruyama *et al.*, 2008). The study found that the numbers of cells are significantly decreased when geraniol and geranium oil are combined with vaginal washing. A 25 μg/mL concentration of geraniol and geranium oil are able to inhibit mycelial growth but not yeast growth (Maruyama *et al.*, 2008).

Other studies have shown that geraniol can produce an antidepressant effect in chronic unpredictable mild stress (CUMS) in mice (Deng *et al.*, 2015). Treatment with geraniol alleviated the depression-related behaviours of exposed mice by restoring their decreased sucrose performance. Another effect of geraniol treatment is the regulation of CUMS-induced pro-inflammatory cytokine IL-1β, which was reversed by inhibiting NF-kB pathway activation and regulating nucleotide binding and oligomerization domain-like receptor family pyrin domain-containing 3 (NLRP3) inflammasome expression (Deng *et al.*, 2015). NF-kB is known to be a key regulator of inflammation, immune response, cell proliferation and cell survival (Jayachandran *et al.*, 2015). Levels of NF-kB can be reduced by pretreatment with geraniol (Khan *et al.*, 2013). Geraniol can enhance free radical scavenging and anti-inflammatory effect (Jayachandran *et al.*, 2015). These show that geraniol could be effective against inflammatory diseases such as shigellosis and Crohn's disease.

There are some experiments which could be undertaken in the future work to test geraniol further, including additional animal models of colitis such as TNBS colitis (Antoniou *et al.,* 2016) and *IL10-/-* mouse (Holgersen *et al.,* 2014) . Holgersen *et al.,* 2014 study used piroxicam administration (in the chow) for induction of entercolitis in *IL10-/-* mouse to evaluate cell involvement in the disease pathogenesis. This *IL10-/-* mouse (mouse model) could be used to investigate the effect of oral administration of geraniol and others terpenes in mouse. In addition, *IL10-/-* mouse (mouse model) could be used to compare with WT mouse in order to determine the effect of geraniol on Il-10. The DSS-induced colitis mouse model used by Fazio *et al*., (2016), and these other colitis models could be used to determine the effect of oral administration of geraniol following AIEC infection. AIEC LF82 are able to colonise and induce colitis in mice expressing CEACAMs (Carvalho *et al.,* 2009). The ability of geraniol to inhibit AIEC LF82 colonisation in the intestinal mucosa and induction of inflammation in CEABAC10 mouse expressing human CEACAMs (including CEACAM6 which is the mannosylated receptor for LF82 fimH interaction) could be investigated as per (Carvalho *et al.,* 2009). Quantification of AIEC LF82 bacteria could be determined in WT or CEABAC10 mice receiving DSS in drinking water before treatment with

geraniol (Carvalho *et al.,* 2009; Sivignon *et al.,* 2015). Here, confocal microscopy analysis of colonic section from mice could be used to determine the effect of geraniol on WT or CEABAC10 mice infected with AIEC LF82. Chronic AIEC infection in streptomycin-treated conventional mice could also be used to test actions of geraniol (Small *et al.,* 2013).

Other monoterpenes such as ocimene, myrcenes, citral, citronellal, citronellol, linalool and others could be used to find further activities on AIEC and *Shigella* infection compared to geraniol. AIEC grow in a low pH (acidic) environment and nutrient-poor medium (Bringer *et al.*, 2007) and data here show that geraniol inhibits AIEC growth in acidic and nutrient-poor medium. The activity of other terpenes could be investigated in acidic, nutrient poor media to compare with geraniol. Radiolabelled geraniol has been used to evaluate the penetration ability of geraniol on human skin *in vitro* (Gilpin & Hui, 2010). Radiolabelled geraniol, such as Deuterium-labelled, geraniol could therefore be used to test the structure of geraniol before and after its inhibitory activities in an acidic environment, such as within the phagolysosomes.

Mass spectrometric analysis could be used to determine for any changes in geraniol structure (Lijima *et al.,* 2004).

Geraniol may have activities inside host cells similar to propolin D. The effect of geraniol on septin cage formation in host cells could also be investigated further. Mostowy *et al.,* 2010 used a septin antibody to investigate septin cage formation in infected host cells with *Shigella*. This work could lead to finding out more information about geraniol as a lead candidate for treatment of AIEC and *Shigella* infections.

Chapter 8: Conclusion

Many Gram-negative bacterial pathogens have the ability to cause disease such as *Shigella* causing dysentery. Some diseases such as Crohn's disease are multifactorial and AIEC infection is one of the major contributing factors. Both dysentery and Crohn's disease are hyperinflammatory in nature. Due to the widespread increase of multiple antibiotic resistant strains, the treatment of bacterial infection has become a major challenge to modern medicine and a global issue in public health. Therefore, this study seeks natural products such as geraniol as an alternative strategy for treating *Shigella* and AIEC infections.

Autophagy is clearly involved in suppression of *S. sonnei* intracellular growth and a few flavonoid compounds including propolin D enhance autophagy activity (Fig. 9). Furthermore, propolin D significantly inhibits the *ΔicsB* mutant intracellular growth compared to its inhibition to wild type *S. sonnei* intracellular growth. This is further evidence that propolin D enhances autophagy as IcsB is the molecular basis for *Shigella* to evade autophagy. Intracellular *S. sonnei* is able to form actin tails in the

presence of propolin D, suggesting propolin D does not enhance septin cage formation for controlling intracellular *S. sonnei*.

Propolin D accumulates in the host cells while other flavonoid compounds do not. Propolin D exhibits anti-*Shigella* activity in reducing M9 minimal medium while eriodictyol does not, suggesting that the side chain of propolin D is the functional moiety for cell penetration as well as inhibition of bacterial growth. Propolin D caused specific stress response to *S. sonnei* and the expression of 4 genes (*dsbA, dkpA, desB* and *spy*) involved in the envelope stress response is significantly changed.

Since the periplasmic oxidoreductase DsbA is vital for *Shigella* survival within the reducing host cell cytosol, I investigated whether propolin D could inhibit DsbA function *in vitro* using purified DsbA, mutant protein DsbA33G and fluorescently labelled Di-E-GSSG. This investigation was extended using geraniol and geranyl acetate which have a similar side chain to propolin D. Geraniol was shown to be

more potent that geranyl acetate in inhibiting reduction of GSSG. Geraniol competitively inhibited the reduction of GSSG.

In vivo experiments using the wax moth *Galleria* larva model has shown that geraniol is able to protect larvae from infection by *S. sonnei* and AIEC. An MTT assay showed that geraniol exhibits no cytotoxicity towards HEK293 cells and macrophages. *In vivo* experiments show *Galleria mellonella* larvae are highly tolerant to geraniol.

In summary, natural products exemplified by geraniol hold great potential in combating infection caused by multiple antibiotic resistant Gram –ve bacterial pathogens. These products can not only target major virulence factors such as DsbA but also enhance innate cellular immunity such as autophagy. The use of these products also offers low risk of antimicrobial resistance. Furthermore, products such as geraniol induce anti-inflammatory cytokines production and work in synergy with antibiotics. These unique features make them favourable for the treatment of bacterial infection.

Chapter 9: References

Achouri S, Wright JA, Evans L, Macleod C, Fraser G, Cicuta P, Bryant CE. 2015. The frequency and duration of *Salmonella*-macrophage adhesion events determines infection efficiency. Philos Trans R Soc Lond B Biol Sci **370:**20140033.

Adams LA, Sharma P, Mohanty B, Ilyichova OV, Mulcair MD, Williams ML, Gleeson EC, Totsika M, Doak BC, Caria S, Rimmer K, Horne J, Shouldice SR, Vazirani M, Headey SJ, Plumb BR, Martin JL, Heras B, Simpson JS, Scanlon MJ. 2015. Application of fragment-based screening to the design of inhibitors of *Escherichia coli* DsbA. Angew Chem Int Ed Engl **54:**2179-2184.

Ali Khan H, Mutus B. 2014. Protein disulfide isomerase a multifunctional protein with multiple physiological roles. Front Chem **2:**70.

Allaoui A, Mounier J, Prevost MC, Sansonetti PJ, Parsot C. 1992. icsB: a *Shigella flexneri* virulence gene necessary for the lysis of protrusions during intercellular spread. Mol Microbiol **6:**1605-1616.

Alonso A, Garcia-del Portillo F. 2004. Hijacking of eukaryotic functions by intracellular bacterial pathogens. Int Microbiol **7:**181-191.

Andrade BF, Braga CP, Dos Santos KC, Barbosa LN, Rall VL, Sforcin JM, Fernandes AA, Fernandes Junior A. 2014. Effect of Inhaling Cymbopogon martinii Essential Oil and Geraniol on Serum Biochemistry Parameters and Oxidative Stress in Rats. Biochem Res Int **2014:**493183.

Antoniou E, Margonis GA, Angelou A, Pikouli A, Argiri P, Karavokyros I, Papalois A, Pikoulis E. 2016. The TNBS-induced colitis animal model: An overview. Ann Med Surg (Lond) **11:**9-15.

Appenzeller-Herzog C. 2011. Glutathione- and non-glutathione-based oxidant control in the endoplasmic reticulum. J Cell Sci **124:**847-855.

Arena ET, Campbell-Valois FX, Tinevez JY, Nigro G, Sachse M, Moya-Nilges M, Nothelfer K, Marteyn B, Shorte SL, Sansonetti PJ. 2015. Bioimage analysis of *Shigella* infection reveals targeting of colonic crypts. Proc Natl Acad Sci U S A **112:**E3282-3290.

Ashkenazi S, Levy I, Kazaronovski V, Samra Z. 2003. Growing antimicrobial resistance of *Shigella* isolates. J Antimicrob Chemother **51:**427-429.

Barnich N, Carvalho FA, Glasser AL, Darcha C, Jantscheff P, Allez M, Peeters H, Bommelaer G, Desreumaux P, Colombel JF, Darfeuille-Michaud A. 2007. CEACAM6 acts as a receptor for adherent-invasive *E. coli*, supporting ileal mucosa colonization in Crohn disease. J Clin Invest **117:**1566-1574.

Blondel CJ, Jimenez JC, Leiva LE, Alvarez SA, Pinto BI, Contreras F, Pezoa D, Santiviago CA, Contreras I. 2013. The type VI secretion system encoded in *Salmonella* pathogenicity island 19 is required for *Salmonella enterica* serotype Gallinarum survival within infected macrophages. Infect Immun **81:**1207-1220.

Bonnet M, Tran Van Nhieu G. 2016. How Shigella Utilizes Ca(2+) Jagged Edge Signals during Invasion of Epithelial Cells. Front Cell Infect Microbiol **6:**16.

Boudeau J, Glasser AL, Masseret E, Joly B, Darfeuille-Michaud A. 1999. Invasive ability of an *Escherichia coli* strain isolated from the ileal mucosa of a patient with Crohn's disease. Infect Immun **67:**4499-4509.

Bourdet-Sicard R, Rudiger M, Jockusch BM, Gounon P, Sansonetti PJ, Nhieu GT. 1999. Binding of the *Shigella* protein IpaA to vinculin induces F-actin depolymerization. EMBO J **18:**5853-5862.

Boyapati R, Satsangi J, Ho GT. 2015. Pathogenesis of Crohn's disease. F1000Prime Rep **7:**44.

Bringer MA, Barnich N, Glasser AL, Bardot O, Darfeuille-Michaud A. 2005. HtrA stress protein is involved in intramacrophagic replication of adherent and invasive Escherichia coli strain LF82 isolated from a patient with Crohn's disease. Infect Immun **73:**712-721.

Bringer MA, Glasser AL, Tung CH, Meresse S, Darfeuille-Michaud A. 2006. The Crohn's disease-associated adherent-invasive *Escherichia coli* strain LF82 replicates in mature phagolysosomes within J774 macrophages. Cell Microbiol **8:**471-484.

Bringer MA, Rolhion N, Glasser AL, Darfeuille-Michaud A. 2007. The oxidoreductase DsbA plays a key role in the ability of the Crohn's disease-associated adherent-invasive *Escherichia coli* strain LF82 to resist macrophage killing. J Bacteriol **189:**4860-4871.

Bromberg J, Darnell JE, Jr. 2000. The role of STATs in transcriptional control and their impact on cellular function. Oncogene **19:**2468-2473.

Brotcke Zumsteg A, Goosmann C, Brinkmann V, Morona R, Zychlinsky A. 2014. IcsA is a *Shigella* flexneri adhesin regulated by the type III secretion system and required for pathogenesis. Cell Host Microbe **15:**435-445.

Burman C, Ktistakis NT. 2010. Autophagosome formation in mammalian cells. Semin Immunopathol **32:**397-413.

Byers B, Goetsch L. 1976. A highly ordered ring of membrane-associated filaments in budding yeast. J Cell Biol **69:**717-721.

Campoy E, Colombo MI. 2009. Autophagy in intracellular bacterial infection. Biochim Biophys Acta **1793:**1465-1477.

Carlberg I, Mannervik B. 1985. Glutathione reductase. Methods Enzymol **113:**484-490.

Carvalho FA, Barnich N, Sivignon A, Darcha C, Chan CH, Stanners CP, Darfeuille-Michaud A. 2009. Crohn's disease adherent-invasive *Escherichia coli* colonize and induce strong gut inflammation in transgenic mice expressing human CEACAM. J Exp Med **206:**2179-2189.

Castanie-Cornet MP, Cam K, Bastiat B, Cros A, Bordes P, Gutierrez C. 2010. Acid stress response in *Escherichia coli*: mechanism of regulation of gadA transcription by RcsB and GadE. Nucleic Acids Res **38:**3546-3554.

Charbonnier JB, Belin P, Moutiez M, Stura EA, Quemeneur E. 1999. On the role of the cis-proline residue in the active site of DsbA. Protein Sci **8:**96-105.

Chassaing B, Rolhion N, de Vallee A, Salim SY, Prorok-Hamon M, Neut C, Campbell BJ, Soderholm JD, Hugot JP, Colombel JF, Darfeuille-Michaud A. 2011. Crohn disease--associated adherent-invasive *E. coli* bacteria target mouse and human Peyer's patches via long polar fimbriae. J Clin Invest **121:**966-975.

Chaudhary SC, Siddiqui MS, Athar M, Alam MS. 2013. Geraniol inhibits murine skin tumorigenesis by modulating COX-2 expression, Ras-ERK1/2 signaling pathway and apoptosis. J Appl Toxicol **33:**828-837.

Chen CN, Wu CL, Lin JK. 2004. Propolin C from propolis induces apoptosis through activating caspases, Bid and cytochrome c release in human melanoma cells. Biochem Pharmacol **67:**53-66.

Chirumbolo S. 2010. The role of quercetin, flavonols and flavones in modulating inflammatory cell function. Inflamm Allergy Drug Targets **9:**263-285.

Cosnes J, Gower-Rousseau C, Seksik P, Cortot A. 2011. Epidemiology and natural history of inflammatory bowel diseases. Gastroenterology **140:**1785-1794.

Cowan MM. 1999. Plant products as antimicrobial agents. Clin Microbiol Rev **12:**564-582.

Crespo R, Wei K, Rodenak-Kladniew B, Mercola M, Ruiz-Lozano P, Hurtado C. 2017. Effect of geraniol on rat cardiomyocytes and its potential use as a cardioprotective natural compound. Life Sci **172:**8-12.

Cushnie TP, Lamb AJ. 2005. Antimicrobial activity of flavonoids. Int J Antimicrob Agents **26:**343-356.

Darfeuille-Michaud A, Boudeau J, Bulois P, Neut C, Glasser AL, Barnich N, Bringer MA, Swidsinski A, Beaugerie L, Colombel JF. 2004. High prevalence of adherent-invasive *Escherichia coli* associated with ileal mucosa in Crohn's disease. Gastroenterology **127:**412-421.

Darfeuille-Michaud A, Neut C, Barnich N, Lederman E, Di Martino P, Desreumaux P, Gambiez L, Joly B, Cortot A, Colombel JF. 1998. Presence of adherent *Escherichia coli* strains in ileal mucosa of patients with Crohn's disease. Gastroenterology **115:**1405-1413.

Datsenko KA, Wanner BL. 2000. One-step inactivation of chromosomal genes in *Escherichia coli* K-12 using PCR products. Proc Natl Acad Sci U S A **97:**6640-6645.

De Fazio L, Spisni E, Cavazza E, Strillacci A, Candela M, Centanni M, Ricci C, Rizzello F, Campieri M, Valerii MC. 2016. Dietary Geraniol by Oral or Enema Administration Strongly Reduces Dysbiosis and Systemic Inflammation in Dextran Sulfate Sodium-Treated Mice. Front Pharmacol **7:**38.

Deng XY, Xue JS, Li HY, Ma ZQ, Fu Q, Qu R, Ma SP. 2015. Geraniol produces antidepressant-like effects in a chronic unpredictable mild stress mice model. Physiol Behav **152:**264-271.

Desbois AP, Coote PJ. 2011. Wax moth larva (*Galleria mellonella*): an in vivo model for assessing the efficacy of antistaphylococcal agents. J Antimicrob Chemother **66:**1785-1790.

Dickinson DA, Forman HJ. 2002. Cellular glutathione and thiols metabolism. Biochem Pharmacol **64:**1019-1026.

Dogan B, Scherl E, Bosworth B, Yantiss R, Altier C, McDonough PL, Jiang ZD, Dupont HL, Garneau P, Harel J, Rishniw M, Simpson KW. 2013. Multidrug resistance is common in *Escherichia coli* associated with ileal Crohn's disease. Inflamm Bowel Dis **19:**141-150.

Dogan B, Suzuki H, Herlekar D, Sartor RB, Campbell BJ, Roberts CL, Stewart K, Scherl EJ, Araz Y, Bitar PP, Lefebure T, Chandler B, Schukken YH, Stanhope MJ, Simpson KW. 2014. Inflammation-associated adherent-invasive *Escherichia coli* are enriched in pathways for use of propanediol and iron and M-cell translocation. Inflamm Bowel Dis **20:**1919-1932.

Doherty GJ, McMahon HT. 2008. Mediation, modulation, and consequences of membrane-cytoskeleton interactions. Annu Rev Biophys **37:**65-95.

Dubey VS, Luthra R. 2001. Biotransformation of geranyl acetate to geraniol during palmarosa (Cymbopogon martinii, Roxb. wats. var. motia) inflorescence development. Phytochemistry **57:**675-680.

Duprez W, Premkumar L, Halili MA, Lindahl F, Reid RC, Fairlie DP, Martin JL. 2015. Peptide inhibitors of the *Escherichia coli* DsbA oxidative machinery essential for bacterial virulence. J Med Chem **58:**577-587.

Eaves-Pyles T, Allen CA, Taormina J, Swidsinski A, Tutt CB, Jezek GE, Islas-Islas M, Torres AG. 2008. *Escherichia coli* isolated from a Crohn's disease patient adheres, invades, and induces inflammatory responses in polarized intestinal epithelial cells. Int J Med Microbiol **298:**397-409.

Economou M, Zambeli S, Michopoulos S. 2009. Incidence and prevalence of Crohn's disease and its etiological influences. Annals of gastroenterology **22:**158-167.

Flanagan PK, Chiewchengchol D, Wright HL, Edwards SW, Alswied A, Satsangi J, Subramanian S, Rhodes JM, Campbell BJ. 2015. Killing of *Escherichia coli* by Crohn's Disease Monocyte-derived Macrophages and Its Enhancement by Hydroxychloroquine and Vitamin D. Inflamm Bowel Dis **21:**1499-1510.

Gilpin S, Hui X, Maibach H. 2010. In vitro human skin penetration of geraniol and citronellol. Dermatitis **21:**41-48.

Gilpin SJ, Hui X, Maibach HI. 2009. Volatility of fragrance chemicals: patch testing implications. Dermatitis **20:**200-207.

Glasser AL, Boudeau J, Barnich N, Perruchot MH, Colombel JF, Darfeuille-Michaud A. 2001. Adherent invasive *Escherichia coli* strains from patients with Crohn's disease survive and replicate within macrophages without inducing host cell death. Infect Immun **69:**5529-5537.

Goldberg MB, Theriot JA. 1995. *Shigella flexneri* surface protein IcsA is sufficient to direct actin-based motility. Proc Natl Acad Sci U S A **92:**6572-6576.

Gouin E, Welch MD, Cossart P. 2005. Actin-based motility of intracellular pathogens. Curr Opin Microbiol **8:**35-45.

Halili MA, Bachu P, Lindahl F, Bechara C, Mohanty B, Reid RC, Scanlon MJ, Robinson CV, Fairlie DP, Martin JL. 2015. Small molecule inhibitors of disulfide bond formation by the bacterial DsbA-DsbB dual enzyme system. ACS Chem Biol **10:**957-964.

Harding CR, Schroeder GN, Collins JW, Frankel G. 2013. Use of *Galleria mellonella* as a model organism to study Legionella pneumophila infection. J Vis Exp doi:10.3791/50964**:**e50964.

Heindl JE, Saran I, Yi CR, Lesser CF, Goldberg MB. 2010. Requirement for formin-induced actin polymerization during spread *of Shigella flexneri*. Infect Immun **78:**193-203.

Heras B, Shouldice SR, Totsika M, Scanlon MJ, Schembri MA, Martin JL. 2009. DSB proteins and bacterial pathogenicity. Nat Rev Microbiol **7:**215-225.

Holgersen K, Kvist PH, Hansen AK, Holm TL. 2014. Predictive validity and immune cell involvement in the pathogenesis of piroxicam-accelerated colitis in interleukin-10 knockout mice. Int Immunopharmacol **21:**137-147.

Holt KE, Baker S, Weill FX, Holmes EC, Kitchen A, Yu J, Sangal V, Brown DJ, Coia JE, Kim DW, Choi SY, Kim SH, da Silveira WD, Pickard DJ, Farrar JJ, Parkhill J, Dougan G, Thomson NR. 2012. Shigella sonnei genome sequencing and phylogenetic analysis indicate recent global dissemination from Europe. Nat Genet **44:**1056-1059.

Holt KE, Thieu Nga TV, Thanh DP, Vinh H, Kim DW, Vu Tra MP, Campbell JI, Hoang NV, Vinh NT, Minh PV, Thuy CT, Nga TT, Thompson C, Dung TT, Nhu NT, Vinh PV, Tuyet PT, Phuc HL, Lien NT, Phu BD, Ai NT, Tien NM, Dong N, Parry CM, Hien TT, Farrar JJ, Parkhill J, Dougan G, Thomson NR, Baker S. 2013. Tracking the establishment of local endemic populations of an emergent enteric pathogen. Proc Natl Acad Sci U S A **110:**17522-17527.

Huang WJ, Huang CH, Wu CL, Lin JK, Chen YW, Lin CL, Chuang SE, Huang CY, Chen CN. 2007. Propolin G, a prenylflavanone, isolated from Taiwanese propolis, induces caspase-dependent apoptosis in brain cancer cells. J Agric Food Chem **55:**7366-7376.

Ibrahim SM, El-Denshary ES, Abdallah DM. 2015. Geraniol, alone and in combination with pioglitazone, ameliorates fructose-induced metabolic syndrome in rats via the modulation of both inflammatory and oxidative stress status. PLoS One **10:**e0117516.

Jayachandran M, Chandrasekaran B, Namasivayam N. 2015. Effect of geraniol, a plant derived monoterpene on lipids and lipid metabolizing enzymes in experimental hyperlipidemic hamsters. Mol Cell Biochem **398:**39-53.

Johannes L, Romer W. 2010. Shiga toxins--from cell biology to biomedical applications. Nat Rev Microbiol **8:**105-116.

Kayath CA, Hussey S, El hajjami N, Nagra K, Philpott D, Allaoui A. 2010. Escape of intracellular Shigella from autophagy requires binding to cholesterol through the type III effector, IcsB. Microbes Infect **12:**956-966.

Khan AQ, Khan R, Qamar W, Lateef A, Rehman MU, Tahir M, Ali F, Hamiza OO, Hasan SK, Sultana S. 2013. Geraniol attenuates 12-O-tetradecanoylphorbol-13-acetate (TPA)-induced oxidative stress and inflammation in mouse skin: possible role of p38 MAP Kinase and NF-kappaB. Exp Mol Pathol **94:**419-429.

Khor B, Gardet A, Xavier RJ. 2011. Genetics and pathogenesis of inflammatory bowel disease. Nature **474:**307-317.

Kishigami S, Ito K. 1996. Roles of cysteine residues of DsbB in its activity to reoxidize DsbA, the protein disulphide bond catalyst of *Escherichia coli*. Genes Cells **1:**201-208.

Kishigami S, Kanaya E, Kikuchi M, Ito K. 1995. DsbA-DsbB interaction through their active site cysteines. Evidence from an odd cysteine mutant of DsbA. J Biol Chem **270:**17072-17074.

Korsmeyer SJ. 1999. BCL-2 gene family and the regulation of programmed cell death. Cancer Res **59:**1693s-1700s.

Krauss E, Agaimy A, Neumann H, Schulz U, Kessler H, Hartmann A, Neurath MF, Raithel M, Mudter J. 2012. Characterization of lymphoid follicles with red ring signs as first manifestation of early Crohn's disease by conventional histopathology and confocal laser endomicroscopy. Int J Clin Exp Pathol **5:**411-421.

Kwon E, Kim DY, Gross CA, Gross JD, Kim KK. 2010. The crystal structure *Escherichia coli* Spy. Protein Sci **19:**2252-2259.

Lai XH, Xu Y, Chen XM, Ren Y. 2015. Macrophage cell death upon intracellular bacterial infection. Macrophage (Houst) **2:**e779.

Lapczynski A, Bhatia SP, Foxenberg RJ, Letizia CS, Api AM. 2008. Fragrance material review on geraniol. Food Chem Toxicol **46 Suppl 11:**S160-170.

Lasica AM, Jagusztyn-Krynicka EK. 2007. The role of Dsb proteins of Gram-negative bacteria in the process of pathogenesis. FEMS Microbiol Rev **31:**626-636.

Lee YK, Lee JA. 2016. Role of the mammalian ATG8/LC3 family in autophagy: differential and compensatory roles in the spatiotemporal regulation of autophagy. BMB Rep **49:**424-430.

Iijima Y, Gang DR, Fridman E, Lewinsohn E, Pichersky E. 2004. Characterization of Geraniol Synthase from the Peltate Glands of Sweet Basil. Plant Physiology **134:**370-379.

Lopez-Romero JC, Gonzalez-Rios H, Borges A, Simoes M. 2015. Antibacterial Effects and Mode of Action of Selected Essential Oils Components against *Escherichia coli* and *Staphylococcus aureus*. Evid Based Complement Alternat Med **2015:**795435.

Lorenzi V, Muselli A, Bernardini AF, Berti L, Pages JM, Amaral L, Bolla JM. 2009. Geraniol restores antibiotic activities against multidrug-resistant isolates from gram-negative species. Antimicrob Agents Chemother **53:**2209-2211.

Lorenzi V, Muselli A, Bernardini AF, Berti L, Pages JM, Amaral L, Bolla JM. 2009. Geraniol restores antibiotic activities against multidrug-resistant isolates from gram-negative species. Antimicrob Agents Chemother **53:**2209-2211.

Luzio JP, Pryor PR, Bright NA. 2007. Lysosomes: fusion and function. Nat Rev Mol Cell Biol **8:**622-632.

Magdalena J, Goldberg MB. 2002. Quantification of Shigella IcsA required for bacterial actin polymerization. Cell Motil Cytoskeleton **51:**187-196.

Mahmoud RY, Stones DH, Li W, Emara M, El-Domany RA, Wang D, Wang Y, Krachler AM, Yu J. 2016. The Multivalent Adhesion Molecule SSO1327 plays a key role in *Shigella sonnei* pathogenesis. Mol Microbiol **99:**658-673.

Man AL, Prieto-Garcia ME, Nicoletti C. 2004. Improving M cell mediated transport across mucosal barriers: do certain bacteria hold the keys? Immunology **113:**15-22.

Marcuzzi A, Crovella S, Pontillo A. 2011. Geraniol rescues inflammation in cellular and animal models of mevalonate kinase deficiency. In Vivo **25:**87-92.

Marcuzzi A, Pontillo A, De Leo L, Tommasini A, Decorti G, Not T, Ventura A. 2008. Natural isoprenoids are able to reduce inflammation in a mouse model of mevalonate kinase deficiency. Pediatr Res **64:**177-182.

Mari M, Morales A, Colell A, Garcia-Ruiz C, Fernandez-Checa JC. 2009. Mitochondrial glutathione, a key survival antioxidant. Antioxid Redox Signal **11:**2685-2700.

Martin HM, Campbell BJ, Hart CA, Mpofu C, Nayar M, Singh R, Englyst H, Williams HF, Rhodes JM. 2004. Enhanced *Escherichia coli* adherence and invasion in Crohn's disease and colon cancer. Gastroenterology **127:**80-93.

Martinez-Medina M, Aldeguer X, Lopez-Siles M, Gonzalez-Huix F, Lopez-Oliu C, Dahbi G, Blanco JE, Blanco J, Garcia-Gil LJ, Darfeuille-Michaud A. 2009. Molecular diversity of *Escherichia coli* in the human gut: new ecological evidence supporting the role of adherent-invasive E. coli (AIEC) in Crohn's disease. Inflamm Bowel Dis **15:**872-882.

Martinez-Medina M, Garcia-Gil LJ. 2014. *Escherichia coli* in chronic inflammatory bowel diseases: An update on adherent invasive *Escherichia coli* pathogenicity. World J Gastrointest Pathophysiol **5:**213-227.

Maruyama N, Takizawa T, Ishibashi H, Hisajima T, Inouye S, Yamaguchi H, Abe S. 2008. Protective activity of geranium oil and its component, geraniol, in combination with vaginal washing against vaginal candidiasis in mice. Biol Pharm Bull **31:**1501-1506.

Matsuoka K, Kanai T. 2015. The gut microbiota and inflammatory bowel disease. Semin Immunopathol **37:**47-55.

Mizushima N, Komatsu M. 2011. Autophagy: renovation of cells and tissues. Cell **147:**728-741.

Mizushima N, Yoshimori T, Ohsumi Y. 2011. The role of Atg proteins in autophagosome formation. Annu Rev Cell Dev Biol **27:**107-132.

Molodecky NA, Kaplan GG. 2010. Environmental risk factors for inflammatory bowel disease. Gastroenterol Hepatol (N Y) **6:**339-346.

Molodecky NA, Soon IS, Rabi DM, Ghali WA, Ferris M, Chernoff G, Benchimol EI, Panaccione R, Ghosh S, Barkema HW, Kaplan GG. 2012. Increasing incidence and prevalence of the inflammatory bowel diseases with time, based on systematic review. Gastroenterology **142:**46-54 e42; quiz e30.

Mostowy S, Bonazzi M, Hamon MA, Tham TN, Mallet A, Lelek M, Gouin E, Demangel C, Brosch R, Zimmer C, Sartori A, Kinoshita M, Lecuit M, Cossart P. 2010. Entrapment of intracytosolic bacteria by septin cage-like structures. Cell Host Microbe **8:**433-444.

Mostowy S, Cossart P. 2011. Autophagy and the cytoskeleton: new links revealed by intracellular pathogens. Autophagy **7:**780-782.

Mpofu CM, Campbell BJ, Subramanian S, Marshall-Clarke S, Hart CA, Cross A, Roberts CL, McGoldrick A, Edwards SW, Rhodes JM. 2007. Microbial mannan inhibits bacterial killing by macrophages: a possible pathogenic mechanism for Crohn's disease. Gastroenterology **133:**1487-1498.

Munz C. 2011. Beclin-1 targeting for viral immune escape. Viruses **3:**1166-1178.

Murbach Teles Andrade BF, Conti BJ, Santiago KB, Fernandes Junior A, Sforcin JM. 2014. Cymbopogon martinii essential oil and geraniol at noncytotoxic concentrations exerted immunomodulatory/anti-inflammatory effects in human monocytes. J Pharm Pharmacol **66:**1491-1496.

Myc A, Pizzolo JG, Dygulski K, Melamed MR. 1992. Increase in acridine orange (AO) fluorescence intensity of monocytes cultured in plastic tissue culture plates as measured by flow cytometry. Cytometry **13:**103-107.

Nazzaro F, Fratianni F, De Martino L, Coppola R, De Feo V. 2013. Effect of essential oils on pathogenic bacteria. Pharmaceuticals (Basel) **6:**1451-1474.

Noge K, Kato M, Mori N, Kataoka M, Tanaka C, Yamasue Y, Nishida R, Kuwahara Y. 2008. Geraniol dehydrogenase, the key enzyme in biosynthesis of the alarm pheromone, from the astigmatid mite Carpoglyphus lactis (Acari: Carpoglyphidae). FEBS J **275:**2807-2817.

Ogawa M, Sasakawa C. 2006. Intracellular survival of Shigella. Cell Microbiol **8:**177-184.

Ogawa M, Yoshimori T, Suzuki T, Sagara H, Mizushima N, Sasakawa C. 2005. Escape of intracellular Shigella from autophagy. Science **307:**727-731.

Ossa JC, Ho NK, Wine E, Leung N, Gray-Owen SD, Sherman PM. 2013. Adherent-invasive *Escherichia coli* blocks interferon-gamma-induced signal transducer and activator of transcription (STAT)-1 in human intestinal epithelial cells. Cell Microbiol **15:**446-457.

Ozkaya A, Sahin Z, Gorgulu AO, Yuce A, Celik S. 2017. Geraniol attenuates hydrogen peroxide-induced liver fatty acid alterations in male rats. J Intercult Ethnopharmacol **6:**29-35.

Pantaloni D, Le Clainche C, Carlier MF. 2001. Mechanism of actin-based motility. Science **292:**1502-1506.

Patel JM. 2008. A Review of Potential Health Benefits of Flavonoids. Lethbridge Undergraduate Research Journal **3**.

Peirano G, Agerso Y, Aarestrup FM, dos Prazeres Rodrigues D. 2005. Occurrence of integrons and resistance genes among sulphonamide-resistant Shigella spp. from Brazil. J Antimicrob Chemother **55:**301-305.

Phalipon A, Sansonetti PJ. 2007. *Shigella's* ways of manipulating the host intestinal innate and adaptive immune system: a tool box for survival? Immunol Cell Biol **85:**119-129.

Prescott NJ, Fisher SA, Franke A, Hampe J, Onnie CM, Soars D, Bagnall R, Mirza MM, Sanderson J, Forbes A, Mansfield JC, Lewis CM, Schreiber S, Mathew CG. 2007. A nonsynonymous SNP in ATG16L1 predisposes to ileal Crohn's disease and is independent of CARD15 and IBD5. Gastroenterology **132:**1665-1671.

Prorok-Hamon M, Friswell MK, Alswied A, Roberts CL, Song F, Flanagan PK, Knight P, Codling C, Marchesi JR, Winstanley C, Hall N, Rhodes JM, Campbell BJ. 2014. Colonic mucosa-associated diffusely adherent afaC+ *Escherichia coli* expressing lpfA and pks are increased in inflammatory bowel disease and colon cancer. Gut **63:**761-770.

Rabbani GH, Teka T, Saha SK, Zaman B, Majid N, Khatun M, Wahed MA, Fuchs GJ. 2004. Green banana and pectin improve small intestinal permeability and reduce fluid loss in Bangladeshi children with persistent diarrhea. Dig Dis Sci **49:**475-484.

Raghukumar R, Vali L, Watson D, Fearnley J, Seidel V. 2010. Antimethicillin-resistant Staphylococcus aureus (MRSA) activity of 'pacific propolis' and isolated prenylflavanones. Phytother Res **24:**1181-1187.

Raivio TL. 2005. Envelope stress responses and Gram-negative bacterial pathogenesis. Mol Microbiol **56:**1119-1128.

Raturi A, Mutus B. 2007. Characterization of redox state and reductase activity of protein disulfide isomerase under different redox environments using a sensitive fluorescent assay. Free Radic Biol Med **43:**62-70.

Rios JL, Recio MC. 2005. Medicinal plants and antimicrobial activity. J Ethnopharmacol **100:**80-84.

Roberts CL, Keita AV, Duncan SH, O'Kennedy N, Soderholm JD, Rhodes JM, Campbell BJ. 2010. Translocation of Crohn's disease *Escherichia coli* across M-cells: contrasting effects of soluble plant fibres and emulsifiers. Gut **59:**1331-1339.

Roberts CL, Keita AV, Parsons BN, Prorok-Hamon M, Knight P, Winstanley C, N OK, Soderholm JD, Rhodes JM, Campbell BJ. 2013. Soluble plantain fibre blocks adhesion and M-cell translocation of intestinal pathogens. J Nutr Biochem **24:**97-103.

Rolhion N, Barnich N, Bringer MA, Glasser AL, Ranc J, Hebuterne X, Hofman P, Darfeuille-Michaud A. 2010. Abnormally expressed ER stress response chaperone Gp96 in CD favours adherent-invasive *Escherichia coli* invasion. Gut **59:**1355-1362.

Sasaki M, Sitaraman SV, Babbin BA, Gerner-Smidt P, Ribot EM, Garrett N, Alpern JA, Akyildiz A, Theiss AL, Nusrat A, Klapproth JM. 2007. Invasive *Escherichia coli* are a feature of Crohn's disease. Lab Invest **87:**1042-1054.

Schroeder GN, Hilbi H. 2008. Molecular pathogenesis of *Shigella* spp.: controlling host cell signaling, invasion, and death by type III secretion. Clin Microbiol Rev **21:**134-156.

Simonsen KT, Nielsen G, Bjerrum JV, Kruse T, Kallipolitis BH, Moller-Jensen J. 2011. A role for the RNA chaperone Hfq in controlling adherent-invasive *Escherichia coli* colonization and virulence. PLoS One **6:**e16387.

Sivignon A, de Vallee A, Barnich N, Denizot J, Darcha C, Pignede G, Vandekerckove P, Darfeuille-Michaud A. 2015. *Saccharomyces cerevisiae* CNCM I-3856 prevents colitis induced by AIEC bacteria in the transgenic mouse model mimicking Crohn's disease. Inflamm Bowel Dis **21:**276-286.

Skoudy A, Mounier J, Aruffo A, Ohayon H, Gounon P, Sansonetti P, Tran Van Nhieu G. 2000. CD44 binds to the *Shigella* IpaB protein and participates in bacterial invasion of epithelial cells. Cell Microbiol **2:**19-33.

Small CL, Reid-Yu SA, McPhee JB, Coombes BK. 2013. Persistent infection with Crohn's disease-associated adherent-invasive *Escherichia coli* leads to chronic inflammation and intestinal fibrosis. Nat Commun **4:**1957.

Solorzano-Santos F, Miranda-Novales MG. 2012. Essential oils from aromatic herbs as antimicrobial agents. Curr Opin Biotechnol **23:**136-141.

Steele D, Riddle M, van de Verg L, Bourgeois L. 2012. Vaccines for enteric diseases: a meeting summary. Expert Rev Vaccines **11:**407-409.

Steinhauer J, Agha R, Pham T, Varga AW, Goldberg MB. 1999. The unipolar *Shigella* surface protein IcsA is targeted directly to the bacterial old pole: IcsP cleavage of IcsA occurs over the entire bacterial surface. Mol Microbiol **32:**367-377.

Subramanian S, Rhodes JM, Hart CA, Tam B, Roberts CL, Smith SL, Corkill JE, Winstanley C, Virji M, Campbell BJ. 2008. Characterization of epithelial IL-8 response to inflammatory bowel disease mucosal *E. coli* and its inhibition by mesalamine. Inflamm Bowel Dis **14:**162-175.

Subramanian S, Roberts CL, Hart CA, Martin HM, Edwards SW, Rhodes JM, Campbell BJ. 2008. Replication of Colonic Crohn's Disease Mucosal *Escherichia coli* Isolates within Macrophages and Their Susceptibility to Antibiotics. Antimicrob Agents Chemother **52:**427-434.

Suzuki T, Franchi L, Toma C, Ashida H, Ogawa M, Yoshikawa Y, Mimuro H, Inohara N, Sasakawa C, Nunez G. 2007. Differential regulation of caspase-1 activation, pyroptosis, and autophagy via Ipaf and ASC in *Shigella*-infected macrophages. PLoS Pathog **3:**e111.

Tamogami S, Agrawal GK, Rakwal R. 2016. Methyl jasmonate elicits the biotransformation of geraniol stored as its glucose conjugate into methyl geranate in Achyranthes bidentata plant. Plant Physiol Biochem **109:**166-170.

Tanida I. 2011. Autophagosome formation and molecular mechanism of autophagy. Antioxid Redox Signal **14:**2201-2214.

Tawfik A, Flanagan PK, Campbell BJ. 2014. *Escherichia coli*-host macrophage interactions in the pathogenesis of inflammatory bowel disease. World J Gastroenterol **20:**8751-8763.

Tchaptchet S, Fan TJ, Goeser L, Schoenborn A, Gulati AS, Sartor RB, Hansen JJ. 2013. Inflammation-induced acid tolerance genes gadAB in luminal commensal *Escherichia coli* attenuate experimental colitis. Infect Immun **81:**3662-3671.

Teh MY, Morona R. 2013. Identification of *Shigella flexneri* IcsA residues affecting interaction with N-WASP, and evidence for IcsA-IcsA co-operative interaction. PLoS One **8:**e55152.

Toreti VC, Sato HH, Pastore GM, Park YK. 2013. Recent progress of propolis for its biological and chemical compositions and its botanical origin. Evid Based Complement Alternat Med **2013:**697390.

Torres AG. 2004. Current aspects of *Shigella* pathogenesis. Rev Latinoam Microbiol **46:**89-97.

Travassos LH, Carneiro LA, Ramjeet M, Hussey S, Kim YG, Magalhaes JG, Yuan L, Soares F, Chea E, Le Bourhis L, Boneca IG, Allaoui A, Jones NL, Nunez G, Girardin SE, Philpott DJ. 2010. Nod1 and Nod2 direct autophagy by recruiting ATG16L1 to the plasma membrane at the site of bacterial entry. Nat Immunol **11:**55-62.

Vazeille E, Chassaing B, Buisson A, Dubois A, de Vallee A, Billard E, Neut C, Bommelaer G, Colombel JF, Barnich N, Darfeuille-Michaud A, Bringer MA. 2016. GipA Factor Supports Colonization of Peyer's Patches by Crohn's Disease-associated *Escherichia Coli*. Inflamm Bowel Dis **22:**68-81.

Veitch NC, Grayer RJ. 2008. Flavonoids and their glycosides, including anthocyanins. Nat Prod Rep **25:**555-611.

Vinothkumar V, Manoharan S, Sindhu G, Nirmal MR, Vetrichelvi V. 2012. Geraniol modulates cell proliferation, apoptosis, inflammation, and angiogenesis during 7,12-dimethylbenz[a]anthracene-induced hamster buccal pouch carcinogenesis. Mol Cell Biochem **369:**17-25.

Watarai M, Tobe T, Yoshikawa M, Sasakawa C. 1995. Disulfide oxidoreductase activity *of Shigella flexneri* is required for release of Ipa proteins and invasion of epithelial cells. Proc Natl Acad Sci U S A **92:**4927-4931.

Weng MS, Liao CH, Chen CN, Wu CL, Lin JK. 2007. Propolin H from Taiwanese propolis induces G1 arrest in human lung carcinoma cells. J Agric Food Chem **55:**5289-5298.

Wine E, Ossa JC, Gray-Owen SD, Sherman PM. 2010. Adherent-invasive *Escherichia coli* target the epithelial barrier. Gut Microbes **1:**80-84.

Wing HJ, Yan AW, Goldman SR, Goldberg MB. 2004. Regulation of IcsP, the outer membrane protease of the *Shigella* actin tail assembly protein IcsA, by virulence plasmid regulators VirF and VirB. J Bacteriol **186:**699-705.

Wright EK, Kamm MA, Teo SM, Inouye M, Wagner J, Kirkwood CD. 2015. Recent advances in characterizing the gastrointestinal microbiome in Crohn's disease: a systematic review. Inflamm Bowel Dis **21:**1219-1228.

Wunderlich M, Glockshuber R. 1993. Redox properties of protein disulfide isomerase (DsbA) from *Escherichia coli*. Protein Sci **2:**717-726.

Xu D, Saeed A, Wang Y, Seidel V, Sandstrom G, Yu J. 2011. Natural products modulate Shigella-host-cell interaction. J Med Microbiol **60:**1626-1632.

Xu D, Yang X, Wang D, Yu J, Wang Y. 2014. Surface display of the HPV L1 capsid protein by the autotransporter *Shigella* IcsA. J Microbiol **52:**77-82.

Xu Y, Eissa NT. 2010. Autophagy in innate and adaptive immunity. Proc Am Thorac Soc **7:**22-28.

Yu J. 1998. Inactivation of DsbA, but not DsbC and DsbD, affects the intracellular survival and virulence of *Shigella flexneri*. Infect Immun **66:**3909-3917.

Yu J, Rossi R, Hale C, Goulding D, Dougan G. 2009. Interaction of enteric bacterial pathogens with murine embryonic stem cells. Infect Immun **77:**585-597.

Zychlinsky A, Fitting C, Cavaillon JM, Sansonetti PJ. 1994. Interleukin 1 is released by murine macrophages during apoptosis induced by Shigella flexneri. J Clin Invest **94:**1328-1332.

Appendices:

Appendix A: List of buffers, solution and media:

Table A 1: list of buffers, solutions and media used in this study.

Buffers and stock solutions	Composition
Acidic, nutrient-poor medium	100 mM bis-Tris, 0.1% w/v Casamino Acids, 0.16% v/v glycerol, and 10 μM $MgCl_2$, pH 5.8
DMEM	10% v/v fetal calf serum, 1 mM sodium pyruvate (Sigma) and 1% v/v non-essential amino acid solution (Sigma)
DNA clean-up solution mix	40 μL of yellow core buffer, 5 μL of 0.09M $MnCl_2$ and 5 μL of DNase I
M9 media	1 g/L ammonium chloride, 6 g/L disodium hydrogen phosphate, 3 g/L potassium dihydrogen phosphate, 0.5 g/L sodium chloride, 2 mL/L 1M magnesium sulfate, 2 mL/L 0.1M calcium chloride and 20 mL/L glucose (Sigma).
PDI/DsbA buffer	0.1M potassium phosphate buffer (pH 7.0) and 2 mM EDTA
phosphate buffer	100 mM potassium phosphate and 2 mM EDTA pH 8.8

protein loading buffer	40% v/v Glycerol, 240 mM Tris/HCl pH 6.8, 8% w/v SDS, 0.04% w/v Bromophenol blue and 5% v/v beta-mercaptoethanol)
protein running buffer	1.44% w/v glycine, 0.3% w/v Tris, 0.1% w/v SDS
SOC media	0.5% w/v Yeast Extract, 2% w/v Tryptone, 10 mM NaCl, 2.5 mM KCl, 10 mM $MgCl_2$, 10 mM $MgSO_4$ and 20 mM glucose.
TAE buffer	4.84 g Tris Base, 1.142 mL Glacial Acetic acid, 2 mL 0.5M EDTA
TBS	25 mM Tris, pH8, 125 mM NaCl
transfer buffer	1.44% w/v glycine, 0.3% w/v Tris, 0.01% w/v SDS, and 20% v/v methanol

Appendix B: NMR data:

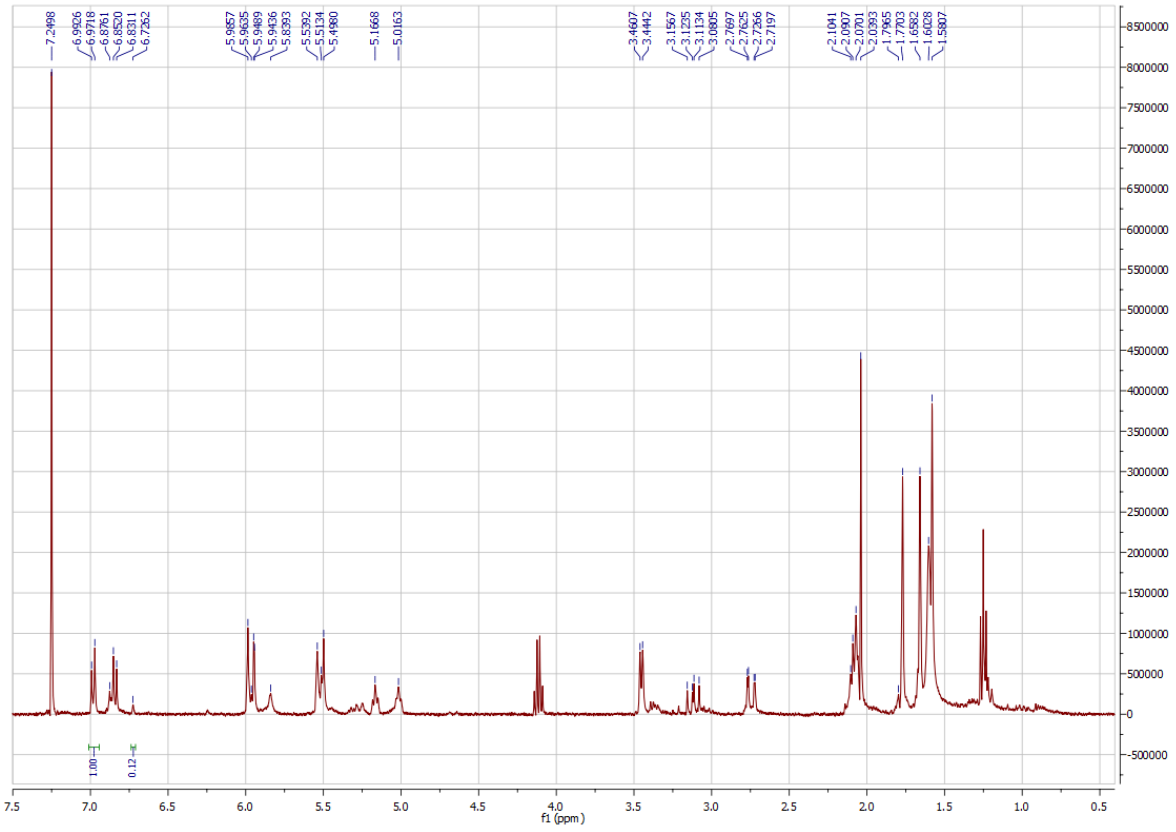

Figure B1: ^{1}H NMR spectrum (400 MHz) of propolin D in $CDCl_3$